Biogeochemical cycling of mercury in terrestrial environments: Emphasis on mercury uptake by black spruce (*Picea mariana*) in peatlands and impacts of invasive earthworms on soil mercury cycling

A Thesis
SUBMITTED TO THE FACULTY OF
UNIVERSITY OF MINNESOTA
BY

Sona Psarska

IN PARTIAL FULFILLMENT OF THE REQUIREMENTS
FOR THE DEGREE OF
MASTER OF SCIENCE

Adviser Edward A. Nater

June 2015

Acknowledgements

First and foremost I would like to express my deepest thanks to my adviser, Dr. Edward Nater, for the opportunity to work with him on different facets of mercury cycling in the environment. Ed has given me invaluable guidance throughout the research process and dedicated many hours of his time to help me become a better student of science through scientific discussion and by giving me opportunities to interact with other scientists. Ed was also extremely instrumental in facilitating and helping with sample collections and for that I am very grateful.

I would like to express a big thank you to Dr. Randall Kolka and Dr. Brandy Toner for serving as committee members and providing guidance and insightful comments that helped me improve in my scientific endeavors. I would like to extend a special thanks to Dr. Randall Kolka for allowing me to collect samples in the peatlands of the Marcell Experimental Forest in Grand Rapids, Minnesota and for providing the majority of my funding as well as invaluable contacts for universities and government agencies outside of Minnesota that were involved in sample collections.

I would like to extend thanks to all of the kind people that were directly or indirectly involved in sample collections without whom this research would have suffered. Big thank you to Tom Malone, Richard Dionne, James Shanley, Paul Hazlett, Dexter Hodder, Roy Rea, Kathy Lewis, Michael Jull, Marilyn Pike, Gordon Putz, Brian Bassard, Nancy Serediak and her neighbor Alan Plourde, Susan Ziegler, Leah Soper, Murray Perrett, Paul Whalen, Darrell Harris and I am sure many others that I may not be aware of. A special thank you to Cyril Lundrigan, a research silviculturalist with the Newfoundland and Labrador Department of Natural Resources, for being an invaluable contact in this province and for helping to facilitate numerous collections and provide helpful information on the local environmental conditions. Additionally, I would like to thank Chris Mahr, Britta Halvorson, Mikhail Mack and Kaleiilima Holt for their assistance in the lab. Thank you to Michael Dolan and Brent Dalzell for allowing me to

use their supplies and equipment for carbon analysis, and to Kyungsoo Yoo and Kathryn Resner for allowing me to use the soil they collected in 2009 for the second part of my research. None of this research would've been possible without the efforts of this group of dedicated people.

I would like to give a special thanks to Michelle Natarajan who was my partner in crime and support system in the lab especially during my first year of graduate school. Thanks to Michelle for keeping me sane, appreciating my weirdness and becoming a true friend in the process. Additionally, I want to thank Michelle and Olga Furman for dedicating many hours to discussion of scientific and other topics with me.

Lastly, I would like to thank my family for their unwavering support throughout my graduate school career. I thank and dedicate my thesis to my parents without whom I would not have accomplished much. I want to give the biggest thank you to my mom for being the most loving and caring person I know and for making me laugh and keeping my spirits up throughout the entire graduate school process.

Abstract

Mercury (Hg) is a naturally occurring element but has become an important environmental pollutant mostly due to human activities such as coal combustion and waste incineration. Mercury is transported and deposited globally with an atmospheric residence time of approximately a year. It can be highly reactive, especially when deposited to aquatic environments, making the biogeochemical cycling of mercury an important area of study. However, most studies have focused heavily on aquatic environments since this is where the methylated organic mercury compounds are found most commonly and become bioaccumulated and biomagnified through the food chain. Despite the fact that organomercury compounds are more toxic, understanding the movement of elemental and ionic mercury through the terrestrial environment is very important since these forms of mercury are ultimately the ones that participate in mercury methylation reactions.

In this thesis, I focus on the deposition of mercury to terrestrial environments. In the first chapter, I focus on the uptake of elemental mercury by black spruce trees in peatland environments to assess their potential ability to be used as passive atmospheric biomonitors. Peatlands are considered to be highly vulnerable to climate change due to their high organic carbon content. With mercury's high affinity for organic matter there is a possibility to see higher rates of mercury volatilization in a warming climate. Therefore, assessing whether black spruce trees could be used as passive monitors of atmospheric mercury could be a quick and relatively inexpensive way to monitor these highly vulnerable ecosystems for changes in elemental mercury dynamics.

In the second chapter, I focus on the impacts of invasive earthworms to mercury cycling in the soil. Hardwood forests in northern Minnesota have developed without earthworms since the last glaciation, however; European earthworms were unintentionally introduced in these forests as a result of human activities. Earthworms feed primarily on organic rich forest floor which coincidentally complexes the largest amounts of mercury. Heavy earthworm invasions result in the complete consumption of the forest floor which undoubtedly alters mercury cycling in the soil. Two mass balance approaches are used to assess the quantity of mercury that is presumably transported from the forest floor into the soil as a result of these invasive soil mixing earthworms.

The terrestrial environment, especially vegetation, is an important sink of mercury. Vegetation takes up elemental mercury and converts it to its ionic form which then remains bound within the leaf making it a potentially viable biomonitor of atmospheric mercury. Additionally, vegetation increases the soil mercury pool by increased deposition of atmospheric mercury to soil primarily through litterfall. In this way vegetation can serve as an important intermediary in the mercury cycle and is an important component of terrestrial systems.

Table of Contents

List of Tables

List of Figures

Chapter 1

Black spruce (*Picea mariana*) needles as a passive monitor of atmospheric mercury: an investigation from various North American sites

1. Introduction

1.1 Atmospheric Mercury Overview

Mercury is a naturally occurring element and can be found in mineral form as the cinnabar ore (HgS), as mercury salts or as organic mercury compounds. Mercury enters the atmosphere and water bodies as a result of natural breakdown of rocks and soil, crustal degassing, and through volcanic eruptions and fires (Schroeder and Munthe 1998). With the dawn of the industrial revolution human activities have significantly impacted the biogeochemical cycling of mercury. Anthropogenic emissions of mercury, mostly through fossil fuel combustion, therefore account for a large fraction of mercury emissions to the environment (Mason et al. 1994; Fitzgerald 1995). 50-75% of Hg emitted is estimated to be from anthropogenic sources (Lindqvist et al. 1991). Mercury is considered a global pollutant due to its highly volatile and reactive nature. Mercury is most toxic when in its organic methylmercury (MeHg) form. This highly toxic form of mercury readily bioaccumulates and biomagnifies through the food chain making it a concern for many organisms including humans (Lindqvist et al. 1991).

In the environment, mercury exists in three oxidation states 0, +1 and +2 (Schroeder and Munthe 1998). The gaseous elemental form of mercury (Hg^0) is the most dominant (>90%) form in the atmosphere (Lindqvist and Rhode 1985; Schroeder et al. 1991). Mercury in the +2 oxidation state (Hg^{2+}), which is associated with particulate phases, only contributes <10% to the overall mercury content of the atmosphere (Schroeder et al. 1991). Methylated gaseous mercury species can also occur in the atmosphere but usually in very negligible amounts (Lin and Pehkonen 1999). Once emitted to the atmosphere, elemental mercury (Hg^0) is transported and deposited globally

with an atmospheric residence time of 6-24 months (Lindqvist and Rhode 1985; Schroeder and Munthe 1998). Atmospheric mercury plays an important role in the overall biogeochemical cycle of mercury. A high percentage of atmospheric mercury is deposited to terrestrial systems where it can become sequestered mainly in soil and vegetation or, if deposited to water bodies, it can continue to actively participate in aquatic chemistry (Sorensen et al. 1994).

1.2 Importance of Vegetation

The biogeochemical cycle of mercury has been extensively studied for many years now, but due to the cycle's complexity there are still many areas in need of elucidation. For example, the interaction of atmospheric mercury with different types of vegetation is one area that would benefit from further study. Forests play an important role in Hg deposition to terrestrial environments. In open areas, which receive the bulk of their atmospheric mercury from precipitation and dry deposition, deposition rates are much smaller than in forested areas, which have the addition of throughfall and littefall (Kolka et al. 2001). The focus of this study will therefore be on vegetation since it plays an important role in the terrestrial biogeochemical cycle as it intercepts the deposition of wet and dry particulate mercury and interacts with gaseous elemental mercury through stomatal openings (Laacouri et al. 2013). Numerous studies, as early as 1978, have shown the direct uptake of Hg^0 through the stomata of plants (Browne and Fang, 1978; Lindberg et al. 1979; Lindberg et al. 1991; Ericksen et al. 2003). However, others have observed that vegetation may also be a source of Hg into the atmosphere depending on the background atmospheric concentrations (Hanson et al. 1995; Lindberg et al. 1998; Leonard et al. 1998; Graydon et al. 2006). In particular, Hanson et al. (1995) introduced

the concept of a compensation point in trees, an atmospheric concentration at which no net exchange of Hg occurs between the leaf and the atmosphere. However, there is great variability between compensation points as they are species specific, and they cannot be used very reliably to model foliar exchanges of Hg with the atmosphere. They also pointed out the need to view vegetation as a dynamic exchange surface, which can act as both a sink or source of Hg, depending on site conditions and background atmospheric levels of Hg^0. With vegetation playing such an important role in the cycling of mercury, more studies should focus on understanding the important interactions of foliage with Hg^0. Root uptake of mercury from soil was shown to be minimal and, therefore, above ground vegetation gets the bulk of its mercury from the atmosphere (Lindberg et al. 1979, Rea et al. 2002, Ericksen et al. 2003; Demers et al. 2007).

Despite the evidence of foliar emissions of Hg, vegetation is considered to be a net sink of mercury due to the ability of leaves to convert elemental mercury into ionic mercury (Hg^{2+}) which then remains bound within the leaf (Du and Fang 1983). Laacouri et al. (2013) found that the majority (>90%) of Hg is bound within leaf tissue with only a small percentage in the cuticle and surface of leaves, which further supports the notion of a vegetation Hg sink. Essentially, there are two pools of gaseous elemental mercury associated with leaves: the exchangeable pool, which has been studied by numerous flux studies (Hanson et al. 1995; Millhollen et al. 2006; Ericksen and Gustin 2004; Stamenkovic and Gustin 2009; Graydon et al. 2006) and the pool that is retained or accumulated within leaves (Rea et al. 2002; Millhollen et al. 2006; Du and Fang 1983; Ericksen et al. 2003). The second pool is important for this study because the retained fraction is relatively easily determined and it provides the potential to use vegetation as a

biomonitor of pollution. Coniferous trees are especially good for Hg related determinations as they show an increase in Hg concentrations with needle age (Wyttenbach and Tobler 1988; Barghigiani et al. 1991; Fleck et al. 1999), while deciduous trees show increasing Hg concentrations with progression of the growing season (Rea et al. 2002; Millhollen et al. 2006; Siwik et al. 2009).

Leaf senescence, especially in deciduous trees, provides an annual input of Hg to the forest floor. Since conifers do not, however, shed their needles all at once but rather continuously at slow rates, they can be used to show the progressive accumulation of atmospheric mercury in needles of different ages, as mentioned above. A number of studies have looked at the possibility of using conifers as bioindicators of pollution (Eriksson et al. 1989; Suchara et al. 2011; Lodenius 2013) not only when it comes to mercury, but other pollutants as well. However, different species behave differently with respect to different pollutants which can make choosing the appropriate biomonitor difficult. With respect to mercury, conifer needles seem to behave logically when it comes to assessing Hg concentrations of needles from different sites (i.e. higher concentrations found near mercury emissions sites), but overall the needles of conifers seem to take up less elemental mercury than other biomonitors such as deciduous trees or lichens and mosses (Lodenius 2013). As Suchara et al. (2011) point out, it is important to consider the issue of scale when choosing a biomonitor. They suggest that spruce may be a biomonitor more suitable for assessing pollution at a local scale, although they analyzed a large suite of contaminants not just mercury (Suchara et al. 2011). A few studies have looked at the Hg concentrations of coniferous needles (Zhang et al. 1995; Fleck et al 1999; Ollerova et al. 2010) with this study hoping to add to that body of knowledge.

1.3 SPRUCE & Atmospheric Mercury Monitoring

The notion to use black spruce (*Picea mariana*) as a passive monitor of atmospheric mercury came from the implications of a large scale climate change study called Spruce and Peatland Responses Under Climatic and Environmental Change (SPRUCE) funded by the Department of Energy and taking place in the USDA Forest Service Marcell Experimental Forest (MEF) near Grand Rapids, Minnesota. The SPRUCE project aims to study a peatland ecosystem under varying temperature and CO_2 levels meant to simulate future climate change warming (mnspruce.ornl.gov). Fifty years of research at the MEF has contributed to our understanding of peatland ecosystems and more specifically peatland hydrology, acid rain impacts, nutrient and carbon cycling, trace gas emissions and mercury behavior within these watersheds (Bartuska and Rains 2011). Numerous mercury related studies have taken place at the MEF (Kolka et al. 1999a; Kolka et al. 1999b; Kolka et al. 2001; Grigal 2000; Jeremiason et al. 2006; Mitchell et al. 2009) providing important background information on mercury dynamics in these systems. Mercury questions related to climate change are also incorporated into the SPRUCE project which sparked my interest in using black spruce, the dominant tree species in these peatlands, as a passive monitor of atmospheric mercury. Within the experimental design of the SPRUCE project are large open top chambers which will encompass entire black spruce trees. Numerous facets of the spruce trees and the peat itself are to be monitored and studied for responses to elevated temperatures and CO_2 levels. The addition of a black spruce biomonitor for changes in Hg concentrations could provide a fairly quick and easy way of monitoring how black spruce trees respond under simulated warming conditions.

Atmospheric monitoring of mercury is necessary especially when we consider its long atmospheric residence time and ability to be transported globally. Transport of atmospheric mercury from emission sources can often contaminate previously pristine sites. This has led to the development of three large scale monitoring efforts in North America: the National Atmospheric Deposition Program's (NADP) Mercury Deposition Network (MDN) and Atmospheric Mercury Network (AMNet) and the Canadian Atmospheric Mercury Measurement Network (CAMNet). In addition to these national monitoring networks, local monitoring efforts by universities and local government agencies also supply important information on mercury's behavior in the atmosphere. The Mercury Deposition Network collects data on total Hg concentration in wet deposition through collectors and gages throughout the U.S. However, sites have been added or removed based on individual decisions and/or funding availability, which makes their distribution fairly uneven (Risch et al. 2014). The Atmospheric Mercury Network (AMNet) was added to collect data on dry deposition; however, dry deposition is more difficult to measure than wet deposition and the measurements are often subject to large errors (Zhang et al. 2009). The monitoring sites are also heavily concentrated in the eastern part of the U.S. While these networks are certainly necessary for continued monitoring of atmospheric mercury on a national scale, this type of monitoring often comes with a high price tag. For example, the upfront cost of operation of one MDN site is well over $10,000 (Monitoring Mercury Deposition 2011). Any additional monitoring, such as for atmospheric methylmercury, would raise the cost considerably. Nonetheless, through the use of data collected by the Canadian Atmospheric Mercury Measurement Network (CAMNet), Temme et al. (2007) were able to show that total gaseous mercury

(TGM) decreased in urban areas of Toronto and Montreal between 1995 and 2005 highlighting the importance of having these networks in use despite their high cost.

As mentioned earlier, the cost of establishing a monitoring site can negatively impact the distribution of these sites and hinder research. This is why the use of biomonitors such as trees or lichens becomes appealing. This type of monitoring usually costs less because there is no major upfront cost associated with establishing the monitoring site. Siwik et al. (2009) highlighted some of the challenges associated with using trees as biomonitors such as the variability of Hg concentrations depending on tree species, leaf age and leaf position. But they also made sure to stress the importance of expanding our knowledge base of different tree species and their storage of elemental mercury and of our continual efforts of using trees as biomonitors precisely because they are a quick, easy and inexpensive way of monitoring changes in atmospheric mercury deposition.

Climate change will undoubtedly impact mercury cycling; therefore, monitoring efforts are more important than ever. Certain ecosystems such as peatlands, which store large amounts of organic matter, are thought to be more vulnerable to climate change. This is important from a mercury perspective because mercury has high affinity for organic matter where it binds strongly with reduced sulfur groups (Skyllberg et al. 2003). If climate change results in faster decomposition of organic matter in peatlands this could release large amounts of mercury into the atmosphere. Therefore, studying the possibility of a black spruce biomonitor may help to indirectly show increasing mercury concentrations in the atmosphere and/or changes in mercury uptake by trees.

1.4 Study Objectives

Building on our previous knowledge of atmospheric mercury and its interactions with vegetation, my objective was to assess the suitability of black spruce as a passive monitor of atmospheric mercury. Black spruce (*Picea mariana*) was chosen as a potential biomonitor due to the growing need to understand and monitor vulnerable ecosystems such as peatlands. Unlike previous studies that mostly focused on one or two sampling locations, this study examines the mercury content of black spruce trees from 19 different peatland sites across North America. By conducting the study over numerous sampling locations, I was able to assess the variability of mercury concentrations through site to site comparisons. I was also able to make finer scale comparisons which show tree to tree variability within a site as well as within tree variability of mercury concentrations. The examination of needles from numerous North American sites allowed me to form a better idea of how Hg concentrations can vary based on the general sampling location. In addition to this, the outcomes of this study allow us to understand whether black spruce can be used as a reliable monitor of atmospheric mercury, especially when considered on a larger scale, or whether it is more suitable for localized determinations of atmospheric mercury.

2. Methods

2.1 Field sites & Climatic Conditions

Black spruce is a common tree species found in peatlands. The collection sites included a mixture of fens- (nutrient rich peatlands) and bogs- (nutrient poor peatlands). Black spruce needles were collected from a total of 19 sites: 11 in U.S. and 8 in Canada. Site breakdown and locations are in Figure 1 and Table 1 in the Appendix I. Collections

took place in the winter of 2014 between January and March. Photosynthesis is substantially impaired in the winter due to cold temperatures (Bergh et al. 1998) which allows for the collection of needles that represent a full year of growth from the 2013 growing season without the confounding effects of new growth. The winter of 2013/2014 was especially cold in the northern U.S and Canada so even collection made in March were still under freezing conditions.

All U.S. sites, except for Alaska, exhibit a strong continental or humid continental climate. Temperatures and precipitation amounts do not vary greatly between the U.S. sites, although the Upper Peninsula of Michigan experiences lake-effect snow so snowfall amounts in this region can be quite high. Black spruce is predominantly found in the taiga or boreal forest biome so a very large climatic variation within its native range is not likely. Inner parts of Alaska, where two of the U.S. sites are found, are considered to have a subarctic continental climate.

Climate of the Canadian sites ranges from humid continental moving from Newfoundland & Labrador in the East to Alberta, with dry continental climate in the west and even semi-arid in some parts of British Columbia. But again the slight climatic variations probably do not have a pronounced effect on black spruce at the various sampling locations. What tends to make a greater difference is whether the samples were collected from a fen or a bog. Trees grow better in fens which are partially fed by groundwater because there are more nutrients available for plant growth. Black spruce in bogs grows very slowly because bogs are typically only fed by precipitation and therefore rather nutrient poor.

In addition to black spruce, balsam fir (*Abies balsamea*) was collected at the Wisconsin (WI) and Michigan (MI_FEN) sites to see how balsam fir needle THg concentrations compare to those of black spruce (Table 3). Balsam fir is often found in more nutrient rich peatlands or on the edges of nutrient poor peatlands.

Lichens were also collected at 11 of the 19 sites based on availability as they have been shown to be acceptable biomonitors of heavy metal pollution (Table 3) (Szczepniak and Biziuk 2003; Sensen and Richardson 2002; Grangeon et al. 2012; Lodenius 2013).

2.2 Sampling

Black spruce collections were made at breast height from trees of approximately the same height to minimize any variability due to sampling location on each tree. 5-7 trees were sampled per site by clipping 3-4 branches from each tree. For the approximate size of branches collected refer to Figure 2 in Appendix I. GPS locations were recorded just for the general site location- not each individual tree within a site (Table 1, Appendix I). Branches were placed in large ziplock bags and stored in a freezer until sample processing and analysis. Balsam fir was also sampled at breast height by clipping branches. For the Wisconsin site, balsam fir samples were taken from the edge of the bog. At the Michigan site, balsam fir was interspersed between black spruce trees as this was a more nutrient rich area. Fruticose lichen species (*Bryoria trichodes, Evernia mesomorpha* and *Usnea subfloridana*) were collected in conjunction with needle collections; however, some sites did not have a sufficient quantity of fruticose lichen for sampling. Lichen was collected from either the same trees as needle collection or, if those trees did not have any appreciable amount of lichen, other trees were sampled; therefore, the amount of lichen collected varied from site to site depending on availability.

Before analysis, branches were processed and dried. Each branch was thoroughly washed in distilled deionized water (DDI) to remove any particles that may have been on the surface of needles and could skew results of analysis. Branches were then handled with gloves and cut into parts to separate needle growth by year. The main focus was to cut at the first year node often easily recognizable due to color changes between 1st year and 2nd year needles (Figure 3, Appendix I). Each sample consisted of needles from two to three twigs based on how many twigs were available from new growth. Once separated by year, needles were placed in open top Teflon vials and dried in the oven at 60°C overnight. Once dry, needles were easily separated from the twigs by a pair of tweezers and stored in Teflon vials at room temperature until analysis. Balsam fir needles were also processed according to the procedures above.

The three different species of lichen collected are all commonly found on black spruce trees. In most cases, the different lichen species were combined if not enough of one kind could be collected from one tree. Lichen was separated from tree branches and care was taken not to include any bark in the sample. They were then dried in the oven overnight at 60°C. To homogenize the sample due to different species being grouped together, the samples were finely ground under liquid nitrogen with a mortar and pestle. After this they were stored in Teflon vials at room temperature until analysis.

2.3 Laboratory Analysis

Samples were analyzed for total mercury (THg) by the double gold amalgamation method (Bloom and Crecelius 1983) using a Brooks Rand Model III cold vapor atomic fluorescence spectroscopy (CVAFS) analyzer via US EPA method 1631. Mercury Guru 2.0 software was used for mercury peak integration. All analyses were conducted

between January and November of 2014. Approximately 0.10-0.20 grams of needle sample was digested with 5 mL of concentrated nitric acid (HNO_3) in an acid clean Teflon vessel at 70°C overnight. As outlined in US EPA method 1631, 1 mL of digested sample was added to a bubbler, reduced by addition of 0.5 mL of stannous chloride ($SnCl_2$) (reduction of Hg^{2+} to volatile Hg^0) and bubbled for 21 minutes with high purity nitrogen gas. Reduced Hg^0 passes through a soda lime trap which absorbs any moisture and acid fumes that may harm the gold sample trap. The gaseous mercury is then captured by a conditioned (standardized) gold sample trap, which after 21 minutes is transferred to the analytical apparatus. The gold sample trap is heated by a coil to 400-500°C while under a constant stream of ultra-pure argon gas. This allows the mercury to be released from the trap and carried via argon to the analytical gold trap. The analytical trap is subsequently heated and the released mercury carried by argon to the CVAFS analyzer. The fluorescence of mercury atoms is detected by a photomultiplier tube and translated into a peak on Mercury Guru 2.0 software. Similarly, approximately 0.20-0.30 grams of lichen sample was digested in 15 mL of concentrated nitric acid and digested in the oven overnight at 70°C. After digestion samples were diluted with DDI water by a factor of 5. 1 mL of the dilution was then analyzed according to the method outlined above.

Bubbler blanks and a standard curve were completed prior to each day of analysis. Bubbler blanks ensured the cleanliness of DDI, acid, carrier gases (pre-cleaned by gold coated scrubber traps) and performance of sample gold traps. A matrix standard curve with eight mercury concentrations (1.6, 0.8, 0.4, 0.2, 0, 0.2, 0.4 and 0.8 ng mL^{-1}) was performed after bubbler blanks to ensure consistent performance of sample gold traps and

analyzer; R^2 higher than 0.995 had to be achieved before any sample analysis could proceed. The working mercury standard used for the development of the standard curve was diluted from TraceCERT Fluka mercury standard (concentration 1001 mg L^{-1} ± 3 mg L^{-1} of Hg).

As outlined in US EPA method 1631, cleanroom techniques and procedures were carried out whenever samples were being handled, digested and analyzed. In addition, all reagents used during sample digestion and analysis were periodically analyzed, remade and purged of Hg to prevent contamination.

Numerous quality assurance and quality control (QA/QC) measures were taken according to US EPA method 1631 including analytical blanks, digestion blanks, analytical standards, sample duplicates, digestion duplicates, matrix spikes and use of National Institute of Standards and Testing (NIST) reference material 2976, freeze-dried mussel tissue. Analytical blanks, standards and duplicates were run approximately every 15-20 samples while matrix spikes and standard reference material (SRM) 2976 were run once per day. Digestion blanks averaged 1-2 per run/day. Overall, blank performance was excellent with a mean of 0.0058 ng mL^{-1} ± 0.0146 ng mL^{-1} giving a final detection limit of 0.0241 ng mL^{-1}. For additional QA/QC statistics please refer to Table 2. All QA/QC recoveries were well within acceptable values.

	Analytical Duplicates	Digestion Duplicates	Analytical Standards	NIST SRM 2976	Matrix Spikes
Count	177	108	176	55	55
Mean	100.3%	101.4%	100.9%	103.7%	99.8%
%RSD	6.9%	10.0%	6.1%	9.9%	9.7%

Table 2. Summary of QA/QC recovery statistics.

The number of needle samples analyzed for each site depended on the overall size and growth of the branches and the ability to distinguish one year old needles from older growth. I analyzed more than 50 samples of one year old needles for every site with the exception of the Alaska sites where I analyzed 46 per site (Table 3). The highest number of samples (103) was analyzed for site CA_AP located in the Avalon Peninsula of Newfoundland. The total number of one year old black spruce needle samples analyzed across all sites is 1,161.

2.4 Statistical Analysis

Statistical analyses were performed within Excel since the bulk of the analyses involved two-sample t-test calculations assuming unequal variance along with rudimentary calculations of mean, standard deviation, etc. Alpha (α) for all t-test calculations was 0.05. Two-sample t-tests were performed to assess within tree, between tree and site to site variability.

3. Results

3.1 Overview: All Sites

Means of THg concentrations were determined for each tree and each site (Table 3). The lowest overall site means are in British Columbia site CA_BC with 7.31 ± 1.83 ng g^{-1} THg, site CA_NF1 with 7.66 ± 1.52 ng g^{-1} THg and site ME near Alton, Maine with 7.89 ± 1.02 ng g^{-1} THg. On the other hand, the highest site average is for a site in Newfoundland CA_NF with 28.49 ± 9.36 ng g^{-1} of THg, which is almost 4 times higher than the lowest observed averages at sites ME and CA_NF1. Similarly, the lowest standard deviation is in the Maine site and the highest in the Newfoundland site CA_NF. The rest of the site averages range between 8 and 23 ng g^{-1} THg.

While an attempt was made to get a representative spread of samples across North America, we were unable to get samples from the Canadian provinces of Saskatchewan, Manitoba or Quebec (although site CA_ON is very close to the Quebec border) due to harsh winter conditions and the reliance on external help for sample collections. Winter sampling can be difficult to execute due to cold temperatures and difficulty in accessing sites that are far from roads and under heavy snow cover. These factors affecting sample collection resulted in an uneven distribution of sites with more sites located in the eastern and central portion of the black spruce native range and only 4 sites in the western portion of the range.

	Black Spruce			Lichen			Balsam Fir		
Site	Count	Range ng g^{-1}	$\bar{x}$ ± SD ng g^{-1}	Count	Range ng g^{-1}	$\bar{x}$ ± SD ng g^{-1}	Count	Range ng g^{-1}	$\bar{x}$ ± SD ng g^{-1}
MN_1FEN	66	8.24 - 29.61	15.29 ± 5.55	NA	NA	NA	NA	NA	NA
MN_2FEN	50	10.55 - 18.26	14.62 ± 2.05	NA	NA	NA	NA	NA	NA
MN_S3FEN	50	16.86 - 36.03	23.59 ± 4.39	2	187.92 - 226.56	207.24 ± 27.32	NA	NA	NA
MN_S1	59	8.43 - 14.84	10.74 ± 1.48	5	107.78 - 149.79	133.44 ± 17.62	NA	NA	NA
MN_S6	50	12.76 - 24.86	17.55 ± 3.09	NA	NA	NA	NA	NA	NA
WI	50	10.22 - 26.07	16.90 ± 3.36	NA	NA	NA	10	12.76 - 21.48	18.29 ± 2.24
MI_FEN	57	8.70 - 16.45	11.99 ± 2.31	NA	NA	NA	20	8.07 - 17.68	14.30 ± 2.27
VT	75	6.03 - 19.98	12.41 ± 2.93	8	91.73 - 209.83	157.63 ± 37.23	NA	NA	NA
ME	52	5.78 - 10.36	7.89 ± 1.02	7	44.69 - 186.71	118.91 ± 47.01	NA	NA	NA
AK1	46	6.84 - 12.54	9.27 ± 1.51	4	195.46 - 203.57	200.05 ± 3.77	NA	NA	NA
AK2	46	6.61 - 12.47	8.83 ±1.26	NA	NA	NA	NA	NA	NA
CA_NF	57	13.64 - 52.22	28.49 ± 9.36	7	161.33 - 456.66	289.96 ± 117.51	NA	NA	NA
CA_NF1	86	4.48 - 10.84	7.66 ± 1.52	NA	NA	NA	NA	NA	NA
NF_BER	51	10.06 - 18.54	13.50 ± 1.75	6	188.97 - 385.39	316.11 ± 76.01	NA	NA	NA
CA_AP	103	7.34 - 25.62	13.87 ± 3.03	8	81.31 - 183.48	141.82 ± 33.55	NA	NA	NA
CA_ON	78	6.03 - 16.78	10.13 ±2.34	NA	NA	NA	NA	NA	NA
CA_ON1	53	4.29 - 15.24	8.57 ± 1.94	12	147.27 - 276.36	210.05 ± 31.02	NA	NA	NA
CA_AL	79	5.98 - 13.77	8.51 ± 1.25	7	131.23 - 174.69	154.64 ± 15.25	NA	NA	NA
CA_BC	53	5.48 - 13.15	7.31 ± 1.83	5	174.17 - 249.62	205.51 ± 27.77	NA	NA	NA

Table 3. Site breakdowns for amounts of black spruce, balsam fir and lichen samples collected. Also showing the range of values from each site and overall site mean ($\bar{x}$) of THg concentrations in ng g^{-1} ± standard deviation. NA signifies that that particular type of sample was not collected at that site.

3.2 Within Tree Variability: Branch to Branch Comparisons

Within tree variability of THg concentrations was assessed for six sites (Table 4) where enough one year old needles were collected from a single branch to warrant a comparison to another branch on the same tree. This was largely influenced by needle availability and size of one year old needles. Two of these sites (VT & CA_NF1) had only one comparison between two branches. For site MN_1FEN within tree variability was assessed for three branches on Tree1 and four branches on Tree5. For site MN_S1 which is the S1 bog at the Marcell Experimental Forest (MEF), six branches on Tree2 and two branches on Tree4 were compared. For the two Newfoundland sites in this batch, site NF_BER had three branches on Tree1 and four branched on Tree2, and site CA_NF four branches on Tree3 compared.

Tree IDs do not hold any special significance and were assigned according to the order in which the trees were processed. Similarly branch IDs (A, B, C, etc.) were assigned sequentially as they were processed. For most of the sites there is no significant ($p > 0.05$) variability within trees (Table 4.1-4.6, Appendix I). Small significant variability can be seen on site MN_1FEN Tree5 between branch A and D with a p value of 0.0384 (Table 4.1, Appendix I). Similarly, S1 bog from the MEF for the most part has no significant variability with the exception of the comparison of Tree2 branches C and F and Tree4 branches A and B with p values of 0.0199 and 0.0183, respectively (Table 4.2, Appendix I). The two Newfoundland sites chosen for within tree variability calculations have a higher percentage of comparisons which turned out to be significant (Table 4). The possible cause of this will be discussed later. All comparisons for site NF_BER Tree1 were significant while only one was significant for Tree2 at that same site (Table

4.5, Appendix I). For site CA_NF, which is the site with the highest THg concentrations, all comparisons are significant except for one (Table 4.6, Appendix I). It is important to keep in mind that the sample sizes for most of these calculations were quite small as it is difficult to get a large number of one year old needle sections from a single branch.

Site	Number of Comparisons	How Many Significant?
MN_1FEN	9	1
MN_S1	16	2
VT	1	0
CA_NF1	1	0
NF_BER	9	4
CA_NF	6	5

Table 4. Summary of sites with within tree variability signifying how many comparisons were significantly different based on a two-sample t-test with alpha (α) of 0.05.

3.3 Within Site Variability: Tree to Tree Comparisons

Tree to tree variability is greater than within tree variability; refer to tables 5.1-5.19 and figures 10.1 – 10.19 in the Appendix I. For most sites, tree to tree comparisons show significant differences with the exception of a few trees in each site. For example, for site MN_S1 4 trees were sampled and compared to each other with a total of 6 comparisons. Out of these, 3 were not significantly different and 3 were (Table 5.4 and Figure 10.4, Appendix I). For site CA_AL with 5 trees so total of 10 comparisons, only 4 comparisons were significantly different (Table 5.18 and Figure 10.18, Appendix I). Site CA_ON1 also had only 4 comparisons that were significantly different out of 10 (Table 5.17 and Figure 10.17, Appendix I), while site MI_FEN had 9 out of 10 comparisons significantly different (Table 5.7 and Figure 10.7, Appendix I). The Alaska sites were the most interesting out of the entire group. At both sites 5 trees were sampled and analyzed. Site AK1 had no significant differences between trees while site AK2 had only one

significant difference and that is between Tree1 and Tree3 with p value of 0.0101 (Table 5.10/Figure 10.10 and Table 5.11/Figure 10.11, Appendix I). Black spruce needles from these two sites show the lowest variability out of all the other sites with a low mean site THg concentration of 9.27 ng g^{-1} for site AK1 and 8.83 ng g^{-1} for site AK2 (Table 3). Standard deviations were also low for the two sites, 1.51 for AK1 and 1.26 for AK2. Site NF_BER had the lowest number of comparisons (3, 2 of them significant) since only 3 trees were analyzed for this site (Table 5.14 and Figure 10.14, Appendix I). The highest number of comparisons (21, 12 of which are significant) were made for site CA_ON where a total of 7 trees was analyzed (Table 5.16 and Figure 10.16, Appendix I).

For sites WI and MI_FEN, where balsam fir was also collected, comparisons were made between balsam fir needles and black spruce needles. At the Wisconsin site, needle samples (n=10) from one balsam fir tree were compared to 5 black spruce trees. 3 of the 5 comparisons were significantly different with p values of 0.0240, 3.82E-05, 0.0027. These values are comparable to the variability observed between black spruce trees. At the Michigan site, two balsam fir trees were sampled (n=10 for each tree) but no significant variability was detected between them ($p = 0.9362$) so they were grouped together for comparisons between black spruce trees. Again the balsam fir needles were compared to needle samples of 5 different black spruce trees with 3 of the comparisons showing significant difference (p values of 3.59E-05, 1.05E-07, 5.47E-08) in THg concentrations. At both the Wisconsin and Michigan sites, the mean THg concentrations of balsam fir needles were higher than black spruce needles, but it is important to keep in mind that the number of samples of balsam fir needles was considerably lower than black spruce samples (Table 3). However, if we consider each black spruce tree within a site

individually at the Wisconsin site, for example, Tree3 had a comparable mean of THg concentrations to the balsam fir needles, 18.70 ng g^{-1} and 18.29 ng g^{-1}, respectively.

3.4 Site to Site Variability

As would be expected the differences in needle Hg concentrations are even more pronounced when site to site comparisons are made. 55 comparisons were made between all U.S. sites out of which only 5 were not significantly different (Table 6 and Figure 11, Appendix I). There was no significant difference between sites MN_1FEN and MN_2FEN; MN_1FEN and WI; MN_S6 and WI; MI_FEN and VT; and AK1 and AK2. The largest significant differences are observed in comparisons of sites AK1, AK2 and ME to the rest of the U.S. sites. This makes sense considering that these 3 sites had some of the lowest mean THg concentrations out of all of the U.S. sites (Table 3). 28 total comparisons were made between the Canadian sites with only 3 comparisons showing no significant difference in THg concentrations (Table 7 and Figure 12, Appendix I). The comparisons which showed no significant difference were between sites CA_NF1 and CA_BC; NF_BER and CA_AP; and CA_ON1 and CA_AL. There seems to be no distinct pattern in the rest of the comparisons, some differences are more pronounced than others. 88 comparisons were made between the U.S. and Canadian sites 6 of which were not significantly different (MN_1FEN, MN_2FEN and CA_AP; MN_S1 and CA_ON; ME, CA_NF1, AK2 and CA_ON1; and AK2 and CA_AL) (Table 8 and Figure 13, Appendix I). Again certain differences are more pronounced with the largest between site MN_2FEN and CA_BC with p value of 9.80E-35.

3.5 Lichen THg concentrations

Lichen THg concentrations were assessed for 11 sites, the means of the concentrations can be seen in Table 3. The lowest mean lichen THg concentration is at site ME with 118.91 ± 47.01 ng g^{-1} which is again one of the sites with the lowest mean THg needle concentrations. Lichens collected from the S1 bog at MEF were also rather low in Hg with a mean concentration of 133.44 ± 17.62 ng g^{-1}. The highest lichen mean THg concentrations are at sites NF_BER and CA_NF with 316.11 ± 76.01 ng g^{-1} and 289.96 ± 117.51 ng g^{-1}, respectively. The standard deviations for both of these sites are quite high and they are the highest out of all the other sites where lichen was collected. Site CA_NF has the highest mean THg needle concentration out of all the sites while site NF_BER has mean needle THg concentration comparable to many of the other sites in the study.

4. Discussion

4.1 Variability at multiple scales

Overall, within tree variability is smaller than tree to tree variability, which is smaller than site to site variability (i.e. within tree variability < between tree variability < site to site variability). Within tree variability is virtually nonexistent except for site CA_NF which shows pronounced variability even in needles that came from the same tree. This variability is most likely related to this site having the highest THg concentrations with the highest standard deviation. Some of this variability may be due to variations in needle collection and processing, although it is unlikely that this would warrant such high variability. The more likely explanation would be that there might be a local emission source of atmospheric Hg leading to elevated concentrations in the needles

as well as lichen. Due to the large number of samples in this study it was unrealistic to do any additional sampling. But it is not expected that most sites would show much if any within tree variability unless the site was heavily polluted. For the most part, variability present within trees is not of concern.

Tree to tree variability is more pronounced and therefore warrants more consideration than within tree variability. The discussion of tree to tree variability can be organized around a few hypotheses including sulfur status of the needles and its effect on retention/oxidation of mercury, and possibly the overall nutritional status and vigor of the trees. In addition, tree to tree variability is likely influenced by a variety of factors such as proximity of sampled trees to one another, consistency in sample collection (ensuring all branches are collected roughly from the same locations on different trees), any unusual site conditions, and sample processing in the lab. In many instances, it can be difficult to find a good number of same size trees with enough needle growth for sampling especially in very nutrient poor areas such as bogs. The conditions of the peatland itself are also important as that can further add to any observed variability in Hg concentrations. For example, needle availability on trees from the S1 bog was rather limited because the trees were quite scraggly (Figure 4, Appendix I). This makes it difficult to get enough one year old needles from just a few branches. Mean THg concentrations of trees within a site can be very similar as is the case for trees from the S1 bog (Figure 10.4, Appendix I), both of the Alaska sites (Figure 10.10 and 10.11, Appendix I), and the Maine site (Figure 10.9, Appendix I). Or there can be quite a difference in means from tree to tree as is the case for sites CA_NF (Figure 10.12, Appendix I), WI (Figure 10.6, Appendix I), MN_S3FEN (Figure 10.3, Appendix I) and MN_S6 (Figure 10.5, Appendix I).

The three MEF sites are within 2 km of each other, there are no known point sources of Hg emissions nearby, and the atmospheric Hg concentrations they are exposed to are probably very similar. Despite of this, two sites from MEF both had higher THg concentrations than the S1 bog. The S3 fen had the highest which is probably due to more nutrients being present in the fen. The higher THg concentrations observed in S6 were interesting to see since this a more nutrient poor area than the S3 fen. However, the needles collected on S6 did look more vigorous than needles collected in S1 (Figure 4, Appendix I). Past research conducted on the S6 bog may also help to shed some light on the higher Hg concentrations. In 2002, Jeremiason et al. (2006) added sulfate to half of the S6 peatland to assess whether this would increase methylmercury production. Sulfate was added via a sprinkler system to the southeastern or experimental portion of the wetland with the northern portion used as a control. This resulted in the addition of a nutrient that was previously not present in very large amounts and was now available for uptake by trees. Considering that mercury has a very high affinity for thiols and reduced sulfur groups (Xia et al. 1999; Hesterberg et al. 2001; Skyllberg et al. 2003), the addition of sulfate could have resulted in greater mercury complexation. A recent study by Wang et al. (2012) has confirmed that the majority of mercury found in leaf tissue of *Brassica juncea* was bound to sulfur. The collection of needles from the S6, which more closely resembles a poor fen, was done in the portion that had previously received these sulfate inputs.

Recently (March 2015), we collected a few additional samples from the S6 peatland in and outside the area of sulfate addition to test this hypothesis. In general, the needles from S6 still look more vigorous than S1 needles regardless of which part of the

bog they came from. The samples were analyzed for sulfur on an Elementar Vario EL analyzer at the University of Minnesota. The needles collected within the sulfate addition of the bog had slightly higher %sulfur values, the mean of a total of 6 samples analyzed was 0.123 %S. The mean of a total of 3 samples analyzed from outside of the sulfate addition was 0.105 %S. While there is a slight difference between the sulfur contents of the two sets of needles, due to the small number of samples analyzed nothing conclusive can be inferred from these results. Additionally, the sulfate that was added in 2006 would most likely not have any effects on the nutrient status of the trees almost a decade later. Despite these findings, the sulfate status of trees may be an interesting area of study for future research questions. The more likely explanation for the elevated mercury levels in the S6 peatland are most likely related to its upland/peatland transision zone- the lagg. The S6 peatland has a large lagg, which makes it slightly richer in nutrients than S1, which has a small lagg. This makes S6 more of a poor fen than a bog and its overall site mean THg concentration therefore appropriately falls between those of the S3 fen and the S1 bog.

The rest of the fen sites in the U.S. had variable THg concentrations which again are most likely due to better growth of trees in nutrient rich areas. The variability of means in trees of the Wisconsin site could be due to sampling location. The black spruce was collected from the edge of the bog due to difficulty of accessing the interior of the bog. It is likely that the collection was made from the lagg rather than the actual bog. A greater amount of nutrients in the lagg could have contributed to the trees growing a little better and therefore having higher THg concentrations.

Interestingly, the two sites with virtually no variability between trees or in site to site comparisons are both in Alaska. This could be due to a shorter growing season in this part of the world leading to less atmospheric mercury being accumulated within needles. Trees with lower overall Hg concentrations tend to show less variability than trees with higher concentrations. It seems that the longer and better these trees grow the more likely it is that there will be greater variability among them. Overall, Alaska is also a more pristine environment than some of the other site locations.

Site CA_ON1, southeast of Lake Nipigon, also appears to be in a fairly pristine area with no development in its vicinity, which is reflected in its overall low THg concentration of 8.57 ng g^{-1}. Site CA_ON close to the border of the Québec province is not much higher in its mean THg concentration with 10.13 ng g^{-1}. Again both of the Ontario sites are not close to any significant human development which seems to be reflected in the Hg concentrations of needles collected from these sites.

Site CA_NF is located near Stephenville Crossing in Newfoundland and Labrador. An open pit gypsum quarry is located in Flat Bay less than 15 km southwest of the site. Although the open pit mine is inactive at the moment, I was informed by a local research silviculturalist that the gypsum has elevated levels of mercury which might be a potential source of atmospheric mercury, especially considering that site CA_NF receives strong winds from the south (Cyril Lundrigan, personal communication, Feb 20, 2015). Gypsum is also a sulfate mineral so it could serve as a potential source of sulfate for trees in this area relating to my sulfate/mercury hypothesis above. Another factor that points to a likely presence of a local source of atmospheric mercury is that the two other sites on the Island of Newfoundland (NF_BER and CA_AP) were considerably lower in their

THg concentrations and not significantly different ($p > 0.05$). The last site (CA_NF1) in this province located on mainland of Labrador on the edge of Lake Melville had comparable THg concentrations to site ME, AK1, AK2 and MN_S1 all of which are on the low end of the spectrum. This site also looks quite pristine with no significant development in its vicinity except a small town of less than 600 people towards the southeast.

As is expected, the highest variability is observed site to site with high variability also present from tree to tree in sites with higher THg concentrations probably due to sampling taking place in fens or close to human developments and possible point sources of atmospheric mercury emissions.

Balsam fir needles seem to respond similarly to black spruce, although at both of the sites from which balsam fir was collected, the mean THg concentrations were higher than those of black spruce. Two sample t-test calculations showed that there was no significant difference between the black spruce and balsam fir needles from the WI site ($p = 0.1429$) while there was a significant difference at the Michigan site ($p = 0.0006$). The sample size of balsam fir from both sites was quite small so drawing major conclusions from these data would probably be unjustifiable. However, the data do point to the possibility of using balsam fir in future studies perhaps in comparison to black spruce at sites that have more nutrients and can support both black spruce and balsam fir growth. Looking at the range of THg concentrations in these samples (Table 3) does show similarities between black spruce and balsam fir needles.

4.2 Overall Trends

The discussion of the overall trends is centered around the premise of a west-to-east increasing trend in atmospheric Hg concentrations due to increasing population and industrial point sources of Hg emissions. Figures 5-9 in Appendix I show the overall trends in the data. As can be seen in figure 5, sites located in the western part of the black spruce native range are all relatively low in terms of their site mean THg concentrations. All of these sites with the exception of AK1 are in relatively pristine areas with no major development in their vicinities. Site AK1 is near Fairbanks but the close proximity to human development does not seem to contribute to any substantial variability in THg needle concentrations or the overall site average. The eastern sites show a bit more variability moving from site to site (explained in previous section). The main site to focus on is site CA_NF, which is close to a gypsum mine that could potentially contribute directly to atmospheric mercury or possibly through inputs of sulfate to the surrounding environment. The central sites (excluding Minnesota) do not show a very large spread in site means although the Wisconsin site is higher than all of the others. As was discussed above, this is likely due to the difficulty we experienced in accessing the bog and the collection of needles from trees on the lagg/upland transition. Variations in THg concentrations of the Minnesota sites have been explained in the previous section. Overall, the sites in the western part of the black spruce range generally show lower THg concentrations than sites in the central and eastern parts of the range. Historically, mercury emissions have been larger in the eastern and central U.S. due to the presence of more coal burning power plants and other human developments. This seems to agree with the trends observed here.

4.3 Lichen Data

Epiphytic lichens have been used as biomonitors of atmospheric pollution for some time now (Lodenius 2013 and references therein). Numerous studies have used lichens to assess atmospheric Hg pollution near point sources but also to assess background levels of Hg in different lichen species (Bargagli and Barghigiani 1991; Bennett and Wetmore 1997; Makholm and Bennett 1998; Sensen and Richardson 2002; Estrade et al. 2010; Blum et al. 2012). The THg contents of lichens collected for this study were all fairly close to natural background levels, which in more pristine areas, do not tend to exceed 250 ng g^{-1}. However, this number is also dependent on the species collected and sampling location. For example, for two sites in a study conducted in Italy Hg lichen concentrations did not exceed 200 ng g^{-1} (Bargagli and Barghigiani 1991). While a study conducted by Makholm and Bennett (1998) reported a background level of 155 ng g^{-1} from a control site in northern Wisconsin. A more recent study by Blum et al. (2012) sampled lichens near the tar sands of Alberta most of which again did not exceed 200 ng g^{-1} of Hg.

For this study, 2 out of 11 sites (CA_NF & NF_BER) seem to have slightly elevated levels of Hg in lichen. Site NF_BER has elevated levels with an overall site mean Hg lichen concentration of 316.11 ng g^{-1} with a higher standard deviation than most of the other sites- 76.01 ng g^{-1} (Table 3). It was not surprising to see elevated levels on site CA_NF since this is the site with the highest mean THg concentration in needles. And again as is the case for needles the standard deviation was highest for lichens sampled at this site. This further points to a possible local source of atmospheric mercury that was discussed in the previous section. Figure 14 in Appendix I shows a regression

analysis between the means of black spruce needles and the means of lichen samples for the sites where both lichen and needles were collected. While the relationship is not very strong (R^2= 0.26) a general trend can be observed where a higher THg needle concentration seems to correspond to higher lichen THg concentration especially for site CA_NF. Most of the sites remain below the 250 ng g^{-1} of Hg line. However, as with black spruce, some variability is still present. Some of this variability may be because different lichen species were combined during sample processing to ensure a sufficient volume for analysis. A study of four different lichen species collected across a transect from the International Falls to Voyageurs National Park in Minnesota showed that there is variability in Hg content of different species; however, none of them exceeded 250 ng g^{-1} (Bennett and Wetmore 1997). Combining different species can undoubtedly skew results, but it is most likely not very significant when dealing with background levels which is the case for most of the sites in this study. Lichens also passively collect pollutants out of the atmosphere throughout the year while for the spruce needles I only focused on the uptake from the previous growing season. In this way their direct comparison may not be the best approach and should perhaps be considered separately in their ability to monitor atmospheric pollution.

4.4 Black Spruce as a Passive Monitor

Considering the results of this study, black spruce could potentially be used to monitor atmospheric mercury in sensitive ecosystems such as peatlands. However, due to the presence of significant variability from tree to tree on almost all sites, sampling should most likely take place from a larger number of trees to account for the variability observed between trees. This is especially recommended for sites that have more

nutrients such as fens or transitional areas between the upland and peatland. It is also very important to consider site conditions when deciding whether or not black spruce should serve as a biomonitor. Sites with better tree growth will have more nutrients available and may allow trees to bind more mercury especially if sulfate is present- although this is still just a hypothesis. Impacts of local sources of mercury also play a role. This is likely the case for site CA_NF where higher THg concentrations were observed and possibly confounded by the potential sulfate additions from gypsum. However, the range of concentrations on this site was also considerably larger than for the rest of the sites (Table 3). This suggests that variability increases with higher Hg concentrations.

The objective of this study however, was to see whether black spruce could be used to passively monitor atmospheric mercury possibly also under climate change conditions. Climate change is a gradual process. If increasing temperatures do lead to greater organic matter decomposition, the release of mercury from decomposition but also from greater volatilization should also be gradual. It should be possible to see gradual increases in Hg content of new growth. However, this is a little bit more challenging with black spruce needles as black spruce tends to have a large portion of orphaned material, or parts of needle growth that grew one year but did not sprout any new growth in subsequent years (Figure 3, Appendix I), when compared to other conifers (Bernier et al. 2007). Consequently, focusing on 1 year old needles is the best approach as it often becomes hard to separate older growth by years. It has also been shown that photosynthesis becomes enhanced under elevated atmospheric CO_2 conditions meaning this may lead to greater mercury uptake (Curtis 1996). However, most of the studies that investigated tree response under elevated CO_2 did not allow for interactions

with other natural stressors such as atmospheric pollutants or soil moisture so it is still largely unclear how the natural environment would respond to elevated CO_2 levels (Karnosky 2003). This is where a study like SPRUCE, a more sophisticated approach to studying the effects of climate change on natural ecosystems than previous studies, can benefit from a relatively simple approach to monitoring atmospheric mercury.

4.5 Limitations of the Study

Many of the limitations of this study are related to sampling locations and sample collection and processing. As can be seen from the variability of data from peatlands at the MEF, even peatlands that are located close to each other can have very different Hg needle concentrations. As previously discussed, I am assuming this to be mainly due to the amount of nutrients present and the overall vigor of the trees. This is important to keep in mind when choosing sample locations. Sample collections may have also introduced some variability as numerous individuals were involved in the collection of needles. There is always some inherent variations in the way protocols are interpreted and executed. Likewise, sample processing was conducted by a number individuals and with the high tendency of black spruce to produce orphaned material it was at times unclear which needles belonged to which year of growth (although first year growth was always easiest to identify). Considering the tree to tree and site to site variability, black spruce would most likely not serve well as a biomonitor of atmospheric mercury on a national scale.

5. Conclusions

This study looked at the possibility of using black spruce needles as a passive monitor of atmospheric mercury mainly to monitor vulnerable ecosystems such as

peatlands. The data from 19 sites from all over North America helped to provide a more complete picture of the mercury content of black spruce needles in different environments and locations. As would be expected and was confirmed by this study, the variability in needles collected from the same tree is very low. I did, however, find considerable variability in certain tree to tree comparisons on the same site. This points to the inherent natural variation in tree growth and how much stomatal uptake of atmospheric mercury could vary between two trees in the same area. This also suggests that monitoring efforts should most likely focus on sampling from a greater number of trees to account for the observed variability. As was expected, site to site variability was even more pronounced. The least variability, with respect to tree-to-tree and site-to-site comparisons, was observed at only two sites, both of which are in Alaska. Alaska has less human development than many of the other sites in the study and a shorter growing season which may lead to less tree growth and subsequent uptake of mercury.

Needles from 3 sites at the Marcell Experimental Forest show how variable mercury content can be presumably based on the nutrient availability of the peatlands. The 3 peatlands are all located within 2 km of each other and yet the mercury content of needles from S3 was twice as high as that of needles from S1. Since S3 is a fen and S1 a bog, this suggests that the higher nutrient availability in S3 not only allows black spruce to grow better than it does in S1, but may also allow it to take up and retain more atmospheric mercury. As discussed earlier, needles from S6 have Hg concentrations in between those of S1 and S3, which is likely because S6 is more of a poor fen than a bog therefore falling between the THg concentrations of the S3 fen and S1 bog. In light of these findings, using black spruce to monitor Hg dynamics in peatlands should, therefore,

be preceded by careful examination of the peatland conditions and how these may affect the vitality of the trees and their ability to uptake Hg.

With the possible exception of site CA_NF, we did not come upon any sites that seemed to be contaminated. That was confirmed by lichen mercury concentrations which were all close to the various background levels determined by other studies mentioned earlier. Lichens will continue to be good biomonitors of atmospheric pollution. On the other hand, conifer needles used for monitoring have the advantage that they are relatively easy to collect and analyze and can provide Hg concentrations from year to year. Black spruce was chosen for this study due to its abundance even in nutrient poor peatlands, but balsam fir seems to also provide a good snapshot of Hg uptake in first year needles and seems to have Hg contents similar to black spruce. However, black spruce would most likely not serve well as a biomonitor as it seems to be easily influenced by local conditions such as nutrient availability and local sources of atmospheric Hg (as on site CA_NF).

Overall, the relative inexpensive act of needle collection and analysis does make this type of monitoring more attractive when compared to more expensive direct monitoring techniques; however, it does have its own caveats as explored and discussed in this study. It can also provide important information on how trees respond and possibly change over time with respect to atmospheric Hg uptake. Regardless of the findings presented here, it will remain important to study vegetation for its ability to take up atmospheric mercury as it plays a crucial role in the biogeochemical cycling of mercury in the environment.

Chapter 2

Impacts of invasive earthworms on the biogeochemical cycle of mercury in soils: Two mass balance approaches to an earthworm invasion in a Northern Minnesota forest

1. Introduction

1.1 Soil Mercury Overview

The second chapter of this thesis explores another component of the mercury cycle- mercury in soil and the impacts of exotic earthworms on its cycling. Mercury in soils originates from three main sources- the atmosphere, natural degassing of the crust and weathering of rocks. The deeper soil horizons are the ones most influenced by mercury as a result of crustal degassing and weathering processes. Surface soil receives most of its mercury from the atmosphere in the form of wet and dry deposition (St. Louis et al. 2001). Forested ecosystems can substantially increase Hg deposition to soil through throughfall and litterfall (Kolka et al. 2001). Deciduous forest systems contribute substantial amounts of mercury via litterfall predominantly at the end of the growing season via leaf senescence. Evergreen forest systems shed needles and leaves continuously at slow rates throughout the year. Litterfall, mainly in the form of leaves, is therefore an important component of the mercury cycle. A study conducted in the Brazilian rainforest found that 50-84% of litter mass was composed predominantly of leaves (Silva-Filho et al. 2006). In this way trees act as an important intermediary in the transfer of atmospheric Hg to soil.

Mercury deposited to soil behaves in two ways. Freshly deposited elemental (Hg^0) mercury has a tendency to preferentially revolatilize, a mechanism named prompt recycling (Selin et al. 2008). The mercury that remains in surface soil is predominantly in ionic forms (Hg^{2+}, Hg_2^{2+}) and mostly bound to humic and fulvic substances (Andersson 1979; Gabriel & Williamson 2004). Mercury has a high affinity for organic matter where it binds strongly with reduced sulfur groups (Skyllberg et al. 2003). Schuster's (1991)

review of mercury behavior in the soil highlights mercury's strong tendency to build complexes with Cl^-, OH^-, S^{2-}, S-containing functional groups of organic ligands, and NH_3 because of their high abundance and stability with mercury. The most important inorganic sorbents of mercury are clay minerals, amorphous oxides, hydroxides, oxyhydroxides of Fe, Mn and Al and amorphous FeS under reducing conditions (Gabriel & Williamson, 2004). pH also plays an important role in mercury adsorption in soil. Studies performed to assess the effects of pH on mercury adsorption showed that in acidic conditions mercury most readily adsorbs to organic substances, while in neutral to alkaline soil conditions mineral components may become more effective sorbents of Hg^{2+} (Andersson, 1979; Schuster, 1991). Mercury's high affinity for organic matter makes it abundant in forest floor and the upper soil layers, which is where most of the mercury derived from atmospheric deposition is found.

1.2 Bioturbation: Emphasis on earthworms

The upper layers of the soil are subject to various physical disturbance mechanisms which affect chemical weathering rates and the cycling of inorganic nutrients and other elements. Bioturbation, the disturbance of soil and sediments by organisms, is one of the most common physical disturbance mechanisms and has been shown to play a critical role in vertically transporting soil minerals and other elements particularly in temperate and tropical environments (Hole 1981; Johnson et al. 2005). Some of the most important bioturbators include ants, termites, earthworms and small fossorial mammals, which physically disturb soil by burrowing for food and shelter (Hole 1981; Schaetzl and Anderson 2005). Earthworms are considered to be the most prominent soil bioturbators (Hendrix and Bohlen 2002) as they occur in virtually every

bioregion on earth and are very effective at moving large quantities of soil (Hendrix et al. 2008; Lee 1985).

Earthworm impacts to soil can become even more pronounced in ecosystems that have developed without them for thousands of years, as is the case for the Northern hardwood forests of the U.S., which have developed without native earthworms since the last glaciation (Bohlen 2004, Hale et al. 2005a, Eisenhauer et al. 2007). Over the past century, these ecosystems have progressively become more and more invaded by exotic European earthworms mainly through their use as fishing bait and through the expansion of agriculture and logging activities (Alban and Berry 1994, Gates 1982). This invasion of non-native organisms into an area that has developed without them for thousands of years can cause significant disturbances to the overall ecosystem.

Earthworms impact soils in numerous ways including alteration of soil physical properties and impacts to the way nutrients and other elements are transported through soil. The majority of earthworm mixing tends to occur in the O (commonly known as forest floor), A and E horizons and upper parts of the B horizon. Most importantly, A horizon thickness tends to increase with the presence of earthworm as they consume the O horizon or forest floor and incorporate organic matter into the immediate horizon below it (Hale et al. 2005b). In general, earthworms tend to decrease soil bulk density through the incorporation of organic matter and the creation of macropores. Additionally, prior to earthworm invasion the soil system is rather heterogeneous but once earthworms invade they homogenize soil materials, thereby reducing soil variability. Such homogenization of the soil system alters elemental cycles which may ultimately result in changes to forest composition and structure (Hale et al. 2005b).

The aim of this study was to assess the impacts of exotic earthworms on the cycling of mercury in the upper layers of the soil. A site in a formerly glaciated hardwood forest in Northern Minnesota was chosen for the study because previous studies at this site show altered elemental biogeochemical cycles due to earthworm invasion (Hale et al. 2005a, Hale et al. 2005b, Hale et al. 2006, Resner et al. 2011; Resner 2013). This previous body of work enabled us to have a better understanding of how earthworms affect the major elemental biogeochemical cycles in the soil such as those of potassium, calcium, magnesium, sodium, phosphorus, carbon, and iron (Resner 2013) while also streamlining our sampling efforts.

Some of the major physical changes observed due to earthworm invasion at this northern Minnesota site include complete loss of the forest floor (O horizon) leading to a subsequent thickening of the A horizon as organic matter is incorporated into upper mineral soil, and changes in soil structure from single grain or fine granular to medium to large granules (Resner 2013). Many of these changes depended upon the particular earthworm ecological group present in the soil. Each ecological group exhibits a unique burrowing tendency which leads to different mixing depths as well as different feeding behaviors (Resner 2013). The three main earthworm ecological groups are anecic species, endogeic species and epigeic species (Table 1). Anecic species burrow deeply into the soil and consume leaf litter while endogeic species mix only within the A horizon and ingest organic matter and mineral material, epigeic species only reside in the litter layer feeding primarily on fungi and bacteria (Frelich et al. 2006; Hale et al. 2007; Hendrix et al. 2008; Resner 2013). Epigeic species tend to invade first followed by endogeic and anecic species at which point the A horizon starts to become thicker.

The most recent research from this transect focused on the effects of earthworms on inorganic nutrients in the soil as well as on soil carbon inventories and organic carbon sorption to mineral surfaces (Lyttle et al. 2014; Resner et al. 2014). Through the use of geochemical normalization techniques, Resner et al. (2014) found that inorganic elements such as Ca, Mg, K and P were enriched in the O horizon prior to invasion but observed almost complete depletions in the heavily invaded areas, which was related to the complete consumption of the forest floor (O horizon) with the arrival of soil mixing earthworm species. Similarly, carbon inventories decreased moving along the transect from least to most invaded and soil mineral surface areas were found to be lower in the A horizon due to the presence of earthworms (Lyttle et al. 2014).

1.3 Geochemical Mass Balance & Normalization Approach

The geochemical mass balance method has been used reliably for some time now to assess elemental mass changes in the soil for a variety of geochemical processes in the earth's surface (Brimhall & Dietrich 1987; Merritts et al. 1992; Riebe et al. 2003; Oh & Richter 2005). Most extensively, it has been used to assess changes in major element chemistry of soil including elements such as Ca, P, K, Mg, Na, Fe, Si and others. Depending on the parent material, most of these elements are present in soils in varying concentrations. Soil weathering and erosional processes affect the concentrations of the major elements in the soil and many studies have utilized the geochemical mass balance to understand how these processes influence the distribution of major elements in soil profiles. However, not until Resner et al. (2014) has this method been used to assess the effects of bioturbation on biogeochemical cycles. The geochemical mass balance has not been as commonly utilized for trace metals found in soil; however, many trace metals

including Pb, Hg, Cu, Cd, Zn, Ni, As, Se and Cr have been studied widely through other techniques. In a study by Jersak et al. (1997), the authors were able to successfully use the geochemical mass balance to study the dynamics of Pb, Cu, Zn, Ni, Co and Cr in three Spodosols of the Northeastern United States, demonstrating that the geochemical mass balance could be used to understand heavy metal distribution in soil. Mercury and lead behave similarly when it comes to their adsorption to organic matter and clay minerals (Evans 1989). Consequently, Hg studies may also benefit from this method.

In this study I utilized the geochemical normalization method to assess fractional and absolute mass changes of mercury in the O and A horizons as this is where most earthworm mixing occurs. With initial invasion the cycling of inorganic elements is impacted and remains so until the soil system reaches a new equilibrium. It is likely that mercury behaves similarly to the inorganic elements examined by Resner et al. (2014) especially considering that mercury is mostly associated with organic matter. Considering that earthworms have the ability to impact and transform biogeochemical cycles of forests that have previously developed without them, it is important to consider how they may be impacting mercury cycling. Most of the mercury taken up by leaves and needles of trees is incorporated into the soil via litterfall. Under worm free conditions, the forest floor (O horizon) tends to be thick and decomposes slowly while also complexing large quantities of mercury. The arrival of invasive earthworms often leads to the complete consumption of the forest floor leaving behind just a small amount of freshly deposited leaf litter. The fate of mercury bound to organic matter in the O horizon following its consumption by earthworms is largely unknown and will be assessed in this study.

1.4 Study Objectives

The overarching objective is to determine what effect earthworms have on the cycling of mercury in forest soils. We will use two mass balance approaches to answer this question. The first approach is based on relatively simple calculations of Hg loadings (mass of Hg per known volume of soil) while the second approach utilizes geochemical normalization using zirconium (Zr, an immobile element) to assess the movement of Hg through the soil profile. These calculations will help us to elucidate the fate of mercury in soils that have been invaded by exotic earthworms as well as determine the relative amount of Hg that is retained in the soil. I hypothesize that earthworms impact the mercury pools of the O and A horizons, which will be determine via the two mass balance approaches. Invasive earthworms feed primarily on organic rich forest floor and mix the remains of those materials into the upper layers of the mineral soil. This is important from a mercury perspective because most of the soil mercury is found in upper soil horizons rich in organic matter.

2. Methods

2.1 Field Site

The field site is located in a sugar maple (*Acer saccharum*) forest in north central Minnesota near Leech Lake (Figure 1 & 2, Appendix II). Additional tree species found in this forest include yellow birch (*Betula alleghaniensis*), paper birch (*Betula papyrifera*), basswood (*Tilia americana*), ironwood (*Ostrya virginiana*) and American elm (*Ulmus americana*) (Hale et al. 2005a). An earthworm invasion transect was established here in 1997 when Hale et al. (2005a; 2005b) conducted their first study on earthworm invasion of forest soils in this area. The transect is located on the east side of Sucker Bay Road.

The construction of the road is thought to be the most likely reason for exotic earthworm invasion in this forest. The most invaded areas are the ones closest to the road with the leading edge of the invasion advancing about 5 meters per year (Resner 2013); therefore, to find uninvaded areas it is necessary to go farther away from the road and deeper into the forest. Earthworm ecological groups and species were identified by both Hale et al. (2005a) and Resner (2013) and can be seen in Table 1.

Ecological group	Taxonomic group	Species
Epigeic	*Dendrobaena*	*Dendrobaena octaedra*, *Dendrodrilus rubidus*
Epi-endogeic	*L. rubellus* (adults)	*Lumbricus rubellus* (adults)
Epi-endogeic/anecic	*L.* juveniles	*Lumbricus* juveniles
Endogeic	*Aporrectodea*	*A. caliginosa*, *A. tuberculata*, *A. trapezoides*, *A. rosea*
Endogeic	*Octolasion*	*Octolasion tyrtaeum*
Anecic	*L. terrestris* (adults)	*Lumbricus terrestris* (adults)

Table 1. Breakdown of all known earthworm species present at the north central Minnesota transect by ecological and taxonomic groups. (Original data from Hale et al. 2005a)

The soil on site is classified as the Warba series which belongs to the taxonomic class of a fine-loamy, mixed, superactive, frigid Haplic Glossudalfs- refer to Appendix III for the official soil series description. Warba soils formed in loamy calcareous glacial till on moraines and typically have a thin (<0.5 m) loess cap. A typical pedon consists of an O, A, E, E/B, B/E, Bt and C horizons. The A and E horizons are typically very fine sandy loams or silt loams while the deeper Bt horizons tend to have more clay and less silt and are classified as clay loams or sandy clay loams. The E horizon tends to extend from the A horizon down to about 35 cm. Below the E horizon is a glossic horizon (E/B or B/E) where the E and Bt horizon materials occupy 15% or more of the horizon. The B/E

horizon ends at a depth of 50 cm followed by Bt horizon material. The Warba soil is extensively found throughout north-central Minnesota and is moderately well to well drained.

2.2 Sampling and Sample Processing

Two sets of soil samples were used in this experiment. The first set of samples were previously collected by Resner (2013) in 2009 as part of her thesis research - (please refer to her thesis for a detailed description of the sampling procedures). Briefly, Resner (2013) collected soil samples from 6 soil pits located at 0, 50, 100, 150, 160, and 190 meters along the transect with the 0 meter pit located closest to the road. We received a subsample of each sample for mercury analysis after the soil had been oven-dried, ground and homogenized.

We collected a second set of samples in summer of 2014 with a 1.8 cm diameter push probe to a depth of 24 cm, which meant sampling well into the E horizon. Deeper sampling was not necessary as it has been shown that the earthworms present on this site mix largely within the A horizon. The soil was separated by horizon as there was a clear change between the O, A, and E horizons even in the earthworm invaded soils. 15 samples were collected in the invaded area of the forest and 15 in an uninvaded area. The uninvaded area was located beyond the least invaded sampling point from Resner (2013), the pit located at 190 meters (Figure 2, Appendix II). We moved approximately 40 meters farther into the forest to ensure the area was free of earthworms. We identified an appropriate spot by checking the thickness of the forest floor (O horizon). In the uninvaded area, 15 forest floor samples were also collected using a sharp knife to cut the forest floor around a metal can of 10 cm diameter (Area = 78.54 cm^2) which served as a

template. Forest floor samples were then carefully lifted and separated from the underlying mineral soil and bagged in the field. The push probe samples of the mineral soils were then collected within the area where the forest floor sample had been removed. All samples were stored in ziplock bags in a cooler for transport to the University of Minnesota.

Soil samples were dried at 105°C for 48 hours, ground with a mortar and pestle, sieved through a 2 mm brass sieve and stored in small ziplock bags until analysis. Likewise, forest floor samples were dried at 95°C for 48 hours and ground in a food processor to homogenize the samples. Soil bulk density was determined for all samples.

2.3 Laboratory Analysis

All soil and forest floor samples were analyzed for total mercury (THg) by the double gold amalgamation method (Bloom and Crecelius 1983) using a Brooks Rand Model III cold vapor atomic fluorescence spectroscopy (CVAFS) analyzer via US EPA method 1631. For a detailed description of this method please refer to Chapter 1 of this thesis; also refer to Table 2 for a summary of the QA/QC recovery statistics. For all soil samples approximately 1 gram of sample was digested in 10 ml of nitric acid (HNO_3) and subsequently diluted by a factor of 5 with DDI prior to analysis. For forest floor samples, 0.5-1.0 gram of sample was digested in 20 ml HNO_3 and subsequently diluted by a factor of 10 with DDI.

	Analytical Duplicates	Digestion Duplicates	Analytical Standards	NIST SRM 2976	Matrix Spikes
Count	29	15	22	7	6
Mean	102.2%	101.3%	102.1%	107.5%	101.7%
%RSD	3.5%	4.5%	4.2%	5.8%	2.8%

Table 2. Summary of QA/QC recovery statistics for all analyzed soil samples.

Resner (2013) conducted a suite of analyses on her soil samples, including total elemental chemistry by inductively coupled plasma mass spectrometry (ICP-MS) at Australian Laboratory Services (ALS) Chemex, exchangeable chemistry by inductively coupled plasma atomic emission spectroscopy (ICP-AES) at the University of Minnesota Research Analytical Lab, and quantitative XRD analysis at the United States Geological Survey (USGS) in Boulder, Colorado.

In addition to THg analysis, samples collected in 2014 were also analyzed for soil organic carbon content by a VarioMax CN Elemental Analyzer at the United States Department of Agriculture- Agricultural Research Service (USDA-ARS) facility located on the St. Paul Campus of the University of Minnesota.

2.4 Geochemical Mass Balance Calculations

In the geochemical mass balance approach the element of interest is normalized to an immobile element such as Zr, Ti or Nb. Zr was chosen as the reference element for these soils. The geochemical mass balance calculations I performed include 2 main equations: fractional mass gains (positive values) or losses (negative values) of an element of interest (τ_j)(Eq. 1) and absolute mass losses or gains of an element of interest (δ_j)(Eq. 2):

$$\tau_j = \left(\frac{C_{j,w}C_{i,p}}{C_{j,p}C_{i,w}}\right) - 1 \qquad \text{Eq. 1}$$

$$\delta_j = \left(C_{j,w} - C_{j,w}\frac{C_{i,w}}{C_{i,p}}\right)\rho_w \Delta h_w \qquad \text{Eq. 2}$$

Where c is the concentration [ppm or mg/g] of the element of interest (*j*) and index element (*i*) in the A horizon (*w*) relative to the underlying loess parent material (E horizon) (*p*). In addition, ρ_w is the soil bulk density (g/cm^3) and Δh is the thickness (cm)

of the A horizon. Positive tau (τ) and delta (δ) values represent mass gains of the element of interest while negative values represent mass losses of the element via leaching, volatilization or biological uptake. Zr is the index element used in these calculations and Hg is the element of interest. The E horizon material underlying A horizon was used as the parent material since almost all of the earthworm mixing happens in the A horizon. Furthermore, the horizons underlying the E horizon have a sandier glacial till parent material and therefore have different Zr concentrations, which confounds tau calculations. Zr is well conserved throughout the E and A horizons and can therefore be used for the geochemical mass balance calculations in these upper soil horizons.

3. Results

3.1 2009 soil vs. 2014 soil

After careful comparison of the two sets of data- the soil collected in 2009 to soil collected in 2014, it became clear that the upper few centimeters of the 2009 soil in pits located at 190, 160, 150 and 100 meters labeled as part of the A horizon by Resner (2013) are actually forest floor. Bulk density and %LOI of these samples strongly resemble the data of the forest floor collected in 2014. Bulk densities are very low and %LOI exceeds 30%, indicating that they are O horizons, not mineral A horizons. Based on these observations the horizon designations of soils in pits 190, 160, 150 and 100 as identified by Resner (2014) were amended to reflect the fact that the upper soil is forest floor and not mineral soil. The amended horizon designations for 2009 soil as compared to the original Resner designations can be seen in Table 4, Appendix II. Since all 2014

soil was only collected to a depth of 24 cm, the data for the 2009 soil were adjusted to reflect the same depth to facilitate comparisons between the two sets of data.

The amended horizon designations of the 2009 soil match well with those described in the 2014 soil. The bulk densities of forest floor are low and do not exceed 0.40 g cm^{-3}. The mass-based THg concentrations (ng g^{-1}) are highest in the forest floor (Table 5 & Table 12, Appendix II) since it is composed primarily of organic matter and much lower in the mineral soil samples. THg concentrations steadily decrease with depth in the mineral soil profile (Tables 6-7 & Tables 13-14, Appendix II).

3.2 Simple Mass Balance Approach: Mercury Pools

I calculated mercury loadings/pools (mass of Hg in a known volume of soil) to assess the mass of mercury transported from the forest floor into the mineral soil following the invasion of soil mixing earthworms. Loadings were determined in a 1m x 1m ($1m^2$ of area) slice of soil and forest floor multiplied by the depth of each horizon. The total loading of each mineral soil profile is the total mass of mercury in 240,000 cm^3 or 0.24 m^3 of mineral soil plus the depth of the forest floor since the mineral soil was sampled to a depth of 24 cm. For the 2009 forest floor samples the total mass of mercury was determined in 40,000 cm^3 of forest floor in pit 190 and 60,000 cm^3 of forest floor in pits 160, 150 and 100. Since forest floor thickness for 2014 samples was not directly measured in the field, I used a uniform thickness of 8 cm (determined from a few representative samples) for all calculations, therefore; the total mass of mercury was determined in 80,000 cm^3 of forest floor for 2014 samples.

The breakdown of loadings in each horizon and the overall profile can be seen in Appendix II, Tables 5-7 for the 2009 soil and Tables 13-15 for the 2014 soil. Since the

2009 and 2014 sampling schemes were not quite the same, pits 190, 160, 150 and 100 from the 2009 soil were grouped together for mean calculations to represent the least invaded soils while pits 50 and 0 were grouped together to represent the most invaded soils. For the 2014 soil, 15 profiles were sampled on each end of the transect (invaded and uninvaded) although 3 profiles from the uninvaded site only had E horizon material with no A horizon present and so were excluded from delta calculations. For the 2009 soil, the Hg loading in the uppermost 24 cm in the least invaded mineral soil is 3.36 mg m^{-2} (Table 6, Appendix II) and 2.30 mg m^{-2} is present in forest floor (Table 5, Appendix II) for a total of 5.66 mg m^{-2}. The Hg loading of the uppermost 24 cm of the most invaded mineral soil is 4.86 mg m^{-2} (Table 7, Appendix II). This means that 1.50 mg m^{-2} (4.86 – 3.36 = 1.50) or 65% of Hg initially present in the forest floor was likely transported into the upper soil horizon in the invaded sites while 0.80 mg m^{-2} (2.30 – 1.50 = 0.80) is unaccounted for. The likely fate of this lost mercury will be discussed in more detail in the discussion section. Likewise, for the 2014 soil Hg loading in the uppermost 24 cm of the uninvaded area is 4.42 mg m^{-2} (Table 13, Appendix II) plus 2.76 mg m^{-2} present in 8 cm of the forest floor (Table 12, Appendix II). Invaded sites have a Hg loading of 5.47 mg m^{-2} to a depth of 24 cm (Table 14, Appendix II). This again shows that (1.06 mg m^{-2}) or 38% of the forest floor Hg mass was likely transported into and retained in the mineral soil of the invaded area while 1.70 mg m^{-2} of Hg was lost.

3.3 Results of Geochemical Mass Balance Calculations

3.3.1 2009 soil

Fractional mass change (τ) calculations show an enrichment of Hg in the A horizon along the entire mineral soil transect (Figure 3, Appendix II). In the least invaded

group (pits 190, 160 and 150), mercury is enriched from the top of the mineral soil horizons to about 10 cm (Table 8, Appendix II) but as we move to the more invaded pits (100, 50 and 0) the enrichment values increase and are also present to a greater depth- about 15 to 17 cm (Table 9, Appendix II). The enrichment values of the top mineral soil increase from 3.9 in the least invaded soil (pit 190) to a value of 7.0 in the most invaded soil (pit 0).

The delta (δ) or absolute mass changes of mercury in forest floor and the A horizon can be seen in Tables 10 and 11 in Appendix II. In general, the delta values are smaller in the A horizon of the least invaded soils (pits 190, 160, 150 and 100) and larger in the A horizon of the most invaded soils (pits 50 and 0). The depth integrated absolute mass changes (δ) of Hg in the A horizons increase from the lowest delta value of 0.0049 μg cm^{-2} observed in pit 150 (Table 10, Appendix II) to 0.1083 μg cm^{-2} observed in the most invaded soil (pit 0) (Table 11, Appendix II). A two-sample t-test shows a significant difference between the deltas of the least invaded and most invaded mineral soils with a p value of 0.0214.

3.3.2 2014 soil

For the 2014 soil, zirconium values were extrapolated based on the relationship between %LOI and Zr values from the 2009 soil. The two end member soils (pit 190 and pit 0) were used to graph the relationship of %LOI to Zr and the subsequent equations were used to calculate Zr values of 2014 soil (uninvaded soil eq.: y= -457.7x +377.31 and invaded soil eq.: y= -964.32x + 408.85), refer to Tables 18-20 in Appendix II for the calculated Zr values. Because we had only determined %C for these soil samples %LOI was calculated based on the conventional Van Bemmelen factor of 1.724, which assumes

that 58% of organic matter is organic carbon (Sutherland 1998). Therefore, a simple calculation of %C multiplied by 1.724 yielded the %LOI values needed for Zr calculations (Tables 18-20, Appendix II).

Fractional mass changes (τ) were not calculated for the 2014 soil due to the way the soil was sampled. The sampling of 2014 soil was not comparable to the way Resner (2013) collected her soil. The 2009 soil was collected in smaller increments (2-3 cm) in the A horizon and larger increments (5-10 cm) in the E horizon. For the 2014 soil, a single core 24 cm long was collected, then split into two horizons, A and E. This means that the mercury concentrations of the 2014 soil represent the overall concentrations of the entire A horizon and E horizon instead of incremental concentrations as is the case for Resner (2013). Collecting soil in smaller increments would have shown the gradual decrease of Hg concentrations as we move down the A horizon. As is the case for the 2009 soil, the top few centimeters of the soil have higher THg concentrations than the subsequent lower depths of the A horizon which allows for the calculation of tau. Since the 2014 soil was not collected in this way tau calculations were not appropriate or comparable to the 2009 soil.

Delta values (δ) or absolute mass changes, however, can be calculated for the 2014 soil and compared to the 2009 soil because these calculations take the overall thickness of the A horizon into consideration. As with the 2009 soil, the same pattern of larger delta values in the invaded mineral soil can be observed in the 2014 soil. The smallest delta value of 0.0013 $\mu g\ cm^{-2}$ is observed in one of the uninvaded soils (Table 16, Appendix II) while the largest is observed in one of the invaded soils (0.0945 $\mu g\ cm^{-2}$) (Table 17, Appendix II). All delta values are reported in Tables 15-17 in Appendix II.

Similarly to 2009 soil, a significant difference is present between the deltas of the invaded and uninvaded mineral soils with a p value of 4.16E-05.

4. Discussion

4.1 Simple Mass Balance vs. Geochemical Mass Balance

After accounting for the mercury that presumably moved from the forest floor into the mineral invaded soil, the loadings of Hg from the simple mass balance show a loss of 0.80 mg Hg m^{-2} in 2009 soil, and 1.7 mg m^{-2} of Hg lost in the 2014 soil. That is a 35% loss in the 2009 soil and a 62% loss of Hg in the 2014 soil (Table 3). Similarly, if we take the mean delta value of the 2009 soil we have 0.0075 µg $cm^{-2}$of Hg in the least invaded soils (pits 190, 160, 150 and 100) and 0.0692 µg cm^{-2} in the most invaded soils (pits 50 and 0) (Table 11, Appendix II). The mean delta value of the combined forest floor from pits 190, 160, 150 and 100 is 0.1375 µg cm^{-2} of Hg (Table 10, Appendix II). Again, we observe that 0.0617 µg cm^{-2} of Hg presumably moved from the forest floor into the A horizon in the invaded mineral soils while 0.0758 µg cm^{-2}, or 55% of the total Hg, is unaccounted for (Table 3).

For the 2014 soils, mean delta values of the invaded and uninvaded soils are 0.0648 and 0.0127 µg cm^{-2}, respectively (Tables 16 & 17, Appendix II). The forest floor has a mean delta value of 0.1410 µg cm^{-2} (Table 15, Appendix II) meaning that 0.0521 µg cm^{-2} of Hg seems to have moved from the forest floor into the A horizon while 0.0889 µg cm^{-2} appears to have been lost; that is a 63% loss of Hg (Table 3). The assumptions I'm making point to a loss of mercury; however, it is possible that some of the mercury that is unaccounted for may be present deeper in the soil profile although it seems more

likely that the lost mercury is a result of volatilization since earthworms at this site do not tend to mix beyond the upper E horizon.

For the 2014 soil samples, the two mass balance approaches seem to agree well when we consider that 62% of the forest floor Hg appears to have been lost using the simple mass balance and 63% appears to be lost using the geochemical mass balance. There is less agreement in the percentages lost in the 2009 soil, 35% from simple mass balance and 55% from geochemical mass balance; but the important message across all soils and mass balance approaches seems to be that there is a definite loss of mercury from the forest floor with the invasion of exotic earthworms. The disparities in the percentage values could partly be explained because the 2009 soil was sampled along a soil transect with variable degrees of invasion while 2014 soil was sampled at only two locations- in the most invaded area and in the uninvaded area. For the sake of comparison, the soil collected in 2009 from 6 different pits along the invasion transect was divided into two groups- the least and most invaded. The least invaded group consists of 4 soil pits while the most invaded of 2 soil pits. For the 2014 soil, we were able to collect 15 different soil profiles in the most invaded area and as well as 15 profiles in the uninvaded area, which provided us with a greater number of samples for comparisons and probably contributed to less variability in this data set.

	Simple Mass Balance	**Geochemical Mass Balance**
2009 soil	35% loss	55% loss
2014 soil	62% loss	63% loss

Table 3. Summary of the percentages of Hg that remain unaccounted for (referred to as a loss) from the forest floor upon earthworm invasion as determined by two different mass balance approaches.

4.2 2009 soil: Fractional mass changes (τ)

The enrichment values calculated for the 2009 soil also demonstrate some general patterns in mercury content of most and least invaded soils. Considering just the top increment of mineral soil (where most of the mineral soil mercury is found) enrichment values in the least invaded pits are around 3.5 and increase to 7.0 in the most invaded pit (Figure 3 and Tables 8-9, Appendix II). That is a substantial increase in enrichment values from the least to the most invaded soils, which seems to agree well with the other calculations discussed in previous sections. In the least invaded pits, tau values are smaller because most of the mercury is in the forest floor and not in the mineral soil horizons. As earthworms invade and consume the forest floor, they incorporate the organic matter plus the associated mercury into the A horizon, thereby increasing the tau enrichment values in these invaded areas.

4.3 2014 soil: Mercury and organic carbon relationship

Since mercury has a very high affinity for organic matter, I used the %C data to graph the relationship of Hg to %C in the uninvaded and invaded mineral soils of the 2014 samples (Figure 4 & 5, Appendix II). A very strong correlation can be seen between Hg and %C in the uninvaded soil (R^2 = 0.92) while a slightly weaker correlation is present in the invaded soils (R^2 = 0.86). Figure 4 (Appendix II) shows that the ratio of Hg to C in the uninvaded soils is relatively constant at approximately 1284 ng g^{-1} while the ratio for invaded soils is only about 566 ng of Hg per g of C (Figure 5, Appendix II). This suggests that the newer organic carbon present in the A horizons of the invaded soils is less decomposed than the organic carbon found in the A horizons of the uninvaded soils.

This further suggests that exotic earthworms are mixing organic carbon from the forest floor into the mineral soil but not decomposing it fully in the heavily invaded areas.

Due to the strong correlation between Hg and C, I used the same mass balance approaches as for Hg to assess the behavior of carbon between uninvaded and invaded soils. The results seem to be in agreement with the Hg results. Loading calculations of the 2009 soil point to a 32% loss of carbon after accounting for the carbon that presumably moved from the forest floor of the least invaded soils to the mineral soil of the most invaded areas (Tables 21-23, Appendix II). Delta (δ) calculations for the 2009 soil samples show a 52% carbon loss or 52% of carbon is unaccounted for based on the geochemical mass balance approach (Tables 24-25, Appendix II). Similarly, for the 2014 soil we observe that 22% of carbon is unaccounted for based on the simple loadings mass balance (Tables 26-28, Appendix II) and 65% is unaccounted for based on the geochemical mass balance delta calculations (Tables 29-31, Appendix II). The percentages of lost carbon for both sets of soil samples using the geochemical mass balance agree well with the same calculations performed for Hg (i.e. 2009 soil: 55% Hg loss with 52% C loss and 2014 soil: 63% Hg loss with 65% C loss). The percentages of lost Hg and C show a little less agreement via the simple mass balance using loadings but only for the 2014 soil samples (i.e. 2009 soil: 35% Hg loss with 32% C loss and 2014 soil: 62% Hg loss with 22% C loss). Considering the very close agreement between Hg and C mass balance calculations, the ratio of Hg to C seems to be relatively constant meaning that if we observe a loss of carbon we should observe a proportional loss of mercury. This further illustrates the close relationship of carbon and mercury and mercury's high affinity for organic matter. It also allows for easier estimates of Hg

content of soils before and after earthworm invasion if we know their organic matter content.

4.4 Loss of Mercury from Forest Floor

Based on both of the mass balance approaches there is a clear loss of Hg with the invasion of exotic earthworms. A little less than half of the Hg from the consumed forest floor is transferred into the upper depths of the A horizon, the remainder appears to be lost. This was an interesting finding since I assumed most of the mercury in the forest floor would remain in the soil system and would simply just be transported from the forest floor into the A horizon. There are a few possible explanations to consider when thinking about this substantial Hg loss.

As is commonly known, most organisms uptake and accumulate heavy metals and other toxins. Numerous studies have looked at the uptake of Hg by earthworms (Talmage and Walton 1993; Zagury et al. 2006; Ernst and Frey 2007; Ernst et al. 2008; Rieder et al. 2011) and it's been shown that the uptake and accumulation varies by ecological group. A study by Rieder et al. (2011) of a series of forest soils found that endogeic species accumulate the largest amounts of Hg, three times as much as epigeic species and twice as much as anecic species. This is mainly attributed to the different burrowing and feeding behaviors of the different ecological groups. For example, anecic species are deep burrowers and consume soils that are lower in Hg content while endogeic species consume litter and mix largely in the upper A horizon where most of the soil Hg is found. While bioaccumulation is certainly an important aspect of mercury cycling the dynamics of earthworm interactions with mercury may be more complicated. It is important to consider what may be happening with the mercury once it is ingested by earthworms.

Some studies have found that earthworms are potentially able to methylate mercury in their gut (Hinton and Veiga 2002; Rieder et al. 2013). In particular, Rieder et al. (2013) focused on the identification of microbes in the gut of *Lumbricus terrestris* L., an anecic species of earthworms, to evaluate the potential of these microbes to methylate mercury. They found bacterial strains predominantly related to the *Firmicutes, Actinobacteria* and *Proteobacteria* phyla and determined that sulfur-reducing bacteria may be to blame for the observed methylation of mercury. Additionally, these bacterial phyla have been found to contain *mer* operon or mercury resistance genes (Robinson and Tuovinen 1984; Osborn et al. 1997; Oregaard and Sorensen 2007; Barkay et al. 2003). The presence of *mer* operon allows organisms to effectively detoxify themselves of mercury. Mercuric reductase (*mer*A) catalyzes the reduction of Hg^{2+} into volatile Hg^{0} , which then readily passes through cell walls, highlighting the importance of this gene to the mercury resistance system (Barkay et al. 2010). Considering that all of the phyla found in the gut of *L. terrestris* are also known to have a high occurrence of mercury resistance genes, it is possible that some mercury taken up by earthworms is lost via *mer*A detoxification and subsequent volatilization.

However, since Rieder et al. (2013) has demonstrated the possibility of mercury methylation within earthworms, there is also the possibility that organomercurial lyase (*mer*B) is involved, which is the detoxifier of organic mercury compounds. The *mer*B enzyme splits the carbon-mercury linkage in organomercury compounds followed by the action of *mer*A to reduce Hg^{2+} to Hg^{0} (Robinson and Tuovinen 1984).

Both the bioaccumulation of mercury within earthworms and possible mercury detoxification within their gut could serve to explain the observed mercury loss from the

forest floor. The mercury detoxification theory could be studied further by specifically testing for the genes involved in mercury resistance of the different strains of bacteria found within the earthworm gut. Mercury flux studies could also be performed in invaded and uninvaded soils to determine whether higher fluxes of elemental mercury are observed in invaded areas demonstrating greater rates of volatilization. Other potential pathways of mercury loss in the invaded soils could be related to leaching of mercury to depths beyond those sampled in this study, erosional losses of mercury-bearing sediments during storm events, and microbial volatilization of mercury from A horizons.

4.5 Limitations of the Study

We could not calculate tau for the samples collected in 2014 because the sampling of the two batches of soil was not the same. The 2009 soil was also sampled in 6 pits along the invasion transect instead of just in the most invaded and uninvaded areas like the 2014 soil. We also collected soil from more profiles in 2014 than the collection in 2009 which makes the 2014 data set more robust. Most of the variability between data sets can be attributed to the location and sampling procedures while some of it is attributed to data manipulation. The pits sampled in 2009 were divided into the least invaded and most invaded soils even though each pit represents a different stage of the earthworm invasion chronosequence. Furthermore, Zr values for the 2014 soil were extrapolated from the 2009 soil but I would not expect the actual Zr values to be very far off since Resner (2013) showed that Zr is pretty well conserved throughout the A and E horizons.

5. Conclusions

By using two different mass balance approaches I was able to demonstrate that the invasion of forested soils by earthworms perturbs the natural mercury biogeochemical cycle in soil. The mass balance calculations demonstrate that a fraction of the forest floor mercury is incorporated into the mineral topsoil as earthworms consume organic rich forest floor and mix within the A horizon. However, the calculations also point to a substantial loss of Hg with earthworm invasion, a 35-63% loss of Hg is observed which is a sizeable quantity of Hg left unaccounted for. Some of this mercury is undoubtedly accumulated within earthworms; however, it is likely, although untested at this time, that the microbes present in their guts could be utilizing the mercury resistance genes (*mer* operon) to detoxify themselves of mercury. This would help to explain the observed loss of Hg from the forest floor upon earthworm invasion.

The two mass balance approaches used in this study produced similar results. In particular, the geochemical mass balance could be useful in studying similar mercury dynamics in soil systems. It is, however, important to be consistent in soil sampling across all study locations to minimize any variability introduced through inconsistent sample collection. Additionally, mercury's high affinity for organic matter is apparent when comparing mercury mass balance calculations to carbon mass balance calculations pointing to the constant nature of the Hg to C ratio. Overall, it is clear that earthworms perturb mercury cycling in the soil when compared to soil systems devoid of these soil mixers. Furthermore, the data presented here strongly point to greater volatilization of mercury in earthworm invaded soils contributing to higher atmospheric Hg inputs from invaded vs. uninvaded soils. In this respect, earthworms speed up the cycling of mercury

through soil. Alternatively, the mercury in worm free areas cycles more slowly and remains sequestered in the soil for a longer period of time.

Bibliography

Alban, D.H., and Berry, E.C. (1994), Effects of earthworm invasion on morphology, carbon and nitrogen of a forest soil, Appl. Soil Ecol*,*1, 243–49, doi: 10.1016/0929-1393(94)90015-9

Andersson, A. (1979) Mercury in soils. In Nriagu JO, ed. The Biogeochemistry of Mercury in the Environment. Amsterdam New York, Oxford: Elsevier/ North Holland Biomedical Press, 79–122.

Bargagli, R. and Barghigiani, C. (1991), Lichen biomonitoring of mercury emission and deposition in mining, geothermal and volcanic areas of Italy, Environmental Monitoring and Assessment, 16, 265-275, doi: 10.1007/BF00397614

Barkay, T., Miller, S. M., and Summers, A. O. (2003), Bacterial mercury resistance from atoms to ecosystems, FEMS Microbiology Reviews, 27, 355-384, doi: 10.1016/S0168-6445(03)00046-9

Barkay, T., Kritee, K., Boyd, E., and Geesey, G. (2010), A thermophilic bacterial origin and subsequent constraints by redox, light and salinity on the evolution of the microbial mercuric reductase, Environmental Microbiology, 12(11), 2904-2917, doi: 10.1111/j.1462-2920.2010.02260.x

Bartuska, A. M. and Rains, M. T., Foreword, Peatland Biogeochemistry and Watershed Hydrology at the Marcell Experimental Forest, edited by Randall K. Kolka, Stephen D. Sebestyen, Elon D. Verry, and Kenneth N. Brooks, CRC Press, 2011, vii-viii, print.

Bennett, J. P. and Wetmore, C. M. (1997), Chemical element concentrations in four lichens on a transect entering Voyageurs National Park, Environmental and Experimental Botany, 37, 174-185, doi: 10.1016/S0098-8472(96)01039-8

Bergh, J., McMurtrie, R. E., and Linder, S. (1998), Climatic factors controlling the productivity of Norway spruce: a model-based analysis, Forest Ecology and Management, 110, 127-139, doi: 10.1016/S0378-1127(98)00280-1

Bernier, P. Y., Lavigne, M. B., Hogg, E. H., and Trofymow, J. A. (2007), Estimating branch production in trembling aspen, Douglas-fir, jack pine, black spruce, and balsam fir, Can. J. For Res, 37, 1024-1033, doi:10.1139/X06-284

Bloom, N. S. and Crecelius, E. A. (1983), Determination of mercury in seawater at sub-nanogram per liter levels, Marine Chemistry, 14, 49-59, doi: 10.1016/0304-4203(83)90069-5

Blum, J. D., Johnson, M. W., Gleason, J. D., Demers, J. D., Landis, M. S., and Krupa, S. (2012), Mercury concentration and isotopic composition of epiphytic tree lichens in the Athabasca oil sands region, Developments in Environmental Science, 11, 373-390, doi: http://dx.doi.org/10.1016/B978-0-08-097760-7.00016-0

Bohlen, P.J., Groffman, P.M., Fahey, T.J., Fisk, M.C., Suarez , E., Pelletier, D.M., and Fahey, R.T. (2004), Ecosystem consequences of exotic earthworm invasion of north temperate forests, Ecosystems, 7, 1–12, doi: 10.1007/s10021-003-0126-z

Brimhall, G.H., and Dietrich, W.E. (1987), Constitutive mass balance relations between chemical composition, volume, density, porosity, and strain in metasomatic hydrochemical systems: Results on weathering and pedogenesis, Geochimica et Cosmochimica Acta, 51, 567-587, doi: 10.1016/0016-7037(87)90070-6

Browne, C. L. and Fang, S. C. (1978), Uptake of mercury vapor by wheat, Plant Physiol, 61, 430-433, doi: http://dx.doi.org.ezp2.lib.umn.edu/10.1104/pp.61.3.430

Curtis, P. S. (1996), A meta-analysis of leaf gas exchange and nitrogen in trees grown under elevated carbon dioxide, Plant, Cell and Environment, 19, 127-137, doi: 10.1111/j.1365-3040.1996.tb00234.x

Demers, J. D., Driscoll, C. T., Fahey, T. J., and Yavitt, J. B. (2007), Mercury cycling in litter and soil in different forest types in the Adirondack region, New York, USA, Ecological Applications, 17(5), 1341-1351, doi: http://dx.doi.org.ezp1.lib.umn.edu/10.1890/06-1697.1

Du, S. -H. and Fang, S. C. (1983), Catalase activity of C_3 and C_4 species and its relationship to mercury vapor uptake, Environmental and Experimental Botany, 23(4), 347-353, doi: 10.1016/0098-8472(83)90009-6

Edwards, S. C., Macleod, C. L., and Lester, J. N. (1998), The bioavailability of copper and mercury to the common nettle (*Urtica dioica*) and the earthworm *Eisenia fetida* from contaminated dredge spoil, Water, Air, and Soil Pollution, 102, 75-90, doi: 10.1023/A:1004993912639

Eisenhauer, N., Partsch, S., Parkinson, D., and Scheu, S. (2007), Invasion of a deciduous forest by earthworms: Changes in soil chemistry, microflora, microarthropods and vegetation, Soil Biology and Biochemistry, 39(5), 1099-1110, doi:10.1016/j.soilbio.2006.12.019

Ericksen, J. A., Gustin, M.S., Schorran, D. E., Johnson, D. W., Lindberg, S. E., and Coleman, J.S. (2003), Accumulation of atmospheric mercury in forest foliage, Atmospheric Environment, 37, 1613-1622, doi:10.1016/S1352-2310(03)00008-6

Ericksen, J. A. and Gustin, M. S. (2004), Foliar exchange of mercury as a function of soil and air mercury concentrations, Science of the Total Environment, 324, 271-279, doi: 10.1016/j.scitotenv.200310.034

Eriksson, G., Jensen, S., Kylin, H., and Strachan, W. (1989), The pine needle as a monitor of atmospheric pollution, Nature, 341, 42-44, doi: 10.1038/341042a0

Ernst, G., and Frey, B. (2007), The effect of feeding behavior on Hg accumulation in the ecophysiologically different earthworms *Lumbricus terrestris* and *Octolaseon cyaneum*: A microcosm experiment, Soil Biology & Biochemistry, 39, 386-390, doi: 10.1016/j.soilbio.2006.07.020

Ernst, G., Zimmermann, S., Christie, P., and Frey, B. (2008), Mercury, cadmium and lead concentrations in different ecophysiological groups of earthworms in forest soils, Environmental Pollution, 156, 1304-1313, doi: 10.1016/j.envpol.2008.03.002

Estrade, N., Carignan, J., and Donard, O. F. X. (2010), Isotope tracing of atmospheric mercury sources in an Urban Area of Northeastern France, Environ. Sci. Technol, 44(16), 6062-6067, doi: 10.1021/es100674a

Evans, L. J. (1989), Chemistry of metal retention by soils, Environ. Sci. Technol, 23(9), 1046-1056, doi: 10.1021/es00067a001

Fitzgerald, W. F. (1995), Is mercury increasing in the atmosphere? The need for an atmospheric mercury network (AMNet), Water, Air, and Soil Pollution, 80, 245-254, doi: 10.1007/BF01189674

Fleck, J. A., Grigal, D. F., and Nater, E. A. (1999), Mercury uptake by trees: an observational experiment, Water, Air, and Soil Pollution, 115, 513-523, doi: 10.1023/A:1005194608598

Frelich, L. E., Hale, C. M., Scheu, S., Holdsworth, A. R., Heneghan, L., Bohlen, P. J., and Reich, P. B. (2006), Earthworm invasion into previously earthworm-free temperate and boreal forests, Biological Invasions, 8(6), 1235-1245, doi:10.1007/s10530-006-9019-3

Gabriel, M. C., and Williamson, D. G. (2004), Principal biogeochemical factors affecting the speciation and transport of mercury through the terrestrial environment, Environ. Geochem. and Health, 26, 421-434, doi: 10.1007/s10653-004-1308-0

Gates, G. E. (1982), Farewell to North American megadriles, Megadrilogica, 4:77.

Grangeon, S., Guédron, S., Asta, J., Sarret, G., and Charlet, L. (2012), Lichen and soil as indicators of an atmospheric mercury contamination in the vicinity of a chlor-alkali plant (Grenoble, France), Ecological Indicators, 13, 178-183, doi: 10.1016/j.ecolind.2011.05.024

Graydon, J. A., St. Louis, V. L., Lindberg, S. E., Hintelmann, H., and Krabbenhoft, D. P. (2006), Investigation of mercury exchange between forest canopy vegetation and the atmosphere using a new dynamic chamber, Environ. Sci. Technol, 40(15), 4680-4688, doi: 10.1021/es0604616

Grigal, D. F., Kolka, R. K., Fleck, J. A., and Nater, E. A. (2000), Mercury budget of an upland-peatland watershed, Biogeochemistry, 50(1), 95-109, doi: 10.1023/A:1006322705566

Grigal, D. F. (2002), Inputs and outputs of mercury from terrestrial watersheds: a review, Environ. Rev, 10, 1-39, doi: 10.1139/a01-013

Hale, C.M., Frelich, L.E., and Reich, P.B. (2005a), Exotic European earthworm invasion dynamics in northern hardwood forests of Minnesota, U.S.A., Ecol Appl., 15, 848–860, doi: 10.1890/03-5345

Hale, C.M., Frelich, L.E., and Reich, P.B. (2005b), Effects of European earthworm invasion on soil characteristics in northern hardwood forests of Minnesota, Ecosystems, 8, 911–927, doi: 10.1007/s10021-005-0066-x

Hale, C.M, Frelich, L.E., and Reich, P.B. (2006), Changes in hardwood forest understory plant communities in response to European earthworm invasions, Ecology, 87(7), 1637-1649, doi: 10.1890/0012-9658(2006)87[1637:CIHFUP]2.0.CO;2

Hale, C. M.E., Reich, P. B., and Pastor, J. (2008), Exotic earthworm effects on hardwood forest floor, nutrient availability and native plants: a mesocosm study, Oecologia, 155(3), 509-18, doi:10.1007/s00442-007-0925-6

Hanson, P. J., Lindberg, S. E., Tabberer, T. A., Owens, J. G., and Kim, K. -H. (1995), Foliar exchange of mercury vapor: evidence for a compensation point, Water, Air, and Soil Pollution, 80, 373-382, doi: 10.1007/BF01189687

Hendrix, P.F., and Bohlen, P.J. (2002), Exotic earthworm invasions in North American: ecological and policy implications, BioScience, 52(9), 801-811, doi: 10.1641/0006-3568(2002)052[0801:EEIINA]2.0.CO;2

Hendrix, P.F., Callaham, M.A., Drake, J.M., Huang, C., James, S.W., Snyder, B.A., and Zhang, W. (2008), Pandora's box contained bait: the global problem of introduced earthworms, The Annual Review of Ecology, Evolution, and Systematics, 39, 593–613, doi: 10.1146/annurev.ecolsys.39.110707.173426

Hesterberg, D., Chou, J. W., Hutchinson, K. J., and Sayers, D. E. (2001), Bonding of Hg(II) to reduced organic sulfur in humic acid as affected by S/Hg ratio, Environ. Sci. Technol, 35(13), 2741-2745, doi: 10.1021/es001960o

Hinton, J. J., and Veiga, M. M. (2002), Earthworms as bioindicators of mercury pollution from mining and other industrial activities, Geochemistry: Exploration, Environment, Analysis, 2, 269-274, doi: 10.1144/1467-787302-031

Hole, F.D. (1981), Effects of animals on soil, Geoderma, 25(1-2), 75-112, doi:10.1016/0016-7061(81)90008-2

Jeremiason, J. D., Engstrom, D. R., Swain, E. B., Nater, E. A., Johnson, B. M., Almendinger, J. E., Monson, B. A., and Kolka, R. K. (2006), Sulfate addition increases methylmercury production in an experimental wetland, Environ. Sci. Technol, 40(12), 3800-3806, doi: 10.1021/es0524144

Jersak, J., Amundson, R., and Brimhall, G., Jr. (1997), Trace metal geochemistry in spodosols of the northeastern United States, Journal of Environmental Quality, 26, 511-521, doi:10.2134/jeq1997.00472425002600020024x

Johnson, D. L. and Braman, R. S. (1974), Distribution of atmospheric mercury species near ground, Environmental Science and Technology, 8(12), 1003-1009, doi: 10.1021/es60102a009

Johnson, D. L., Domier, J. E. J., and Johnson, D. N. (2005), Reflections on the nature of soil and its biomantle, Annals of the Association of American Geographers, 95(1), 11–31, doi: http://www.jstor.org/stable/3694030

Karnosky, D. F. (2003), Impacts of elevated atmospheric CO2 on forest trees and forest ecosystems: knowledge gaps, Environment International, 29, 161-169, doi: 10.1016/S0160-4120(02)00159-9

Kolka, R. K., Grigal, D. F., Nater, E. A., and Verry, E. S. (1999a), Mercury and organic carbon relationships in streams draining forested upland/peatland watersheds, Journal of Environmental Quality, 28(3), 766-775, doi: 10.2134/jeq1999.00472425002800030006x

Kolka, R. K., Nater, E. A., Grigal, D. F., Verry, E. S. (1999b), Atmospheric inputs of mercury and organic carbon into a forested upland/bog watershed, Water, Air, and Soil Pollution, 113(1), 273-294, doi: 10.1023/A:1005020326683

Kolka, R. K., Grigal, D. F., Nater, E. A., and Verry, E. S. (2001), Hydrologic cycling of mercury and organic carbon in a forested upland-bog watershed, Soil Science Society of America Journal, 65(3), 897-905, doi: 10.2136/sssaj2001.653897x

Laacouri, A., Nater, E. A., and Kolka, R. K. (2013), Distribution and uptake dynamics of mercury in leaves of common deciduous trees species in Minnesota, USA, Environ. Sci. Technol, 47, 10462-10470, doi: dx.doi.org/10.1021/es401357z

Lee, K.E. (1985), Earthworms – Their ecology and relationships with soils and land use. Academic Press, Sydney, Australia.

Leonard, T. L., Taylor, G. E., Jr., Gustin, M. S., and Fernandez, G. C. J. (1998), Mercury and plants in contaminated soils: 1. Uptake, partitioning and emission to the atmosphere, Environmental Toxicology and Chemistry, 17(10), 2063-2071, doi: 10.1002/etc.5620171024

Lin, C. -J. and Pehkonen, S. O. (1999), The chemistry of atmospheric mercury: a review, Atmospheric Environment, 33, 2067-2079, doi: 10.1016/S1352-2310(98)00387-2

Lindberg, S. E., Jackson, D. R., Huckabee, J. W., Janzen, S. A., Levin, M. J., and Lund, J. R. (1979), Atmospheric emission and plant uptake of mercury from agricultural soils near the Almadén mercury mine, Journal of Environmental Quality, 8(4), 572-578, doi: 10.2134/jeq1979.00472425000800040026x

Lindberg, S. E., Hanson, P. J., Meyers, T. P., and Kim, K. -H. (1998), Air/surface exchange of mercury vapor over forests – the need for a reassessment of continental biogenic emissions, Atmospheric Environment, 32(5), 895-908, doi: 10.1016/S1352-2310(97)00173-8

Lindqvist, O. and Rodhe, H. (1985), Atmospheric mercury – a review, Tellus, 37B, 136-159, doi: 10.1111/j.1600-0889.1985.tb00062.x

Lindqivst, O., Johansson, K., Aastrup, M., Andersson, A., Bringmark, L., Hovsenius, G., Hakanson, L., Iverfeldt, A., Meili, M., and Timm, B. (1991), Mercury in the Swedish environment – recent research on causes, consequences and corrective methods, Water, Air, and Soil Pollution, 55, xi-xiii, doi: 10.1007/BF00542429

Lodenius, M. (2013), Use of plants for biomonitoring of airborne mercury in contaminated areas, Environmental Research, 125, 113-123, doi: http://dx.doi.org/10.1016/j.envres.2012.10.014

Lyttle, A., Yoo, K., Hale, C.M., Aufdenkampe, A., Sebestyen, S. (2011), Carbon-mineral interactions along an earthworm invasion gradient at a sugar maple forest in northern Minnesota, Applied Geochemistry, 26, S85-S88, doi: 10.1016/j.apgeochem.2011.03.037

Lyttle, A., Yoo, K., Hale, C., Aufdenkampe, A., Sebestyen, S., Resner, K., and Blum, A. (2014), Impact of exotic earthworms on organic carbon sorption on mineral surfaces and soil carbon inventories in a northern hardwood forest, Ecosystems, 18, 16-29, doi: 10.1007/s10021-014-9809-x

Makholm, M. M. and Bennett, J. P. (1998), Mercury accumulation in transplanted *Hypogymnia physodes* lichens downwind of Wisconsin chlor-alkali plant, Water, Air, and Soil Pollution, 102, 427-436, doi: 10.1023/A:1004977717769

Mason, R. P., Fitzgerald, W. F., and Morel, F. M. M. (1994), The biogeochemical cycling of elemental mercury: anthropogenic influences, Geochimica et Cosmochimica Acta, 58(15), 3191-3198, doi: 10.1016/0016-7037(94)90046-9

Merritts, D.J., Chadwick, O.A., Hendricks, D.M., Brimhall, G.H., and Lewis, C.J. (1992), The mass balance of soil evolution on late quaternary marine terraces, northern California, Geological Society of America Bulletin, 104, 1456-1470, doi: 10.1130/0016-7606(1992)104<1456:TMBOSE>2.3.CO;2

Millhollen, A. G., Gustin, M. S., and Obrist, D. (2006), Foliar mercury accumulation and exchange for three tree species, Environ. Sci. Technol, 40(19), 6001-6006, doi: 10.1021/es0609194

Mitchell, C. P. J., Branfireun, B. A., Kolka, R. A. (2009), Methylmercury dynamics at the upland-peatland interface: topographic and hydrogeochemical controls, Water Resources Research, 45(2), W02406, doi: 10.1029/2008WR006832

Monitoring Mercury Deposition, National Atmospheric Deposition program, 2011, http://nadp.sws.uiuc.edu/lib/brochures/mdn.pdf

Obrist, D. (2007), Atmospheric mercury pollution due to losses of terrestrial carbon pools?, Biogeochemistry, 85, 119-123, doi: 10.1007/s10533-007-9108-0

Oh, N.H., and Richter, D.D. (2005), Elemental translocation and loss from three highly weathered soil-bedrock profiles in the southeastern United States, Geoderma, 126, 5-25, doi: 10.1016/j.geoderma.2004.11.005

Ollerová, H., Marušková, A., Kontrišová, O., and Plieštiková, L. (2010), Mercury accumulation in *Picea abies* (L.) Karst. Needles with regard to needle age, Polish Journal of Environmental Studies, 19(6), 1401-1404, ISSN: 1230-1485

Oregaard, G., and Sorensen, S. J. (2007), High diversity of bacterial mercuric reductase genes from surface and sub-surface floodplain soil (Oak Ridge, USA), International Society for Microbial Ecology Journal, 1, 453-467, doi: 10.1038/ismej.2007.56

Osborn, A. M., Bruce, K. D., Strike, P., and Ritchie, D. A. (1997), Distribution, diversity and evolution of the bacterial mercury resistance (*mer*) operon, FEMS Microbiology Reviews, 19, 239-262, doi: http://dx.doi.org/10.1111/j.1574-6976.1997.tb00300.x

Rea, A. W., Lindberg, S. E., Scherbatskoy, T., and Keeler, G. J. (2002), Mercury accumulation in foliage over time in two northern mixed-hardwood forests, Water, Air, and Soil Pollution, 133, 49-67, doi: 10.1023/A:1012919731598

Resner, K., Yoo, K., Hale, C.M., Aufdenkampe, A., and Sebestyen, S. (2011), Elemental and mineralogical changes in soils due to bioturbation along an earthworm invasion chronosequence in Northern Minnesota, Applied Geochemistry, 26, S127-S131, doi: 10.1016/j.apgeochem.2011.03.047

Resner, K. (2013), Impacts of earthworm bioturbation on elemental cycles in soils: An application of a geochemical mass balance to an earthworm invasion chronosequence in a sugar maple forest in Northern Minnesota, Master's thesis, Department of Soil, Water and Climate, University of Minnesota, St. Paul, Minnesota, United States.

Resner, K., Yoo, K., Sebestyen, S., Aufdenkampe, A., Hale, C., Lyttle, A., and Blum, A. (2014), Invasive earthworms deplete key soil inorganic nutrients (Ca, Mg, K, and P) in a northern hardwood forest, Ecosystems, 18, 89-102, doi: 10.1007/s10021-014-9814-0

Riebe, C., Kirchener, J.W., and Finkel, R.C. (2003), Long-term rates of chemical weathering and physical erosion from cosmogenic nuclides and geochemical mass balance, Geochimica et Cosmochimica Acta, 67, 4411-4427, doi: 10.1016/S0016-7037(03)00382-X

Rieder, S. R., Brunner, I., Horvat, M., Jacobs, A., and Frey, B. (2011), Accumulation of mercury and methylmercury by mushrooms and earthworms from forest soils, Environmental Pollution, 159, 2861-2869, doi: 10.1016/j.envpol.2011.04.040

Rieder, S. R., Brunner, I., Daniel, O., Liu, B., and Frey, B. (2013), Methylation of merucry in earthworms and the effects of mercury on the associated bacterial communities, PLOS ONE, 8(4), e61215, doi: 10.1371/journal.pone.0061215

Risch, M. R., Kenski, D. M., and Gay, D. A. (2014), A great Lakes atmospheric mercury monitoring network: evaluation and design, Atmospheric Environment, 85, 109-122, doi: http://dx.doi.org/10.1016/j.atmosenv.2013.11.050

Robinson, J. B., and Tuovinen, O. H. (1984), Mechanisms of microbial resistance and detoxification of mercury and organomercury compounds: physiological, biological, and genetic analyses, Microbiological Reviews, 48(2), 95-124, PMCID: PMC373215

Sackett, T. E., Smith, S. M., and Basiliko, N. (2013), Indirect and direct effects of exotic earthworms on soil nutrient and carbon pools in North American temperate forests, Soil Biology & Biochemistry, 57, 459-467, doi: http://dx.doi.org/10.1016/j.soilbio.2012.08.015

Schaetzl, R., and Anderson, S. (2005), Soils: Genesis and Geomorphology, New York: Cambridge University Press.

Schroeder, W. H., Yarwood, G., and Niki, H. (1991), Transformation processes involving mercury species in the atmosphere – results from a literature survey, Water, Air, and Soil Pollution, 56, 653-666, doi: 10.1007/BF00342307

Schroeder, W. H. and Munthe, J. (1998), Atmospheric mercury – an overview, Atmospheric Environment, 32(5), 809-822, doi: 10.1016/S1352-2310(97)00293-8

Schuster, E. (1991), The behavior of mercury in the soil with special emphasis on complexation and adsorption processes- A review of the literature, Water, Air, and Soil Pollution, 56, 667-680, doi: 10.1007/BF00342308

Selin, N. E., Jacob, D. J., Yantosca, R. M., Strode, S., Jaegl´e, L., and Sunderland, E. M. (2008), Global 3-D land-oceanatmosphere model for mercury: present-day versus preindustrial cycles and anthropogenic enrichment factors for deposition, Glob. Biogeochem. Cycles, 22, GB2011, doi: 10.1029/2007GB003040

Sensen, M. and Richardson, D. H. S. (2002), Mercury levels in lichens from different host trees around a chloralkali plant in New Brunswick, Canada, The Science of the Total Environment, 293, 31-45, doi: 10.1016/S0048-9697(01)01135-4

Silva-Filho, E. V., Machado, W., Oliveira, R. R., Sella, S. M., and Lacerda, L. D. (2006), Mercury deposition through litterfall in an Atlantic Forest at Ilha Grande, Southeast Brazil, Chemosphere, 65, 2477-2484, doi:10.1016/j.chemosphere.2006.04.053

Siwik, E. I. H., Campbell, L. M., and Mierle, G. (2009), Fine-scale mercury trends in temperate deciduous tree leaves from Ontario, Canada, Science of the Total Environment, 407, 6275-6279, doi: 10.1016/j.scitotenv.2009.08.044

Skyllberg, U., Qian, J., Frech, W., Xia, K., and Bleam, W. F. (2003), Distribution of mercury, methyl mercury and organic suphur species in soil, soil solution and stream of a boreal forest catchment, Biogeochemistry, 64, 53-76, doi: 10.1023/A:1024904502633

Sorensen, J. A., Glass, G. E., and Schmidt, K. W. (1994), Regional patterns of wet mercury deposition, Environ. Sci. Technol, 28, 2025-2032, doi: 10.1021/es00061a010

Stamenkovic, J. and Gustin, M. S. (2009), Nonstomatal versus stomatal uptake of atmospheric mercury, Environ. Sci. Technol, 43(5), 1367-1372, doi: 10.1021/es801583a

St. Louis, V., Rudd, J. W. M., Kelly, C. A., Hall, B. D., Rolfhus, K. R., Scott, K. J., Lindberg, S. E., and Dong, W. (2001), Importance of the forest canopy to fluxes of methyl mercury and total mercury to boreal ecosystems, Environmental Science and Technology, 35, 3089–3098, doi: 10.1021/es001924p

Suchara, I., Sucharova, J., Hola, M., Reimann, C., Boyd, R., Filzmoser, P., and Englmaier, P. (2011), The performance of moss, grass, and 1- and 2-year old spruce needles as bioindicators of contamination: A comparative study at the scale of the Czech Republic, Science of the Total Environment, 409, 2281-2297, doi: 10.1016/j.scitotenv.2011.02.003

Sutherland, R. A. (1998), Loss-on-ignition estimates of organic matter and relationships to organic carbon in fluvial bed sediments, Hydrobiologia, 389, 153-167, doi: 10.1023/A:1003570219018

Szczepaniak, S. and Biziuk, M. (2003), Aspects of the biomonitoring studies using mosses and lichens as indicators of metal pollution, Environmental Research, 93, 221-230, doi: 10.1016/S0013-9351(03)00141-5

Talmage, S. S., and Walton, B. T. (1993), Food chain transfer and potential renal toxicity of mercury to small mammals at a contaminated terrestrial field site, Ecotoxicology, 2, 243-256, doi: 10.1007/BF00368533

Temme, C., Blanchard, P., Steffen, A., Banic, C., Beauchamp, S., Poissant, L., Tordon, R., and Wiens, B. (2007), Trend, seasonal and multivariate analysis study of total gaseous mercury data from the Canadian atmospheric mercury measurement network (CAMNet), Atmospheric Environment, 41, 5423-5441, doi: 10.1016/j.atmosenv.2007.02.021

U.S. Environmental Protection Agency, 2002, Method 1631, Revision E: Mercury in Water by Oxidation, Purge and Trap, and Cold Vapor Atomic Fluorescence Spectrometry, U.S. Gov. Office,Washington, DC, http://water.epa.gov/scitech/methods/cwa/metals/mercury/upload/2007_07_10_methods_method_mercury_1631.pdf

Wang, J., Feng, X., Anderson, C. W. N., Wang, H., Zheng, L., and Hu, T. (2012), Implications of mercury speciation in thiosulfate treated plants, Environ. Sci. Technol, 46, 5361-5368, doi: dx.doi.org/10.1021/es204331a

Wyttenbach, A. and Tobler, L. (1988), The seasonal variation of 20 elements in Ist and 2nd year needles of Norway spruce, *Picea abies* (L.) Karst, Trees, 2, 52-64, doi: 10.1007/BF01196345

Xia, K., Skyllberg, U. L., Bleam, W. F., Bloom, P. R., Nater, E. A., and Helmke, P. A. (1999), X-ray absorption spectroscopic evidence for the complexation of Hg(II) by reduced sulfur in soil humic substances, Environ. Sci. Technol, 33(2), 257-261, doi: 10.1021/es980433q

Zagury, G. J., Neculita, C.-M., Bastien, C., and Deschenes L. (2006), Mercury fractionation, bioavailability, and ecotoxicity in highly contaminated soils from chlor-alkali plants, Environmental Toxicology & Chemistry, 25(4), 1138-1147, doi: 10.1897/05-302R.1

Zhang, L., Planas, D., and Qian, J. -L. (1995), Mercury concentrations in black spruce (*Picea mariana* mill B.S.P.) and lichens in boreal Quebec, Canada, Water, Air, and Soil Pollution, 81, 153-161, doi: 10.1007/BF00477262

Zhang, L., Wright, L. P., and Blanchard, P. (2009), A review of current knowledge concerning dry deposition of atmospheric mercury, Atmospheric Environment, 43, 5853-5864, doi: 10.1016/j.atmosenv.2009.08.019

Appendix I

Figure 1. Location of all sites. 11 sites are located in the U.S. and 8 sites are in Canada. Outside image shows locations of the 3 sites at the Marcell Experimental Forest which are too close together to be seen at the large scale of the original image. The arrow points to the one point on the map that represents all 3 of the MEF sites.
Image Source: Google Earth.

Figure 2. Showing the approximate size of branches collected. Image credit: Sona Psarska

Figure 3. Showing the differences in color between new growth and older growth. Image credit: Sona Psarska

Figure 4. Comparison of needles from S1 (top) and S6 (bottom). S6 needles are longer and more vigorous. Images credit: Sona Psarska

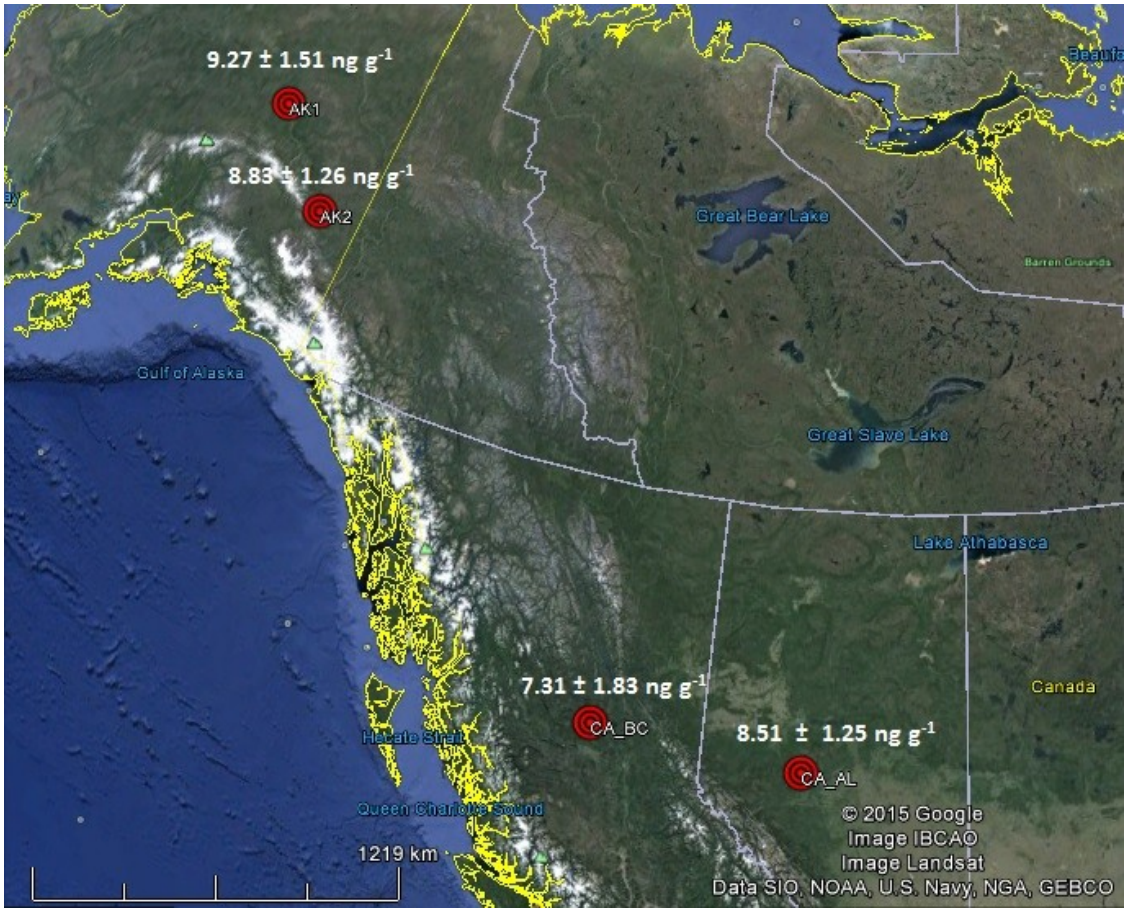

Figure 5. Locations of all western sites showing mean THg black spruce needle concentrations ± standard deviation. Image Source: Google Earth

Figure 6. Locations of all eastern sites showing mean THg black spruce needle concentrations ± standard deviation. Image Source: Google Earth

Figure 7. Locations of all central sites showing mean THg black spruce needle concentrations ± standard deviation. Image Source: Google Earth

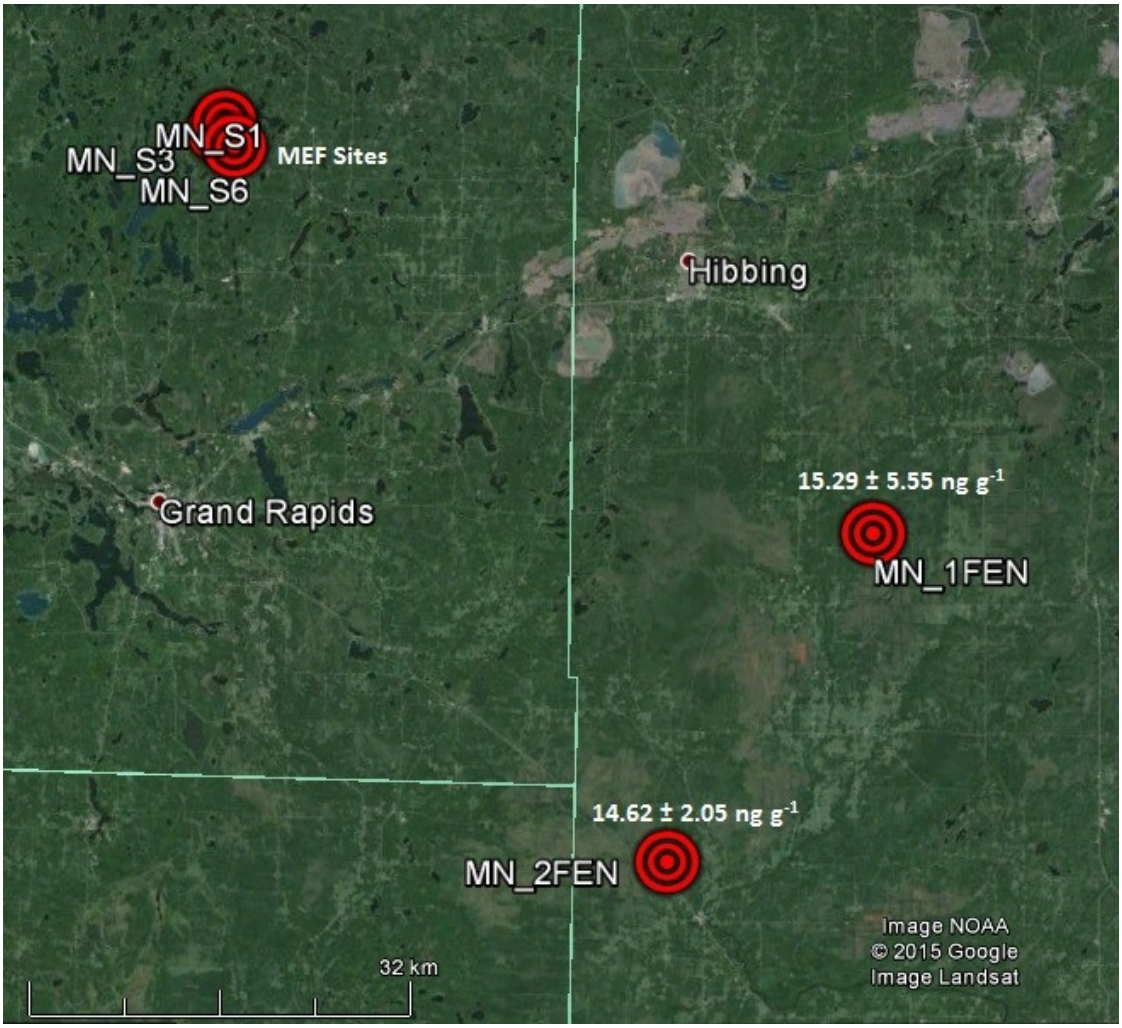

Figure 8. Locations of Minnesota fen sites showing mean THg black spruce needle concentrations ± standard deviation. Image Source: Google Earth

Figure 9. Locations of Minnesota Marcell Experimental Forest sites showing mean THg black spruce needle concentrations ± standard deviation. Image Source: Google Earth

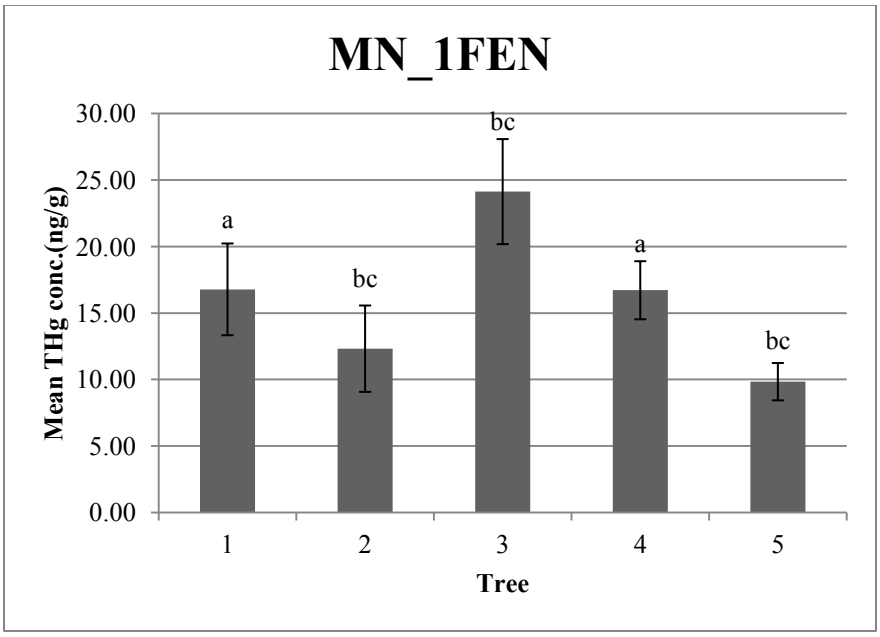

Figure 10.1. Showing MN_1FEN mean THg concentrations in ng g^{-1} (± 1 SD) for each tree. Means with different letters are significantly different ($p < 0.05$). bc notation signifies that the mean is significantly different from all of the other trees.

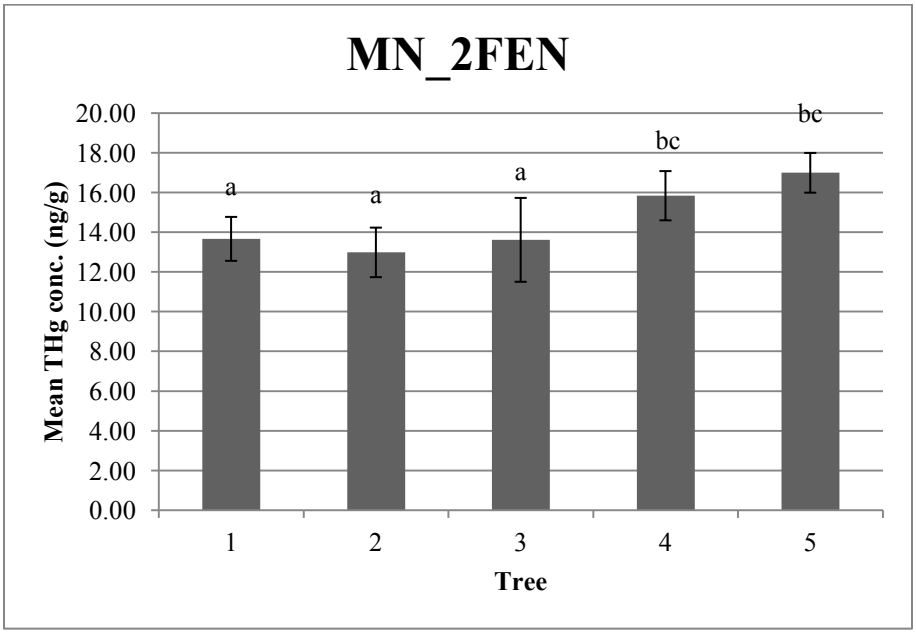

Figure 10.2. Showing MN_2FEN mean THg concentrations in ng g^{-1} (± 1 SD) for each tree. Means with different letters are significantly different ($p < 0.05$). bc notation signifies that the mean is significantly different from all of the other trees.

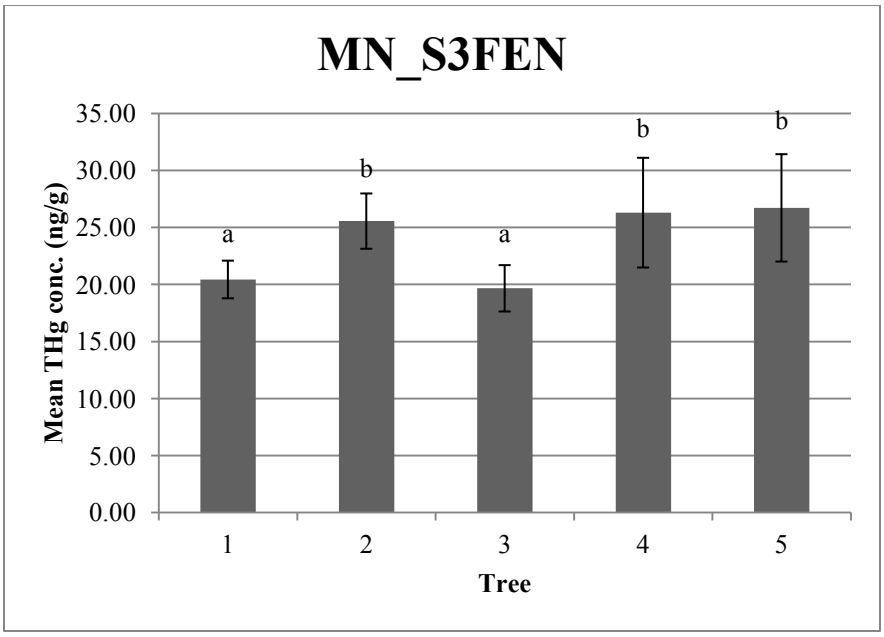

Figure 10.3. Showing MN_S3FEN mean THg concentrations in ng g^{-1} (± 1 SD) for each tree. Means with different letters are significantly different ($p < 0.05$).

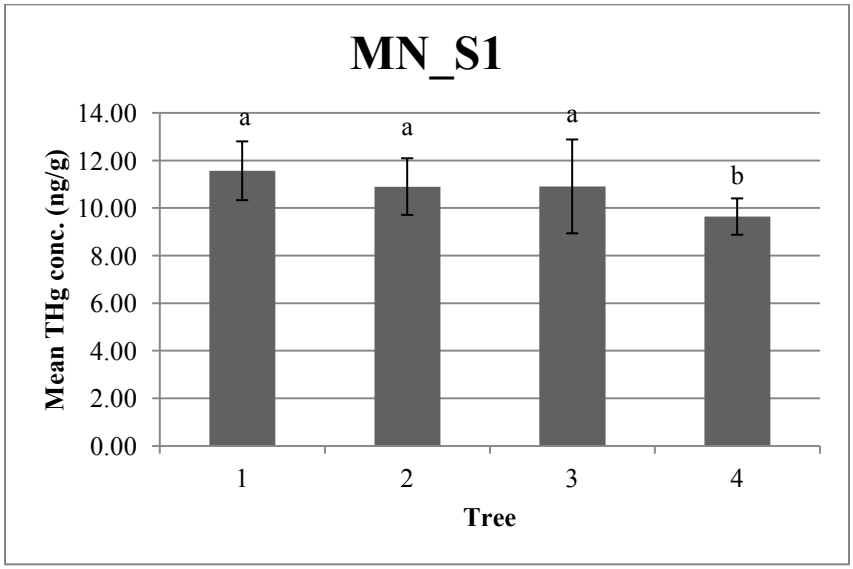

Figure 10.4. Showing MN_S1 mean THg concentrations in ng g^{-1} (± 1 SD) for each tree. Means with different letters are significantly different ($p < 0.05$).

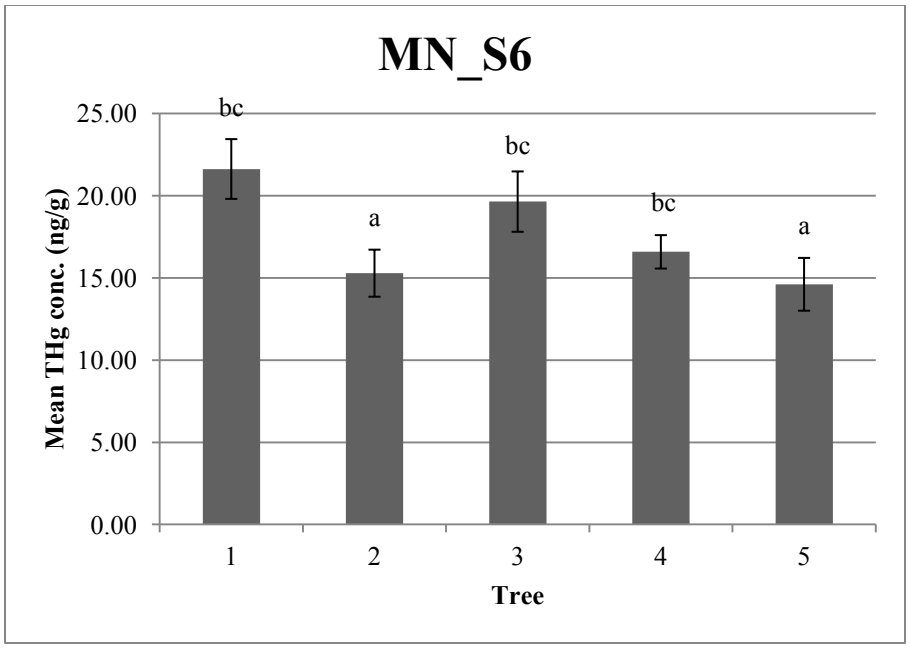

Figure 10.5. Showing MN_S6 mean THg concentrations in ng g^{-1} (± 1 SD) for each tree. Means with different letters are significantly different ($p < 0.05$). bc notation signifies that the mean is significantly different from all of the other trees.

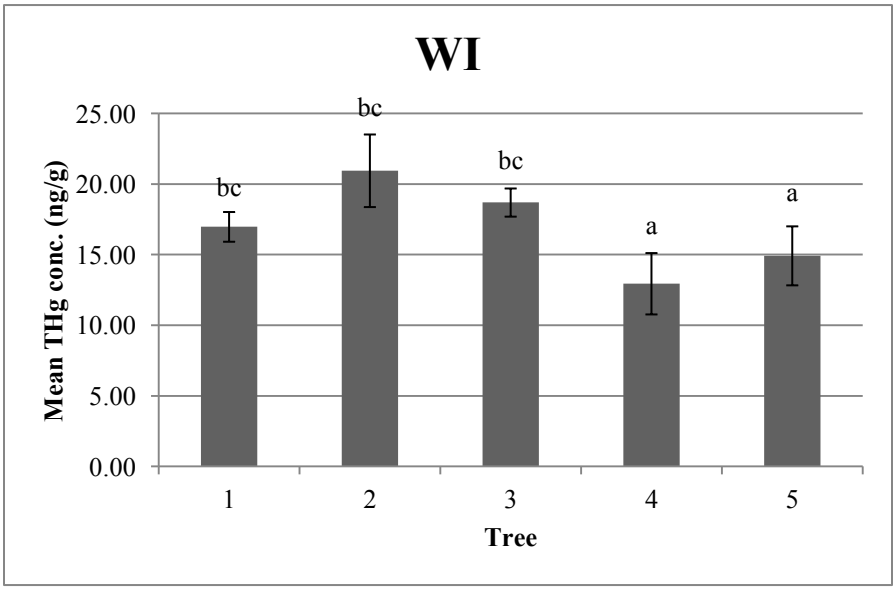

Figure 10.6. Showing WI mean THg concentrations in ng g^{-1} (± 1 SD) for each tree. Means with different letters are significantly different ($p < 0.05$). bc notation signifies that the mean is significantly different from all of the other trees.

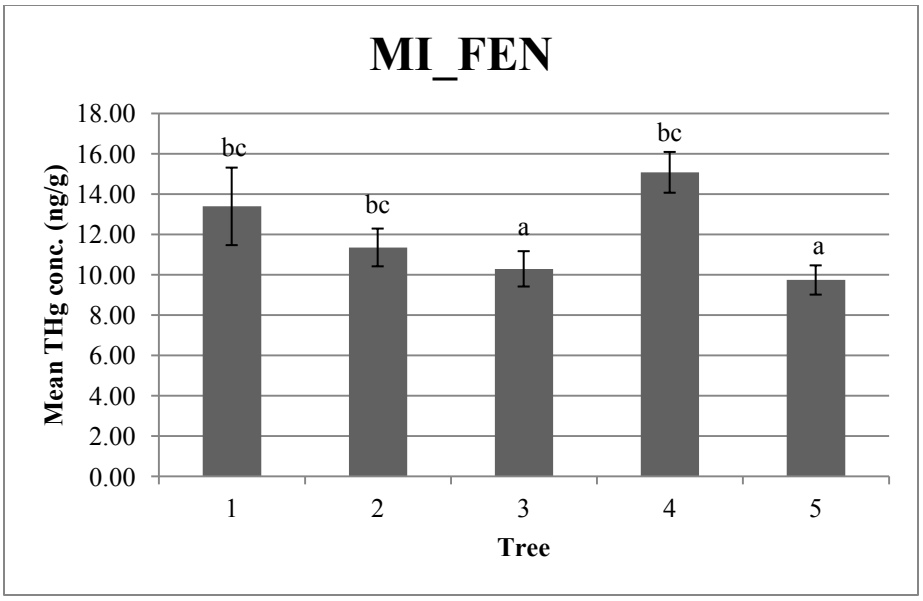

Figure 10.7. Showing MI_FEN mean THg concentrations in ng g^{-1} (± 1 SD) for each tree. Means with different letters are significantly different ($p < 0.05$). bc notation signifies that the mean is significantly different from all of the other trees.

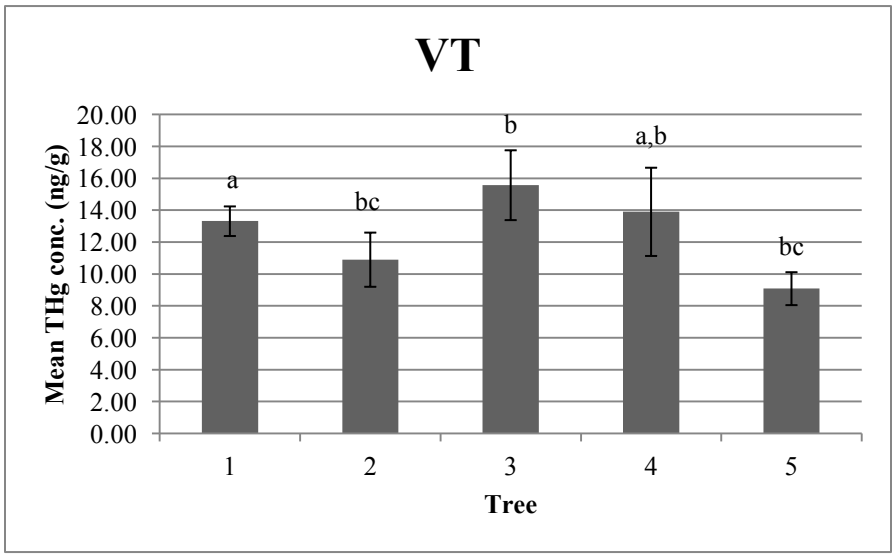

Figure 10.8. Showing VT mean THg concentrations in ng g^{-1} (± 1 SD) for each tree. Means with different letters are significantly different ($p < 0.05$). bc notation signifies that the mean is significantly different from all of the other trees.

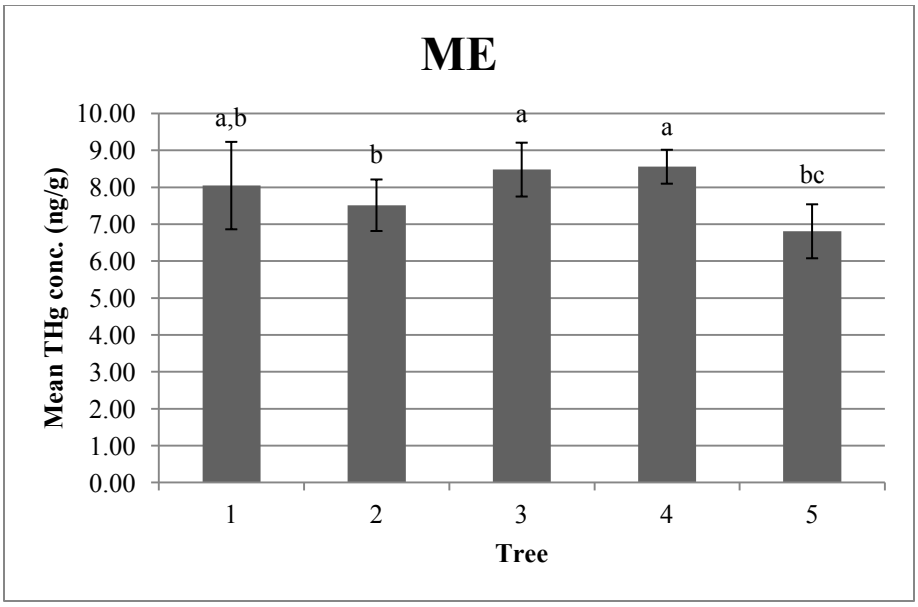

Figure 10.9. Showing ME mean THg concentrations in ng g^{-1} (± 1 SD) for each tree. Means with different letters are significantly different ($p < 0.05$). bc notation signifies that the mean is significantly different from all of the other trees.

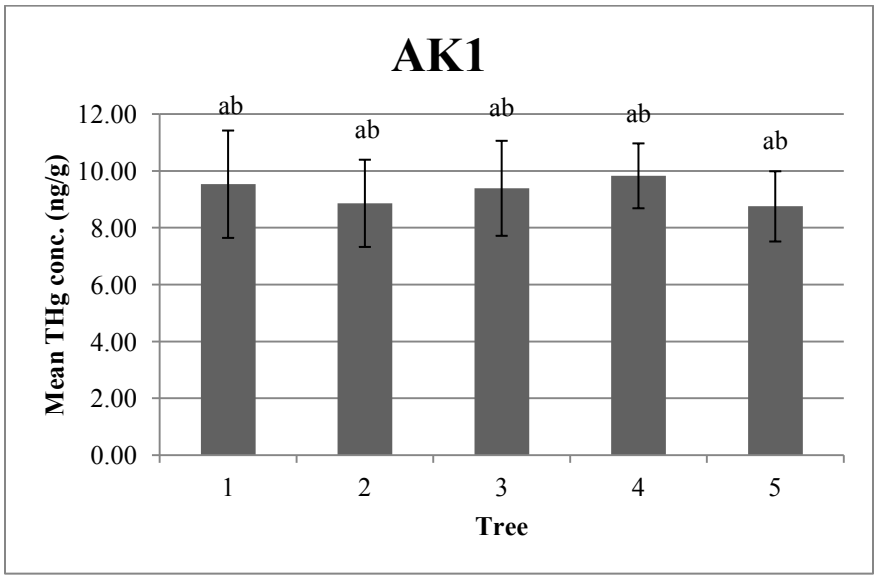

Figure 10.10. Showing AK1 mean THg concentrations in ng g^{-1} (± 1 SD) for each tree. Means with different letters are significantly different ($p < 0.05$). ab notation signifies that the mean is not significantly different from all of the other trees.

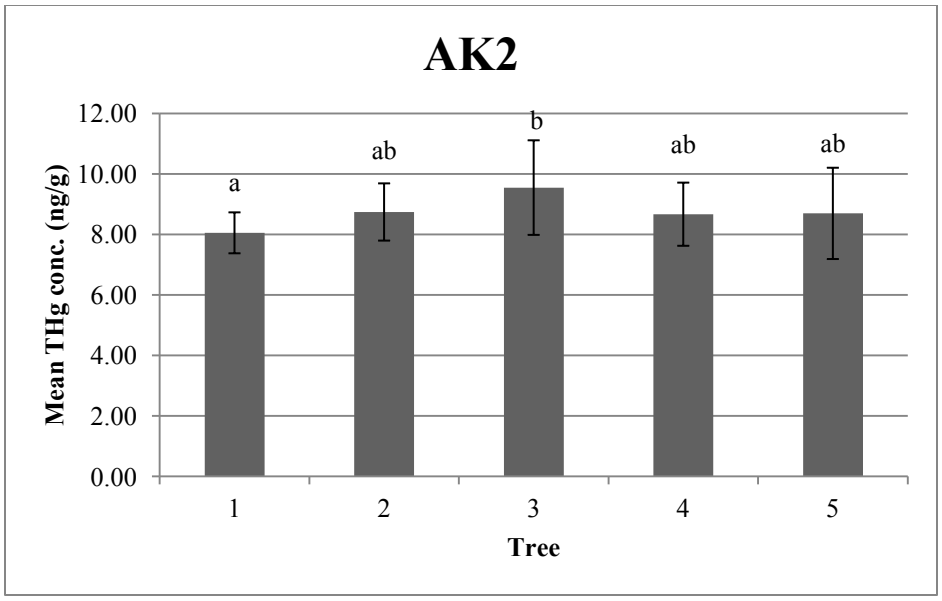

Figure 10.11. Showing AK2 mean THg concentrations in ng g^{-1} (± 1 SD) for each tree. Means with different letters are significantly different ($p < 0.05$). ab notation signifies that the mean is not significantly different from all of the other trees.

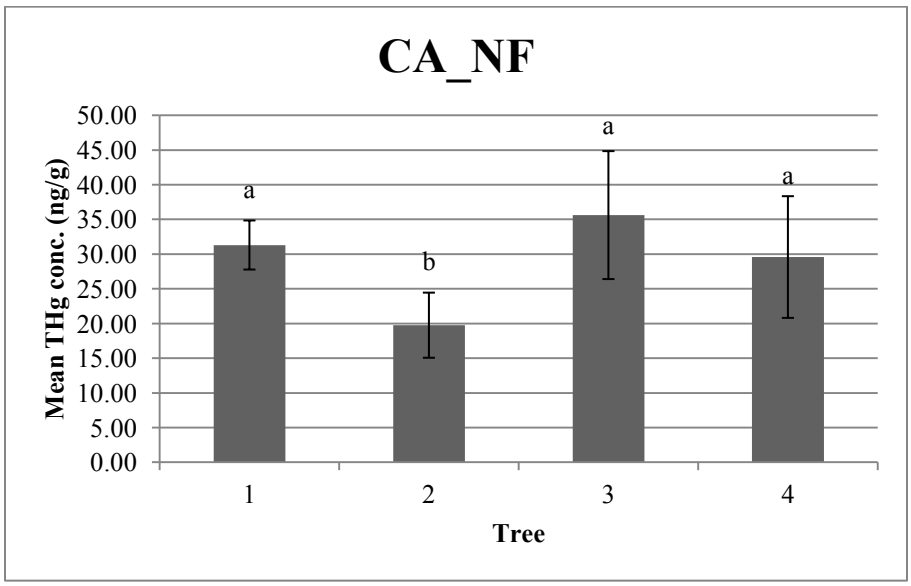

Figure 10.12. Showing CA_NF mean THg concentrations in ng g^{-1} (± 1 SD) for each tree. Means with different letters are significantly different ($p < 0.05$).

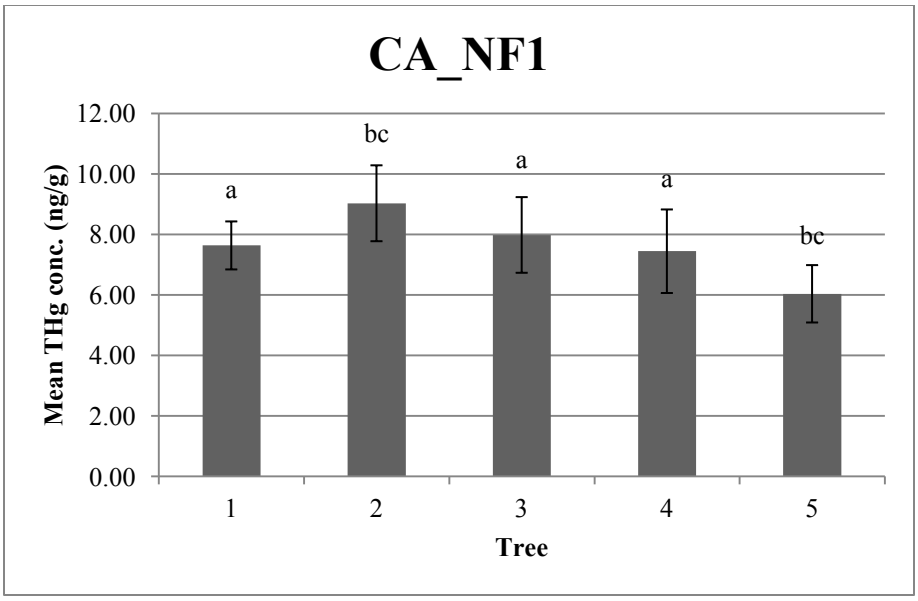

Figure 10.13. Showing CA_NF1 mean THg concentrations in ng g^{-1} (± 1 SD) for each tree. Means with different letters are significantly different ($p < 0.05$). bc notation signifies that the mean is significantly different from all of the other trees.

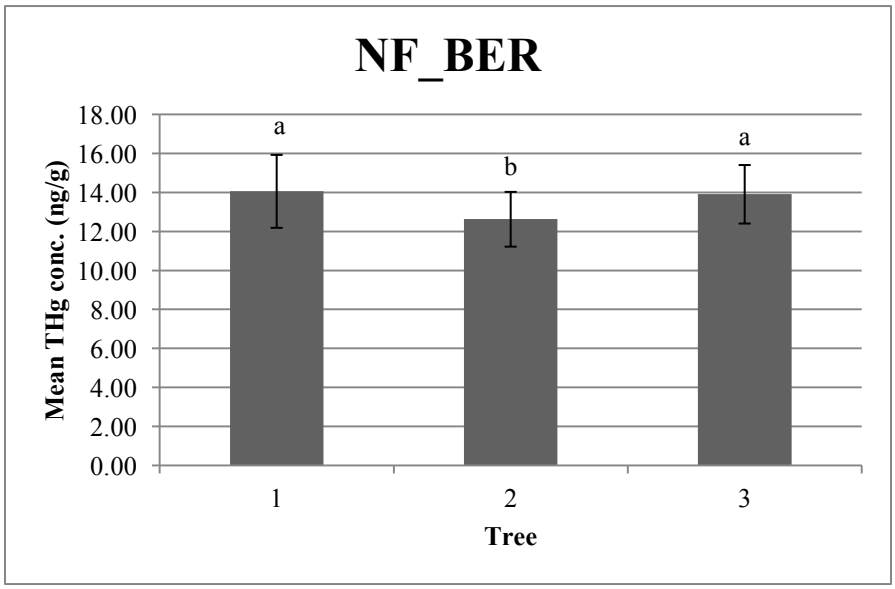

Figure 10.14. Showing NF_BER mean THg concentrations in ng g^{-1} (± 1 SD) for each tree. Means with different letters are significantly different ($p < 0.05$).

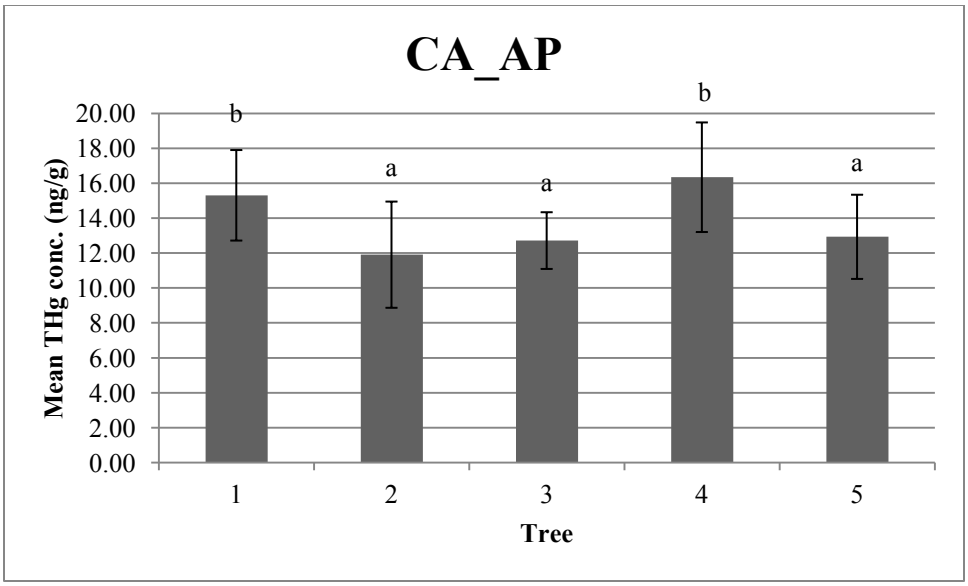

Figure 10.15. Showing CA_AP mean THg concentrations in ng g^{-1} (± 1 SD) for each tree. Means with different letters are significantly different ($p < 0.05$).

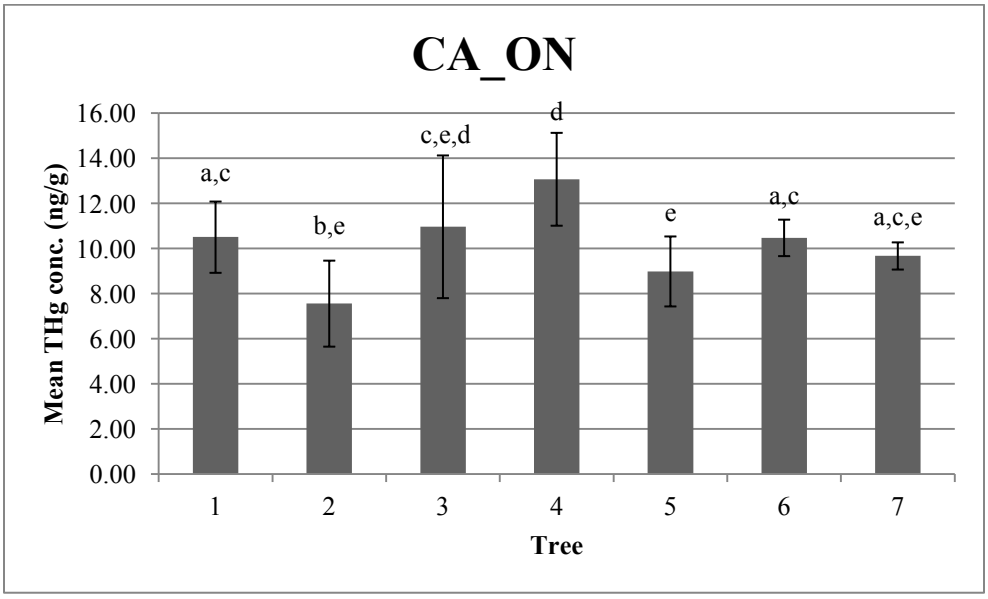

Figure 10.16. Showing CA_ON mean THg concentrations in ng g^{-1} (± 1 SD) for each tree. Means with different letters are significantly different ($p < 0.05$).

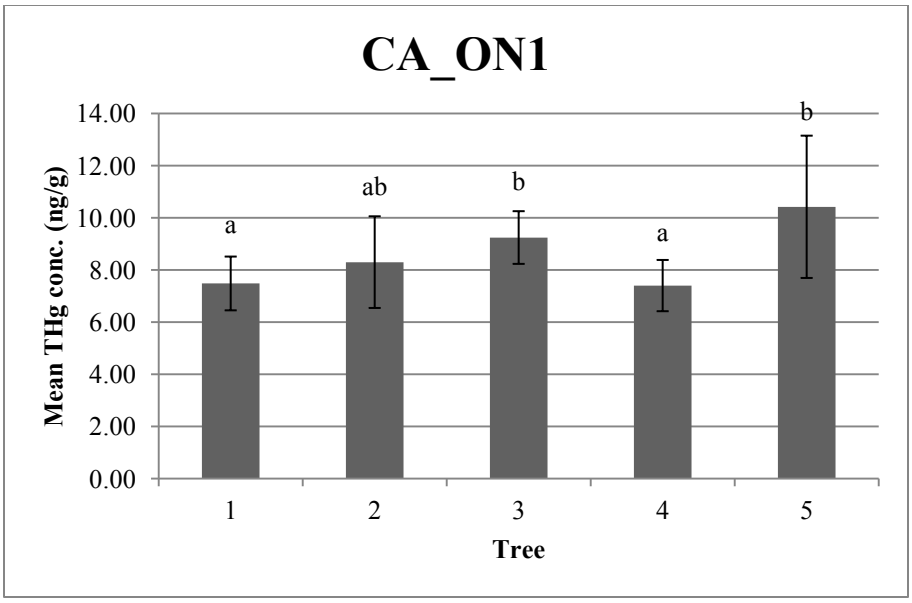

Figure 10.17. Showing CA_ON1 mean THg concentrations in ng g^{-1} (± 1 SD) for each tree. Means with different letters are significantly different ($p < 0.05$). ab notation signifies that the mean is not significantly different from all of the other trees.

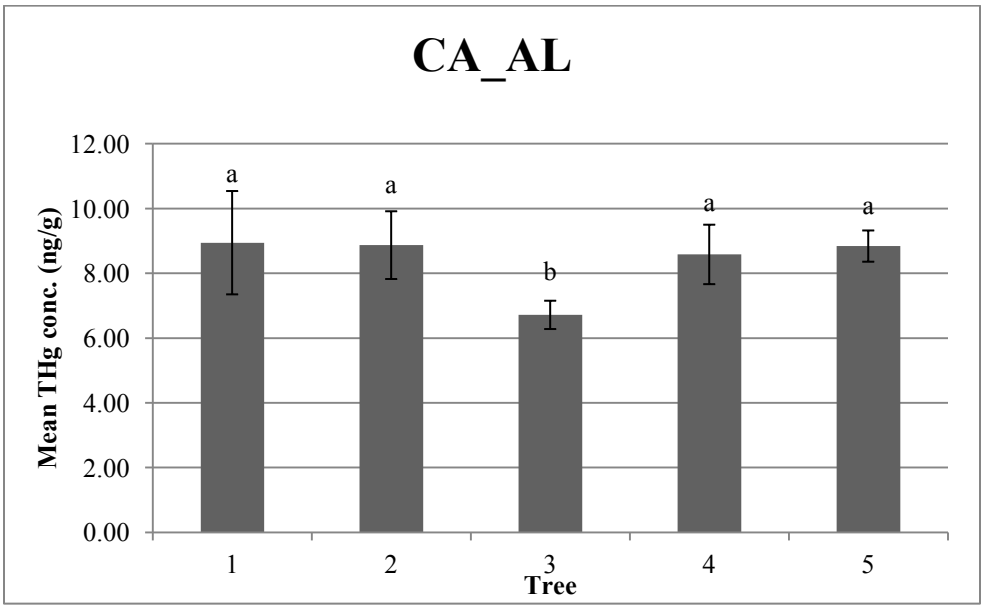

Figure 10.18. Showing CA_AL mean THg concentrations in ng g^{-1} (± 1 SD) for each tree. Means with different letters are significantly different ($p < 0.05$).

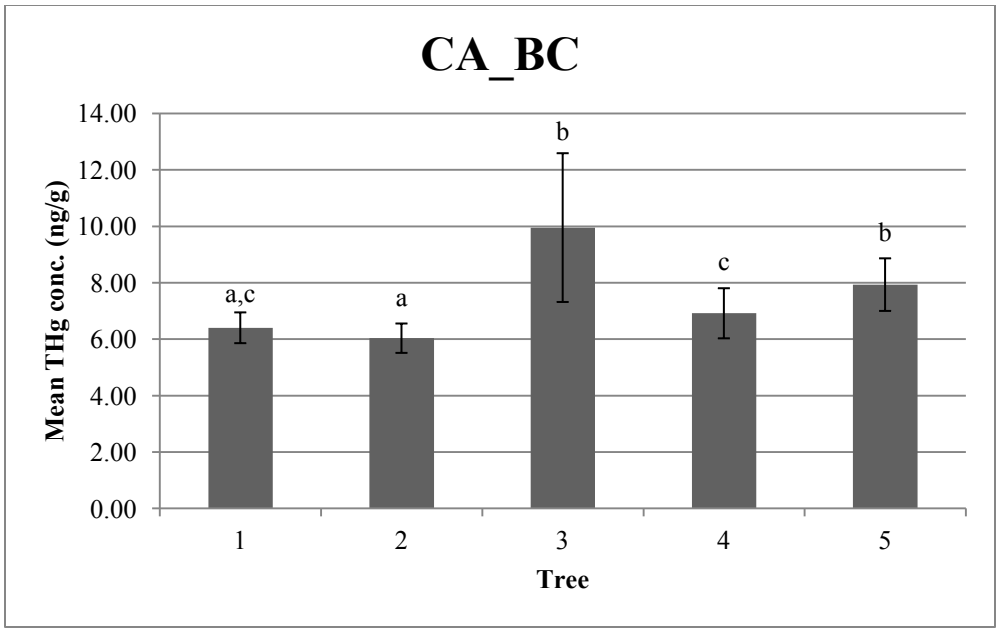

Figure 10.19. Showing CA_BC mean THg concentrations in ng g^{-1} (± 1 SD) for each tree. Means with different letters are significantly different ($p < 0.05$).

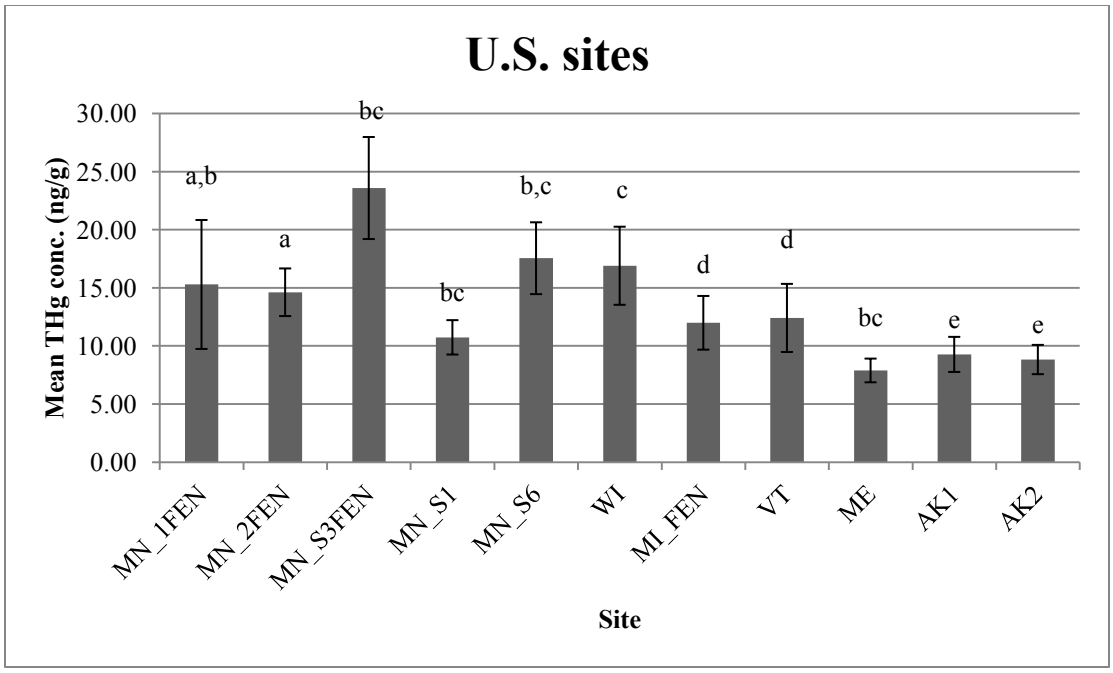

Figure 11. Showing mean THg concentrations in ng g^{-1} (± 1 SD) for each U.S. site. Means with different letters are significantly different ($p < 0.05$). bc notation signifies that the mean is significantly different from all of the other sites.

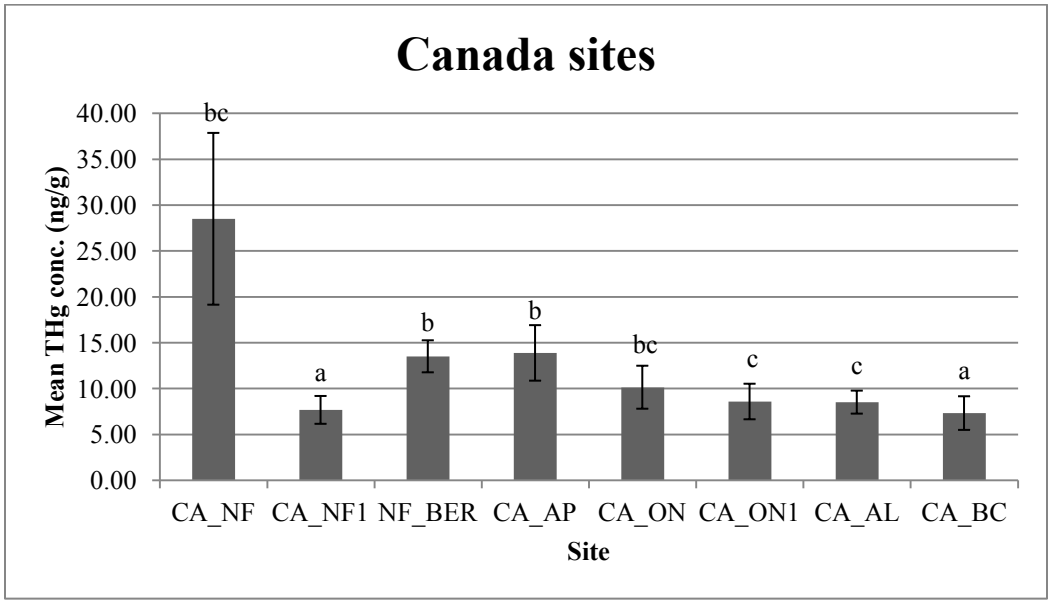

Figure 12. Showing mean THg concentrations in ng g^{-1} (± 1 SD) for each Canada site. Means with different letters are significantly different ($p < 0.05$). bc notation signifies that the mean is significantly different from all of the other sites.

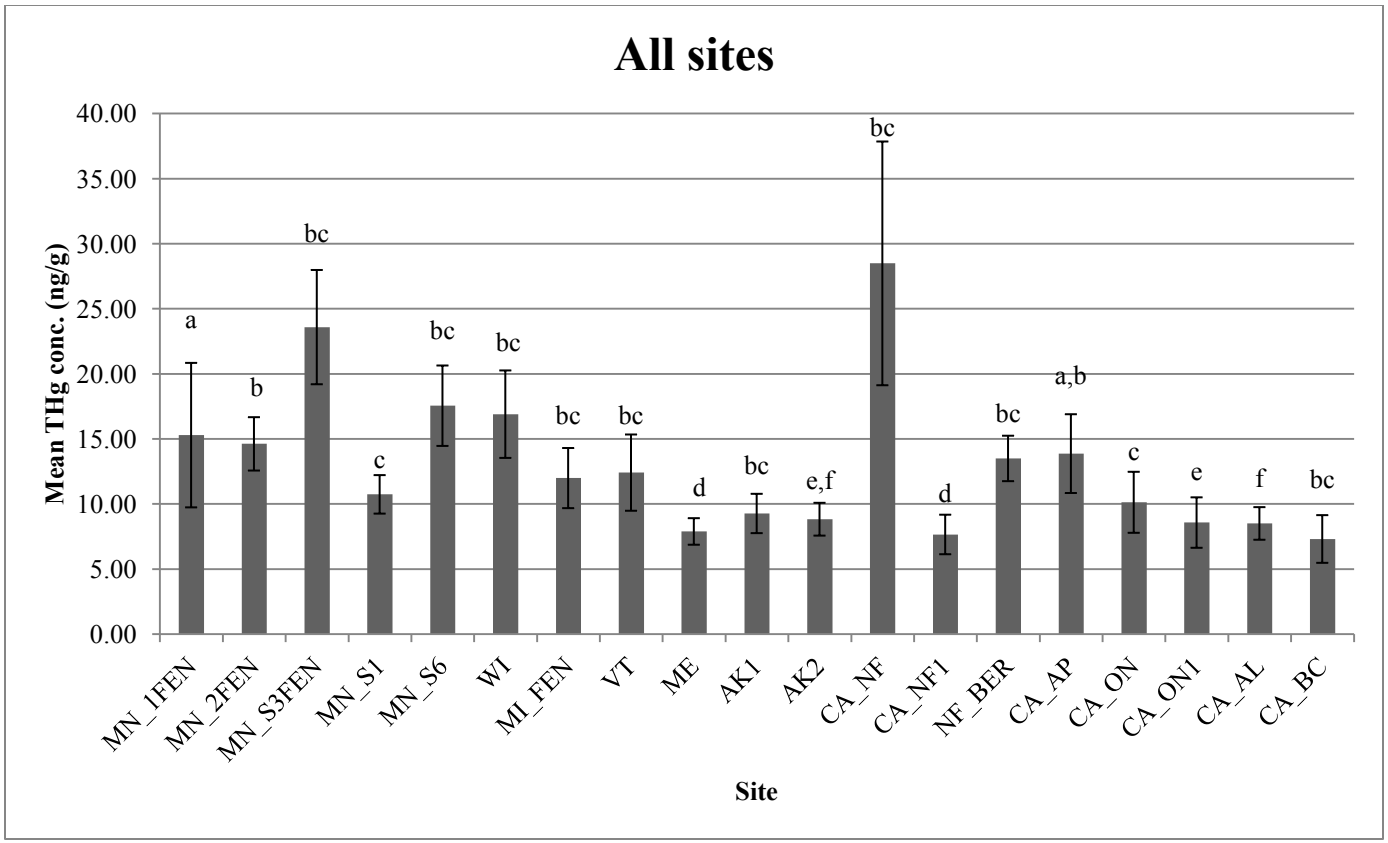

Figure 13. Showing mean THg concentrations in ng g^{-1} (± 1 SD) for all site. Means with different letters are significantly different ($p < 0.05$). bc notation signifies that the mean is significantly different from all of the other sites.

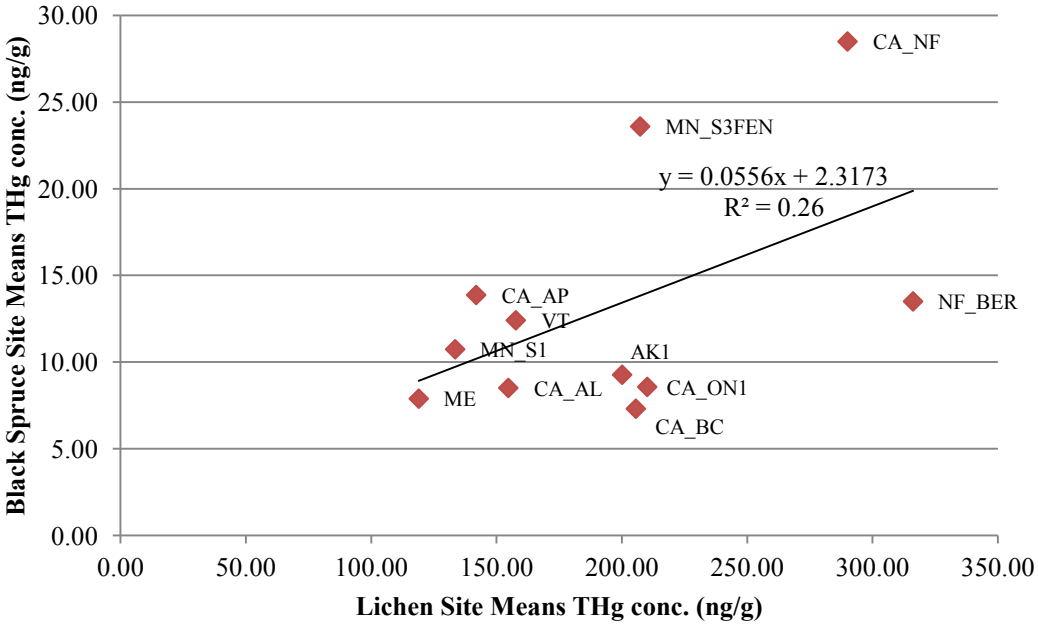

Figure 14. Showing the relationship between the black spruce site means and lichen site means for all sites where lichen was collected (MN_S3FEN, MN_S1, VT, ME, AK1, CA_NF, NF_BER, CA_AP, CA_ON1, CA_AL and CA_BC).

Tables 1. GPS locations of all U.S and Canada sites.

U.S. samples							
Site ID	**State**	**Map Datum**	**UTM Zone**	**Northing**	**Easting**	**Latitude**	**Longitude**
1FEN	MN	NAD 83	15N	5229735	520729	47.22	-92.73
2FEN	MN	NAD 83	15N	5201702	503617	46.97	-92.95
S3FEN	MN	NAD 83	15N	5263860	465058	47.53	-93.46
S6	MN	NAD 83	15N	5263065	464530	47.52	-93.47
S1	MN	NAD 83	15N	5261777	465910	47.51	-93.45
FEN	MI	NAD 83	16N	5093205	439889	45.99	-87.78
WI	WI	NAD 83	15N	5103889	727636	46.05	-90.06
ME	ME	NAD 83	19N	4988582	519843	45.05	-68.75
VT	VT	NAD 83	18N	4908150	720011	44.29	-72.24
AK1	AK	NAD 83	6N	7193990	458362	64.87	-147.88
AK2	AK	NAD 83	7N	7008557	393695	63.19	-143.11

Canada samples							
Site ID	**Province**	**Map Datum**	**UTM Zone**	**Northing**	**Easting**	**Latitude**	**Longitude**
CA_NF	NF&L	NAD 83	21N	5367596	396646	48.45	-58.40
CA_NF1	NF&L	NAD 83	20N	5942156	689905	53.59	-60.13
CA_AP	NF&L	NAD 83	22T	5238757	328598	47.28	-53.27
NF_BER	NF&L	NAD 83	21N	5612118	490792	50.66	-57.13
CA_ON	ON	NAD 83	17N	5432718	572840	49.04	-80.00
CA_ON1	ON	NAD 83	16N	5477614	311257	49.42	-89.60
CA_AL	AL	NAD 83	11U	6015975	553943	54.29	-116.17
CA_BC	BC	NAD 83	10N	6060101	419291	54.68	-124.25

Table 4.1. Site MN_1FEN within tree comparisons for tree 1 & 5. Showing p values of two sample t-test.

Tree/Branch	1C n=6	1D n=5
1B n=8	0.8042	0.5049
1C n=6		0.6591

Tree/Branch	5B n=5	5C n=6	5D n=4
5A n=4	0.4578	0.0840	**0.0384**
5B n=5		0.1835	0.0612
5C n=6			0.5110

Table 4.2. Site MN_S1 within tree comparisons for tree 2 & 4. Showing p values of two sample t-test.

Tree/Branch	2B n=3	2C n=4	2D n=3	2E n=4	2F n=4
2A n=3	0.9610	0.7325	0.9702	0.4795	0.6719
2B n=3		0.5433	0.9776	0.2886	0.3570
2C n=4			0.3052	0.4478	**0.0199**
2D n=3				0.2265	0.1193
2E n=4					0.0977

Tree/Branch	4B n=4
4A n=4	**0.0183**

Table 4.3. Site VT within tree comparison for tree 5. Showing p value of two sample t-test.

Tree/Branch	5C n=4
5B n=5	0.4625

Table 4.4. Site CA_NF1 within tree comparison for tree 1. Showing p value of two sample t-test.

Tree/Branch	1B n=6
1A n=4	0.4411

Table 4.5. Site NF_BER within tree comparisons for tree 1 & 2. Showing p values of two sample t-test.

Tree/Branch	1B n=5	1C n=5
1A n=7	**0.0006**	**0.0314**
1B n=5		**0.0006**

Tree/Branch	2C n=3	2D n=4	2E n=4
2A n=6	0.3922	0.2384	0.9121
2C n=3		**0.0462**	0.3458
2D n=4			0.1221

Table 4.6. Site CA_NF within tree comparisons for tree 3. Showing p values of two sample t-test.

Tree/Branch	3C n=5	3D n=3	3E n=3
3B n=6	**0.0360**	**2.48E-05**	**0.0008**
3C n=5		**0.0029**	**0.0061**
3D n=3			0.7162

Table 5.1. Top half shows summary of statistics for each tree and bottom half shows p values of two sample t-tests for site MN_1FEN.

MN_1FEN	# of samples	Mean	StDev
Tree1	21	16.78	3.45
Tree2	12	12.32	3.25
Tree3	10	24.13	3.95
Tree4	6	16.71	2.18
Tree5	17	9.84	1.40
Total	**66**	**15.29**	**5.55**

Tree	2	3	4	5
1	**0.0011**	**0.0001**	0.9550	**3.9E-09**
2		**7.8E-07**	**0.0043**	**0.0261**
3			**0.0003**	**6.4E-07**
4				**0.0002**

Table 5.2. Top half shows summary of statistics for each tree and bottom half shows p values of two sample t-tests for site MN_2FEN.

MN_2FEN	# of samples	Mean	StDev
Tree1	10	13.67	1.11
Tree2	10	12.99	1.25
Tree3	10	13.62	2.11
Tree4	10	15.84	1.24
Tree5	10	17.00	1.00
Total	**50**	**14.62**	**2.05**

Tree	2	3	4	5
1	0.2130	0.9490	**0.0006**	**1.4E-06**
2		0.4281	**7.0E-05**	**4.1E-07**
3			**0.0117**	**0.0005**
4				**0.0350**

Table 5.3. Top half shows summary of statistics for each tree and bottom half shows p values of two sample t-tests for site MN_S3FEN.

MN_S3FEN	# of samples	Mean	StDev
Tree1	11	20.44	1.65
Tree2	11	25.56	2.43
Tree3	10	19.67	2.03
Tree4	10	26.30	4.81
Tree5	8	26.72	4.71
Total	**50**	**23.59**	**4.39**

Tree	2	3	4	5
1	**1.8E-05**	0.3538	**0.0037**	**0.0068**
2		**8.0E-06**	0.6676	0.5372
3			**0.0017**	**0.0033**
4				0.8547

Table 5.4. Top half shows summary of statistics for each tree and bottom half shows p values of two sample t-tests for site MN_S1.

MN_S1	# of samples	Mean	StDev
Tree1	10	11.57	1.24
Tree2	21	10.90	1.19
Tree3	15	10.91	1.97
Tree4	13	9.64	0.76
Total	**59**	**10.74**	**1.48**

Tree	2	3	4
1	0.1742	0.3167	**0.0007**
2		0.9883	**0.0007**
3			**0.0329**

Table 5.5. Top half shows summary of statistics for each tree and bottom half shows p values of two sample t-tests for site MN_S6.

MN_S6	# of samples	Mean	StDev	
Tree1	10	21.63	1.82	
Tree2	10	15.29	1.43	
Tree3	10	19.64	1.84	
Tree4	10	16.59	1.02	
Tree5	10	14.61	1.61	
Total	**50**	**17.55**	**3.09**	
Tree	**2**	**3**	**4**	**5**
1	**1.2E-07**	**0.0260**	**2.3E-06**	**3.5E-08**
2		**1.7E-05**	**0.0327**	0.3331
3			**0.0004**	**3.9E-06**
4				**0.0050**

Table 5.6. Top half shows summary of statistics for each tree and bottom half shows p values of two sample t-tests for site WI.

WI	# of samples	Mean	StDev	
Tree1	10	16.98	1.05	
Tree2	10	20.95	2.57	
Tree3	10	18.70	1.00	
Tree4	10	12.95	2.17	
Tree5	10	14.92	2.09	
Total	**50**	**16.90**	**3.36**	
Tree	**2**	**3**	**4**	**5**
1	**0.0007**	**0.0014**	**0.0002**	**0.0158**
2		**0.0240**	**5.9E-07**	**2.4E-05**
3			**3.9E-06**	**0.0002**
4				0.0527

Table 5.7. Top half shows summary of statistics for each tree and bottom half shows p values of two sample t-tests for site MI_FEN.

MI_FEN	# of samples	Mean	StDev
Tree1	9	13.40	1.92
Tree2	9	11.36	0.94
Tree3	20	10.30	0.88
Tree4	13	15.08	1.01
Tree5	6	9.74	0.73
Total	**57**	**11.99**	**2.31**

Tree	2	3	4	5
1	**0.0144**	**0.0009**	**0.0344**	**0.0003**
2		**0.0114**	**5.4E-08**	**0.0024**
3			**9.8E-13**	0.1504
4				**7.3E-09**

Table 5.8. Top half shows summary of statistics for each tree and bottom half shows p values of two sample t-tests for site VT.

VT	# of samples	Mean	StDev
Tree1	14	13.31	0.93
Tree2	16	10.90	1.70
Tree3	13	15.57	2.19
Tree4	16	13.90	2.77
Tree5	16	9.08	1.03
Total	**75**	**12.41**	**2.93**

Tree	2	3	4	5
1	**5.3E-05**	**0.0033**	0.4342	**2.1E-12**
2		**2.4E-06**	**0.0011**	**0.0012**
3			0.0805	**3.4E-08**
4				**3.0E-06**

Table 5.9. Top half shows summary of statistics for each tree and bottom half shows p values of two sample t-tests for site ME.

ME	# of samples	Mean	StDev
Tree1	12	8.05	1.18
Tree2	10	7.51	0.70
Tree3	10	8.48	0.73
Tree4	10	8.56	0.46
Tree5	10	6.81	0.73
Total	**52**	**7.89**	**1.02**

Tree	2	3	4	5
1	0.2075	0.3073	0.1891	**0.0074**
2		**0.0073**	**0.0012**	**0.0404**
3			0.7779	**7.3E-05**
4				**1.2E-05**

Table 5.10. Top half shows summary of statistics for each tree and bottom half shows p values of two sample t-tests for site AK1.

AK1	# of samples	Mean	StDev
Tree1	9	9.53	1.89
Tree2	11	8.86	1.53
Tree3	9	9.39	1.67
Tree4	9	9.83	1.14
Tree5	8	8.76	1.24
Total	**46**	**9.27**	**1.51**

Tree	2	3	4	5
1	0.4031	0.8664	0.6948	0.3265
2		0.4755	0.1237	0.8685
3			0.5258	0.3836
4				0.0849

Table 5.11. Top half shows summary of statistics for each tree and bottom half shows p values of two sample t-tests for site AK2.

AK2	# of samples	Mean	StDev
Tree1	9	8.06	0.68
Tree2	9	8.75	0.95
Tree3	10	9.55	1.56
Tree4	10	8.67	1.04
Tree5	8	8.70	1.51
Total	**46**	**8.83**	**1.26**

Tree	2	3	4	5
1	0.0771	**0.0101**	0.0748	0.2959
2		0.1475	0.9617	0.8783
3			0.1613	0.1926
4				0.8525

Table 5.12. Top half shows summary of statistics for each tree and bottom half shows p values of two sample t-tests for site CA_NF.

CA_NF	# of samples	Mean	StDev
Tree1	11	31.29	3.54
Tree2	18	19.74	4.69
Tree3	16	35.60	9.22
Tree4	12	29.56	8.77
Total	**57**	**28.49**	**9.36**

Tree	2	3	4
1	**5.5E-08**	0.1043	0.5379
2		**3.0E-06**	**0.0029**
3			0.0902

Table 5.13. Top half shows summary of statistics for each tree and bottom half shows p values of two sample t-tests for site CA_NF1.

CA_NF1	# of samples	Mean	StDev
Tree1	18	7.64	0.79
Tree2	19	9.03	1.25
Tree3	13	7.99	1.25
Tree4	20	7.45	1.38
Tree5	16	6.04	0.95
Total	**86**	**7.66**	**1.52**

Tree	2	3	4	5
1	**0.0003**	0.3901	0.6268	**1.1E-05**
2		**0.0282**	**0.0011**	**2.9E-09**
3			0.2785	**0.0001**
4				**0.0019**

Table 5.14. Top half shows summary of statistics for each tree and bottom half shows p values of two sample t-tests for site NF_BER

NF_BER	# of samples	Mean	StDev
Tree1	22	14.06	1.87
Tree2	19	12.63	1.40
Tree3	10	13.91	1.50
Total	**51**	**13.50**	**1.75**

Tree	2	3
1	**0.0082**	0.8109
2		**0.0392**

Table 5.15. Top half shows summary of statistics for each tree and bottom half shows p values of two sample t-tests for site CA_AP.

CA_AP	# of samples	Mean	StDev
Tree1	20	15.31	2.59
Tree2	17	11.91	3.04
Tree3	25	12.72	1.63
Tree4	21	16.35	3.14
Tree5	20	12.93	2.41
Total	**103**	**13.87**	**3.03**

Tree	2	3	4	5
1	**0.0010**	**0.0005**	0.2554	**0.0047**
2		0.3274	**9.5E-05**	0.2717
3			**4.6E-05**	0.7340
4				**0.0004**

Table 5.16. Top half shows summary of statistics for each tree and bottom half shows p values of two sample t-tests for site CA_ON.

CA_ON	# of samples	Mean	StDev
Tree1	12	10.51	1.58
Tree2	11	7.56	1.91
Tree3	11	10.97	3.16
Tree4	10	13.07	2.06
Tree5	11	8.99	1.55
Tree6	10	10.48	0.81
Tree7	13	9.67	0.60
Total	**78**	**10.13**	**2.34**

Tree	2	3	4	5	6	7
1	**0.0007**	0.6692	**0.0049**	**0.0302**	0.9542	0.1088
2		**0.0075**	**5.6E-06**	0.0692	**0.0004**	**0.0041**
3			0.0859	0.0820	0.6282	0.2087
4				**8.9E-05**	**0.0030**	**0.0005**
5					**0.0137**	0.1900
6						**0.0182**

Table 5.17. Top half shows summary of statistics for each tree and bottom half shows p values of two sample t-tests for site CA_ON1.

CA_ON1	# of samples	Mean	StDev
Tree1	10	7.48	1.03
Tree2	12	8.30	1.76
Tree3	11	9.24	1.01
Tree4	10	7.40	0.98
Tree5	10	10.42	2.73
Total	**53**	**8.57**	**1.94**

Tree	2	3	4	5
1	0.1918	**0.0009**	0.8579	**0.0078**
2		0.1284	0.1478	0.0511
3			**0.0004**	0.2243
4				**0.0071**

Table 5.18. Top half shows summary of statistics for each tree and bottom half shows p values of two sample t-tests for site CA_AL.

CA_AL	# of samples	Mean	StDev
Tree1	13	8.94	1.60
Tree2	30	8.87	1.05
Tree3	12	6.71	0.44
Tree4	12	8.58	0.92
Tree5	12	8.84	0.48
Total	**79**	**8.51**	**1.25**

Tree	2	3	4	5
1	0.8777	**0.0003**	0.4907	0.8240
2		**1.1E-11**	0.3884	0.9003
3			**9.5E-06**	**1.2E-10**
4				0.4020

Table 5.19. Top half shows summary of statistics for each tree and bottom half shows p values of two sample t-tests for site CA_BC.

CA_BC	# of samples	Mean	StDev
Tree1	12	6.41	0.55
Tree2	12	6.04	0.52
Tree3	9	9.96	2.64
Tree4	10	6.92	0.89
Tree5	10	7.94	0.93
Total	**53**	**7.31**	**1.83**

Tree	2	3	4	5
1	0.1035	**0.0032**	0.1332	**0.0004**
2		**0.0023**	**0.0150**	**5.1E-05**
3			**0.0081**	0.0542
4				**0.0226**

Table 6. Summary of p values for all comparisons between US sites.

Site	MN_2FEN	MN_S3FEN	MN_S1	MN_S6	WI	MI_FEN	VT	ME	AK1	AK2
MN_1FEN	0.3724	**6.05E-15**	**1.15E-08**	**6.23E-03**	0.0554	**2.88E-05**	**2.80E-04**	**3.23E-16**	**1.75E-12**	**1.00E-13**
MN_2FEN		**2.26E-20**	**1.48E-18**	**2.72E-07**	**9.96E-05**	**8.92E-09**	**2.23E-06**	**4.53E-32**	**1.50E-25**	**2.54E-28**
MN_S3FEN			**1.90E-27**	**5.73E-12**	**2.40E-13**	**1.49E-26**	**4.83E-26**	**4.60E-31**	**2.21E-30**	**1.33E-30**
MN_S1				**3.96E-22**	**3.48E-18**	**8.22E-04**	**3.47E-05**	**3.94E-21**	**2.78E-06**	**1.64E-10**
MN_S6					0.3141	**3.75E-17**	**3.08E-15**	**4.09E-29**	**6.49E-27**	**1.25E-27**
WI						**2.25E-13**	**1.29E-11**	**1.19E-25**	**1.04E-22**	**8.41E-24**
MI_FEN							0.3526	**1.09E-19**	**1.45E-10**	**8.83E-14**
VT								**1.02E-21**	**3.50E-12**	**1.83E-15**
ME									**1.43E-06**	**1.11E-04**
AK1										0.1382

Table 7. Summary of p values for all comparisons between Canadian sites.

Site	CA_NF1	NF_BER	CA_AP	CA_ON	CA_ON1	CA_AL	CA_BC
CA_NF	**9.17E-24**	**2.29E-17**	**4.73E-17**	**2.14E-21**	**4.24E-23**	**9.40E-23**	**1.78E-24**
CA_NF1		**2.12E-35**	**1.39E-40**	**9.12E-13**	**4.33E-03**	**1.29E-04**	0.2507
NF_BER			0.3368	**4.60E-16**	**1.00E-24**	**6.53E-30**	**9.31E-33**
CA_AP				**3.05E-17**	**6.92E-27**	**2.45E-34**	**2.50E-36**
CA_ON					**6.35E-05**	**3.54E-07**	**3.40E-12**
CA_ON1						0.8254	**8.28E-04**
CA_AL							**8.18E-05**

Table 8. Summary of p values for all comparisons between US and Canadian sites.

Site	CA_NF	CA_NF1	NF_BER	CA_AP	CA_ON	CA_ON1	CA_AL	CA_BC
MN_1FEN	**8.88E-15**	**6.69E-17**	**1.58E-02**	0.0606	**4.87E-10**	**2.82E-14**	**1.10E-14**	**9.87E-18**
MN_2FEN	**5.05E-16**	**1.98E-34**	**3.83E-03**	0.0729	**1.06E-20**	**4.10E-28**	**9.27E-30**	**9.80E-35**
MN_S3FEN	**6.85E-04**	**6.87E-32**	**8.38E-23**	**2.04E-22**	**7.15E-30**	**1.24E-32**	**3.36E-30**	**2.52E-34**
MN_S1	**1.31E-20**	**4.46E-23**	**3.09E-14**	**2.00E-15**	0.0658	**2.30E-09**	**1.00E-15**	**1.68E-18**
MN_S6	**4.76E-12**	**2.25E-30**	**6.74E-12**	**4.43E-10**	**9.80E-25**	**1.68E-29**	**1.25E-27**	**4.29E-33**
WI	**6.73E-13**	**1.38E-26**	**1.52E-08**	**5.46E-07**	**2.57E-20**	**4.65E-25**	**3.85E-24**	**1.02E-28**
MI_FEN	**2.31E-19**	**3.81E-21**	**2.00E-04**	**2.07E-05**	**1.10E-05**	**1.88E-13**	**2.24E-16**	**5.84E-21**
VT	**7.68E-19**	**4.33E-23**	**1.03E-02**	**1.47E-03**	**3.98E-07**	**4.26E-15**	**3.69E-18**	**9.10E-23**
ME	**2.24E-23**	0.2881	**1.05E-32**	**1.81E-38**	**1.96E-11**	**2.58E-02**	**2.43E-03**	**4.86E-02**
AK1	**2.60E-22**	**8.61E-08**	**2.30E-22**	**2.04E-24**	**1.45E-02**	**4.79E-02**	**4.97E-03**	**7.64E-08**
AK2	**1.07E-22**	**6.39E-06**	**1.06E-26**	**1.02E-29**	**1.11E-04**	0.4229	0.1631	**4.68E-06**

Appendix II

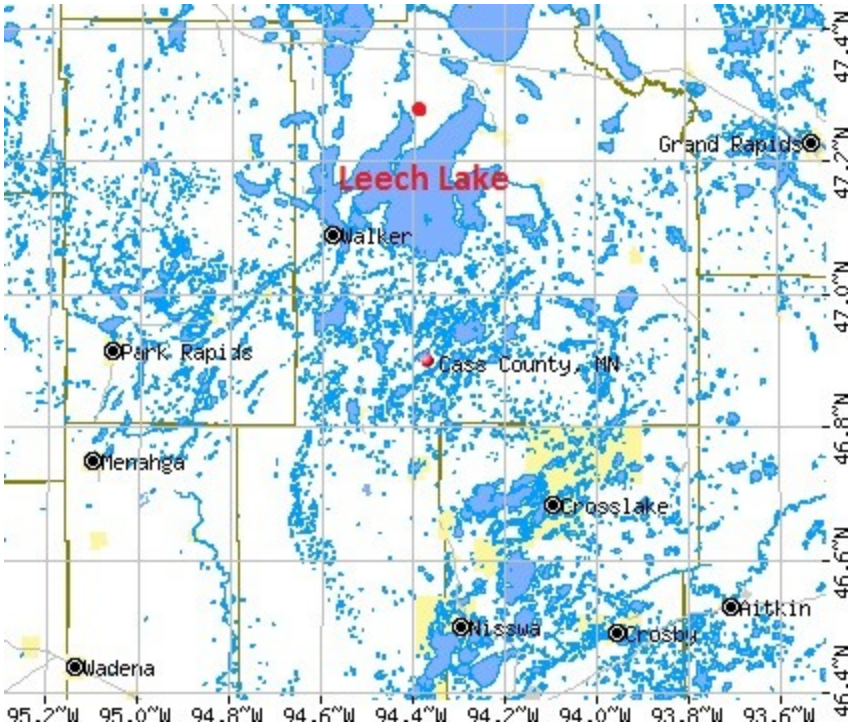

Figure 1. The general location of the earthworm invasion transect (red dot) by northern parts of Leech Lake. Image Source: www.city-data.com

Figure 2. Close up of the earthworm invasion transect. For 2009 soil, pit 0 is located at the red circle labeled begin transect and pit 190 is located at the red circle labeled end transect. 2014 soil was collected from the invaded area indicated by the yellow pin on the left side while the uninvaded area extends 40 meters (yellow uninvaded pin) past the end of the original earthworm transect. Image source: Google Earth

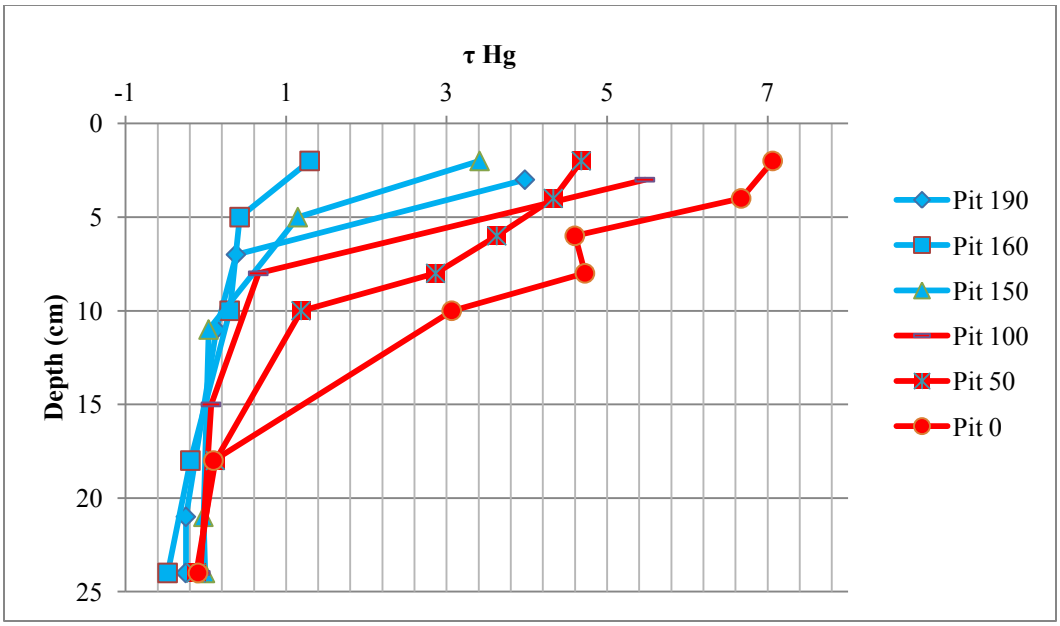

Figure 3. Graphed tau values of all mineral soil pits from 2009 samples. Blue markers represent least invaded soils and red markers represent most invaded soils.

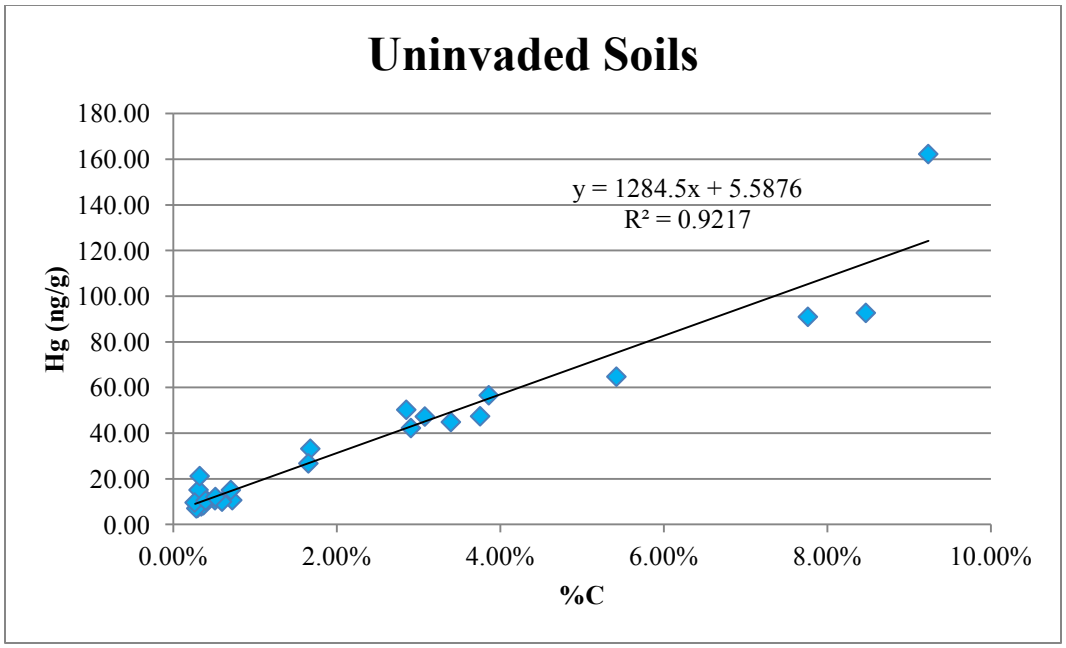

Figure 4. Relationship of Hg (ng/g) to %C in the uninvaded mineral soils of 2014 samples.

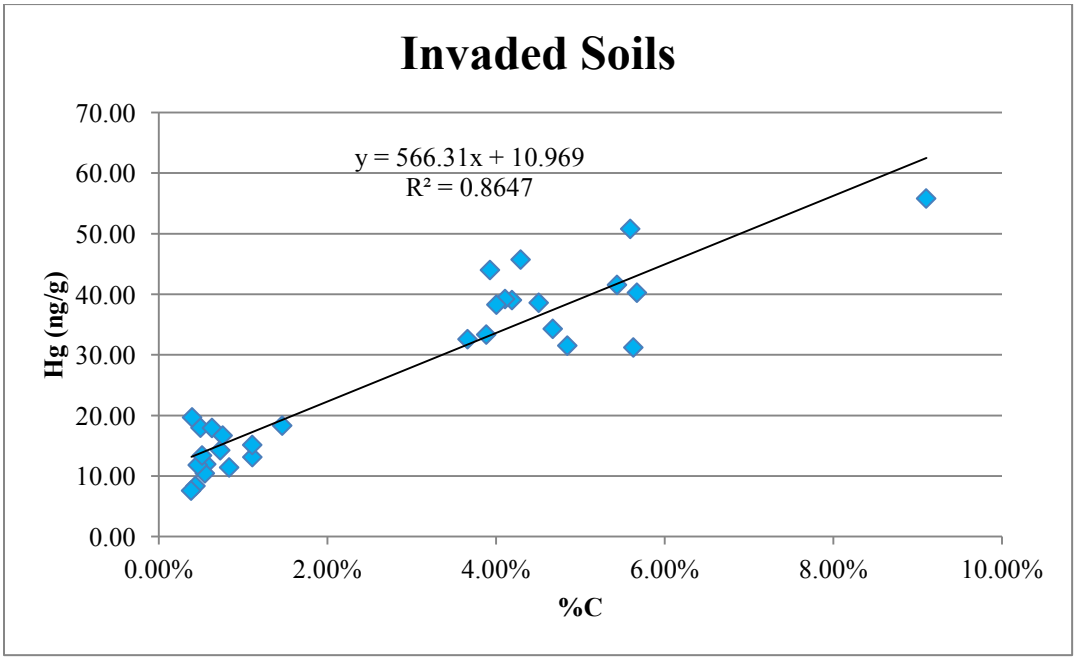

Figure 5. Relationship of Hg (ng/g) to %C in the invaded mineral soils of 2014 samples.

Table 4. Showing the original horizon designations from Resner (2013) and the amended new designations based on the bulk density and %LOI of the samples.

Pit	BD (g/cm^3)	%LOI	Depth (cm)	Resner Horizon Designations	New Depth (cm)	New Horizon Designations
190	0.27	59.90%	0-2	1A1		FF
	0.27	53.50%	2-4	1A1		FF
	0.86	11.20%	4-7	1A2	0-3	A
	0.81	3.64%	7-11	loess	3-7	E
	0.81	2.84%	11-15	loess	7-11	E
	1.13	1.72%	15-25	loess	11-21	E
	1.13	1.17%	25-35	loess	21-24	E
160	0.24	65.60%	0-2	1A1		FF
	0.24	54.10%	2-4	1A1		FF
	0.24	30.20%	4-7	1A2		FF
	0.61	8.29%	7-9	1A2	0-2	A
	0.61	5.03%	9-12	A-loess	2-5	A
	1	3.30%	12-17	loess	5-10	E
	1.2	1.92%	17-25	loess	10-18	E
	1.31	1.70%	25-35	1Bw1	18-24	E
150	0.33	66.90%	0-2	1A1		FF
	0.33	55.30%	2-4	1A1		FF
	0.33	32.60%	4-6	1A1		FF
	0.5	8.66%	6-8	1A2	0-2	A
	0.5	4.30%	8-11	1A2	2-5	A
	0.9	2.33%	11-17	A-loess	5-11	E
	1.24	1.38%	17-27	loess	11-21	E
	1.24	1.76%	27-37	loess	21-24	E
100	0.24	32.40%	0-2	1A		FF
	0.24	26.40%	2-4	1A		FF
	0.24	22.00%	4-6	1A		FF
	0.24	13.20%	6-9	1A	0-3	A
	0.56	3.33%	9-14	loess-A	3-8	A
	1.3	2.06%	14-21	loess	8-15	E
	1.3	1.70%	21-31	loess	15-24	E

Table 5. Summary of Hg loadings in the forest floor (FF) of the least invaded pits of the 2009 samples with the overall mean Hg loading in FF reported at the bottom. Forest floor thickness is 6 cm for pits 160, 150 and 100; and 4 cm for pit 190.

Pit	Thickness (cm)	Horizon	BD (g/cm^3)	Hg (ng/g)	Hg Loading (mg/m^2)
190	2	FF	0.27	140.82	0.76
	2	FF	0.27	158.99	0.86
				Hg Loading sum	1.62
160	2	FF	0.24	211.11	1.01
	2	FF	0.24	211.22	1.01
	2	FF	0.24	129.71	0.93
				Hg Loading sum	2.96
150	2	FF	0.33	167.62	1.11
	2	FF	0.33	184.36	1.22
	2	FF	0.33	137.38	0.91
				Hg Loading sum	3.23
100	2	FF	0.24	108.13	0.52
	2	FF	0.24	103.20	0.50
	2	FF	0.24	81.59	0.39
				Hg Loading sum	1.41
Mean Hg loading in FF = 2.30					

Table 6. Summary of Hg loadings to a depth of 24 cm in mineral soil profiles of the least invaded pits of the 2009 samples with the overall mean Hg loading reported at the bottom.

Pit	Depth (cm)	Horizon	BD (g/cm^3)	Hg (ng/g)	Hg Loading (mg/m^2)
190	0-3	A	0.86	47.26	1.22
	3-7	E	0.81	14.47	0.47
	7-11	E	0.81	11.99	0.39
	11-21	E	1.13	8.1	0.92
	21-24	E	1.13	8.13	0.28
				Hg Loading sum	3.27
160	0-2	A	0.61	39.45	0.48
	2-5	A	0.61	25.61	0.47
	5-10	E	1	23.93	1.2
	10-18	E	1.2	15.19	1.46
	18-24	E	1.31	9.9	0.78
				Hg Loading sum	4.38
150	0-2	A	0.5	41.63	0.42
	2-5	A	0.5	21.56	0.32
	5-11	E	0.9	10.68	0.58
	11-21	E	1.24	10.15	1.26
	21-24	E	1.24	10.3	0.38
				Hg Loading sum	2.96
100	0-3	A	0.24	53.91	0.39
	3-8	A	0.56	15.72	0.44
	8-15	E	1.3	10.29	0.94
	15-24	E	1.3	9.05	1.06
				Hg Loading sum	2.82
Mean Hg loading in least invaded soil (combined pits 190, 160, 150, 100)= 3.36					

Table 7. Summary of Hg loadings to a depth of 24 cm in mineral soil profiles of the most invaded pits of the 2009 samples with the overall mean Hg loading reported at the bottom.

Pit	Depth (cm)	Horizon	BD (g/cm^3)	Hg (ng/g)	Hg Loading (mg/m^2)
50	0-2	A	0.55	59.71	0.66
	2-4	A	0.55	58.46	0.64
	4-6	A	0.55	52.15	0.57
	6-8	A	0.55	45.01	0.5
	8-10	A	0.55	26.93	0.3
	11-18	E	1.09	14.09	1.07
	18-24	E	1.32	11.14	0.88
				Hg Loading sum	4.62
0	0-2	A	0.67	53.14	0.71
	2-4	A	0.67	56.63	0.76
	4-6	A	0.67	44.71	0.6
	6-8	A	0.67	48.26	0.65
	8-10	A	0.67	37.77	0.51
	10-18	E	1.14	12.78	1.17
	18-24	E	1.1	10.8	0.71
				Hg Loading sum	5.1
Mean Hg Loading in most invaded soil (combined pits 50 and 0) = 4.86					

Table 8. Summary of tau (τ) values in mineral soil profiles of the least invaded pits of the 2009 samples.

Pit	Depth (cm)	Horizon	BD (g/cm^3)	Hg (ppm)	Zr (ppm)	τ Hg
190	0-3	A	0.86	0.0473	326.05	3.98
	3-7	E	0.81	0.0145	360.65	0.38
	7-11	E	0.81	0.0120	364.31	0.13
	11-21	E	1.13	0.0081	369.44	-0.25
	21-24	E	1.13	0.0081	371.95	-0.25
			E horizon mean	0.0107	366.59	
160	0-2	A	0.61	0.0395	382.67	1.30
	2-5	A	0.61	0.0256	400.59	0.42
	5-10	E	1	0.0239	410.09	0.30
	10-18	E	1.2	0.0152	417.67	-0.19
	18-24	E	1.31	0.0099	418.88	-0.47
			E horizon mean	0.0187	415.55	
150	0-2	A	0.5	0.0416	417.40	3.41
	2-5	A	0.5	0.0216	444.04	1.15
	5-11	E	0.9	0.0107	456.07	0.04
	11-21	E	1.24	0.0101	461.88	-0.03
	21-24	E	1.24	0.0103	459.56	-0.01
			E horizon mean	0.0104	459.17	
100	0-3	A	0.24	0.0539	406.02	5.47
	3-8	A	0.56	0.0157	462.95	0.66
	8-15	E	1.3	0.0103	470.28	0.07
	15-24	E	1.3	0.0090	472.35	-0.07
			E horizon mean	0.0097	471.32	

Table 9. Summary of tau (τ) values in mineral soil profiles of the most invaded pits of the 2009 samples.

Pit	Top	Horizon	BD (g/cm^3)	Hg (ppm)	Zr (ppm)	τ Hg
50	0-2	A	0.55	0.0597	334.37	4.68
	2-4	A	0.55	0.0585	348.78	4.33
	4-6	A	0.55	0.0522	358.52	3.63
	6-8	A	0.55	0.0450	370.41	2.87
	8-10	A	0.55	0.0269	391.40	1.19
	11-18	E	1.09	0.0141	400.00	0.12
	18-24	E	1.32	0.0111	402.52	-0.12
			E horizon mean	0.0126	401.26	
0	0-2	A	0.67	0.0531	200.30	7.07
	2-4	A	0.67	0.0566	224.41	6.67
	4-6	A	0.67	0.0447	242.73	4.60
	6-8	A	0.67	0.0483	256.23	4.73
	8-10	A	0.67	0.0378	282.36	3.07
	10-18	E	1.14	0.0128	354.11	0.10
	18-24	E	1.1	0.0108	362.88	-0.10
			E horizon mean	0.0118	358.49	

Table 10. Summary of delta (δ) values in the forest floor of the least invaded pits of the 2009 samples with the mean delta value reported at the bottom.

Pit	Horizon	BD (g/cm^3)	Hg (ppm)	Zr (ppm)	%LOI	δ Hg ($\mu g/cm^2$)
190	FF	0.27	0.1408	103.15	59.9	0.0546
	FF	0.27	0.1590	132.44	53.5	0.0548
					δ sum	0.1095
160	FF	0.24	0.2111	67.81	65.6	0.0848
	FF	0.24	0.2112	130.99	54.1	0.0694
	FF	0.24	0.1297	262.30	30.2	0.0230
					δ sum	0.1772
150	FF	0.33	0.1676	61.54	66.9	0.0958
	FF	0.33	0.1844	132.42	55.3	0.0866
	FF	0.33	0.1374	271.12	32.6	0.0371
					δ sum	0.2195
100	FF	0.24	0.1081	295.28	32.4	0.0194
	FF	0.24	0.1032	329.88	26.4	0.0149
	FF	0.24	0.0816	355.26	22	0.0096
					δ sum	0.0439
Mean of δ sums for FF: 0.1375						

Table 11. Summary of delta (δ) values for A horizons of all soil profiles of the 2009 samples with the mean delta values reported at the bottom.

Pit	Depth (cm)	Horizon	BD (g/cm^3)	Hg (ppm)	Zr (ppm)	δ Hg ($\mu g/cm^2$)
190	0-3	A	0.86	0.0473	326.05	0.0135
					δ sum	0.0135
160	0-2	A	0.61	0.0395	382.67	0.0038
	2-5	A	0.61	0.0256	400.59	0.0017
					δ sum	0.0055
150	0-2	A	0.5	0.0416	417.40	0.0038
	2-5	A	0.5	0.0216	444.04	0.0011
					δ sum	0.0049
100	0-3	A	0.24	0.0539	406.02	0.0054
	3-8	A	0.56	0.0157	462.95	0.0008
					δ sum	0.0062
50	0-2	A	0.55	0.0597	334.37	0.0109
	2-4	A	0.55	0.0585	348.78	0.0084
	4-6	A	0.55	0.0522	358.52	0.0061
	6-8	A	0.55	0.0450	370.41	0.0038
	8-10	A	0.55	0.0269	391.40	0.0007
					δ sum	0.0300
0	0-2	A	0.67	0.0531	200.30	0.0314
	2-4	A	0.67	0.0566	224.41	0.0284
	4-6	A	0.67	0.0447	242.73	0.0193
	6-8	A	0.67	0.0483	256.23	0.0184
	8-10	A	0.67	0.0378	282.36	0.0107
					δ sum	0.1083
Mean δ for least invaded soils (pits 190, 160, 150, 100)= 0.0075						
Mean δ for most invaded soils (pits 50, 0)= 0.0692						

Table 12. Summary of Hg loadings in the forest floor (FF) of the uninvaded soils of the 2014 samples with the overall mean Hg loading in FF reported at the bottom. Thickness of all forest floor samples is 8 cm.

Sample ID	Thickness (cm)	Horizon	BD (g/cm^3)	Hg (ng/g)	Hg Loading (mg/m^2)
1	8	FF	0.20	168.94	2.67
2	8	FF	0.16	198.29	2.49
3	8	FF	0.17	181.45	2.44
4	8	FF	0.21	146.87	2.42
5	8	FF	0.21	162.15	2.78
6	8	FF	0.19	153.67	2.29
7	8	FF	0.32	160.53	4.12
8	8	FF	0.25	185.32	3.69
9	8	FF	0.28	191.02	4.28
10	8	FF	0.20	115.38	1.85
11	8	FF	0.23	121.35	2.24
12	8	FF	0.19	115.58	1.77
13	8	FF	0.22	141.90	2.53
14	8	FF	0.36	99.97	2.90
15	8	FF	0.19	197.07	2.96
				Mean Hg loading in FF	2.76

Table 13. Summary of Hg loadings to a depth of 24 cm in the uninvaded mineral soils of the 2014 samples with the mean Hg loading reported at the bottom.

Sample ID	Depth (cm)	Horizon	BD (g/cm^3)	Hg (ng/g)	Hg Loading (mg/m^2)
1	0-4	A	0.9	50.25	1.81
1	4-24	E	1.27	11.18	2.83
2	0-3	A	0.96	47.28	1.35
2	3-24	E	1.29	11.86	3.21
3	0-3	A	0.84	42.24	1.06
3	3-24	E	1.33	7.93	2.21
4	0-4	A	0.51	90.96	1.85
4	4-24	E	1.3	10.65	2.76
5	0-1	A	0.73	44.88	1.49
5	1-24	E	1.3	10.63	2.9
6	0-5	A	1.01	33.18	1.68
6	5-24	E	1.32	7.25	1.82
7	0-4	A	0.86	26.77	0.92
7	4-24	E	1.33	15.14	4.04
8	0-5	A	0.87	47.41	2.07
8	5-24	E	1.23	8.44	1.96
9	0-5	A	0.42	92.68	1.95
9	5-24	E	1.2	15.08	3.44
10	0-5	A	0.7	56.6	1.98
10	5-24	E	1.3	7.08	1.75
11	0-5	A	0.46	64.74	1.49
11	5-24	E	1.11	10	2.11
12	0-24	E	1.34	21.18	6.82
13	0-24	E	1.39	9.61	3.2
14	0-24	E	1.28	10.47	3.22
15	0-3.5	A	0.54	162.25	3.04
15	3.5-24	E	1.35	12.03	3.32
Mean Hg loading in uninvaded soil = 4.42					

Table 14. Summary of Hg loadings to a depth of 24 cm in the invaded mineral soils of the 2014 samples with the mean Hg loading reported at the bottom.

Sample ID	Depth (cm)	Horizon	BD (g/cm^3)	Hg (ng/g)	Hg Loading (mg/m^2)
1	0-8	A	0.78	34.31	2.14
1	8-24	E	1.3	8.37	1.74
2	0-13	A	0.64	31.23	2.59
2	13-24	E	1.05	13.13	1.52
3	0-11	A	0.71	41.56	3.23
3	11-24	E	1.03	11.96	1.6
4	0-9	A	0.77	31.54	2.18
4	9-24	E	1.16	10.46	1.83
5	0-10	A	1.04	33.36	3.48
5	10-24	E	1.39	7.6	1.48
6	0-13	A	0.75	40.27	3.93
6	13-24	E	1.29	11.42	1.62
7	0-11	A	0.73	50.81	4.09
7	11-24	E	1.53	11.82	2.34
8	0-15	A	0.57	55.83	4.77
8	15-24	E	1.4	15.14	1.91
9	0-9	A	0.89	44.02	3.52
9	9-24	E	1.16	13.4	2.32
10	0-8	A	0.95	39.06	2.97
10	8-24	E	1.13	17.99	3.26
11	0-10	A	0.82	45.74	3.77
11	10-24	E	1.18	17.94	2.97
12	0-11	A	0.73	39.23	3.14
12	11-24	E	1	18.33	2.39
13	0-10	A	0.86	38.3	3.31
13	10-24	E	1.15	19.69	3.18
14	0-10	A	0.72	38.61	2.77
14	10-24	E	1.1	14.26	2.19
15	0-11	A	0.92	32.6	3.3
15	11-24	E	1.18	16.69	2.55
Mean Hg loading in invaded soil = 5.47					

Table 15. Summary of Hg delta (δ) values in the forest floor of the uninvaded pits of the 2014 samples with the mean delta value reported at the bottom.

Sample	Horizon	BD (g/cm^3)	Hg (ppm)	Zr (ppm)	%LOI	δ Hg ($\mu g/cm^2$)
1	FF	0.20	0.1689	199.94	38.75%	0.1236
2	FF	0.16	0.1983	176.24	43.93%	0.1308
3	FF	0.17	0.1814	186.02	41.79%	0.1225
4	FF	0.21	0.1469	213.48	35.79%	0.1032
5	FF	0.21	0.1621	204.50	37.76%	0.1255
6	FF	0.19	0.1537	218.89	34.61%	0.0950
7	FF	0.32	0.1605	231.43	31.87%	0.1545
8	FF	0.25	0.1853	182.60	42.54%	0.1886
9	FF	0.28	0.1910	192.74	40.33%	0.2055
10	FF	0.20	0.1154	160.93	47.27%	0.1055
11	FF	0.23	0.1213	79.01	65.17%	0.1767
12	FF	0.19	0.1971	173.24	44.59%	0.1580
					Mean δ value	0.1408

Table 16. Summary of Hg delta (δ) values in the uninvaded mineral soil of the 2014 samples with the mean delta value reported at the bottom.

Sample	Horizon	Depth (cm)	BD (g/cm^3)	Hg (ppm)	Zr (ppm)	δ Hg ($\mu g/cm^2$)
1	A	0-4	0.90	0.0502	354.31	0.0087
2	A	0-3	0.96	0.0473	355.67	0.0059
3	A	0-3	0.84	0.0422	357.98	0.0045
4	A	0-4	0.51	0.0910	335.68	0.0183
5	A	0-1	0.73	0.0449	356.77	0.0014
6	A	0-5	1.01	0.0332	362.12	0.0053
7	A	0-4	0.86	0.0268	365.06	0.0013
8	A	0-5	0.87	0.0474	355.61	0.0099
9	A	0-5	0.42	0.0927	334.89	0.0187
10	A	0-5	0.70	0.0566	351.40	0.0120
11	A	0-5	0.46	0.0647	347.68	0.0100
12	A	0-3.5	0.54	0.1622	303.05	0.0562
					Mean δ value	0.0127

Table 17. Summary of Hg delta (δ) values in the invaded mineral soil of the 2014 samples with the mean delta value reported at the bottom.

Sample	Horizon	Depth (cm)	BD (g/cm^3)	Hg (ppm)	Zr (ppm)	δ Hg ($\mu g/cm^2$)
1	A	0-8	0.78	0.0343	299.54	0.0407
2	A	0-13	0.64	0.0312	283.65	0.0543
3	A	0-11	0.71	0.0416	286.87	0.0711
4	A	0-9	0.77	0.0315	296.67	0.0423
5	A	0-10	1.04	0.0334	312.65	0.0546
6	A	0-13	0.75	0.0403	282.95	0.0870
7	A	0-11	0.73	0.0508	284.26	0.0945
8	A	0-15	0.57	0.0558	225.90	0.1766
9	A	0-9	0.89	0.0440	311.92	0.0543
10	A	0-8	0.95	0.0391	307.59	0.0494
11	A	0-10	0.82	0.0457	305.88	0.0626
12	A	0-11	0.73	0.0392	308.95	0.0391
13	A	0-10	0.86	0.0383	310.65	0.0536
14	A	0-10	0.72	0.0386	302.31	0.0477
15	A	0-11	0.92	0.0326	316.35	0.0437
					Mean δ value	0.0648

Table 18. Summary of calculated Zr values for forest floor in the uninvaded soils of 2014 samples. Zr values were calculated based on the following equation:
y= -457.7x + 377.31, where x is the LOI fraction and y the calculated Zr value.

Sample ID	Horizon	% C	% LOI	Calc. Zr
1	FF	22.48%	38.75%	199.94
2	FF	25.48%	43.93%	176.24
3	FF	24.24%	41.79%	186.02
4	FF	20.76%	35.79%	213.48
5	FF	21.90%	37.76%	204.50
6	FF	20.08%	34.61%	218.89
7	FF	18.49%	31.87%	231.43
8	FF	24.68%	42.54%	182.60
9	FF	23.39%	40.33%	192.74
10	FF	27.42%	47.27%	160.93
11	FF	37.80%	65.17%	79.01
12	FF	9.08%	15.66%	305.64
13	FF	17.56%	30.27%	238.77
14	FF	11.26%	19.41%	288.47
15	FF	25.86%	44.59%	173.24

Table 19. Summary of calculated Zr values for the uninvaded soils of 2014 samples. Zr values were calculated based on the following equation:
y = -457.7x + 377.31, where x is the LOI fraction and y the calculated Zr value.

Sample ID	Depth (cm)	Horizon	% C	% LOI	Calc. Zr
1	0-4	A	2.85%	4.92%	354.80
1	4-24	E	0.35%	0.60%	374.54
2	0-3	A	3.08%	5.31%	353.01
2	3-24	E	0.38%	0.65%	374.35
3	0-3	A	2.91%	5.02%	354.35
3	3-24	E	0.34%	0.59%	374.59
4	0-4	A	7.77%	13.39%	316.04
4	4-24	E	0.72%	1.25%	371.59
5	0-1	A	3.40%	5.86%	350.49
5	1-24	E	0.51%	0.88%	373.26
6	0-5	A	1.68%	2.90%	364.06
6	5-24	E	0.30%	0.52%	374.94
7	0-4	A	1.66%	2.85%	364.25
7	4-24	E	0.31%	0.54%	374.85
8	0-5	A	3.76%	6.48%	347.67
8	5-24	E	0.37%	0.64%	374.38
9	0-5	A	8.47%	14.61%	310.45
9	5-24	E	0.71%	1.22%	371.73
10	0-5	A	3.86%	6.66%	346.84
10	5-24	E	0.28%	0.49%	375.06
11	0-5	A	5.42%	9.35%	334.52
11	5-24	E	0.60%	1.03%	372.58
12	0-24	E	0.33%	0.56%	374.74
13	0-24	E	0.26%	0.46%	375.22
14	0-24	E	0.40%	0.69%	374.17
15	0-3.5	A	9.24%	15.93%	304.42
15	3.5-24	E	0.52%	0.89%	373.22

Table 20. Summary of calculated Zr values for the invaded soils of 2014 samples. Zr values were calculated based on the following equation:
y = -964.32x + 408.85, where x is the LOI fraction and y the calculated Zr value.

Sample ID	Depth (cm)	Horizon	% C	% LOI	Calc. Zr
1	0-8	A	4.67%	8.06%	299.54
1	8-24	E	0.44%	0.75%	369.99
2	0-13	A	5.63%	9.71%	283.65
2	13-24	E	1.11%	1.91%	358.78
3	0-11	A	5.44%	9.37%	286.87
3	11-24	E	0.56%	0.97%	367.87
4	0-9	A	4.85%	8.36%	296.67
4	9-24	E	0.55%	0.94%	368.15
5	0-10	A	3.89%	6.70%	312.65
5	10-24	E	0.38%	0.66%	370.87
6	0-13	A	5.67%	9.78%	282.95
6	13-24	E	0.84%	1.44%	363.36
7	0-11	A	5.59%	9.64%	284.26
7	11-24	E	0.46%	0.80%	369.55
8	0-15	A	9.10%	15.70%	225.90
8	15-24	E	1.11%	1.91%	358.81
9	0-9	A	3.93%	6.77%	311.92
9	9-24	E	0.51%	0.89%	368.70
10	0-8	A	4.19%	7.22%	307.59
10	8-24	E	0.50%	0.85%	369.01
11	0-10	A	4.29%	7.40%	305.88
11	10-24	E	0.63%	1.09%	366.75
12	0-11	A	4.11%	7.08%	308.95
12	11-24	E	1.47%	2.53%	352.89
13	0-10	A	4.01%	6.91%	310.65
13	10-24	E	0.40%	0.68%	370.67
14	0-10	A	4.51%	7.77%	302.31
14	10-24	E	0.73%	1.26%	365.11
15	0-11	A	3.66%	6.32%	316.35
15	11-24	E	0.76%	1.31%	364.63

Table 21. Summary of C loadings in the forest floor (FF) of the least invaded pits of the 2009 samples with the overall mean C loading in FF reported at the bottom. Forest floor thickness is 6 cm for pits 160, 150 and 100; and 4 cm for pit 190.

Pit	Thickness (cm)	Horizon	BD (g/cm^3)	C (mg/g)	C Loading (kg/m^2)
190	2	FF	0.27	347.45	1.88
	2	FF	0.27	310.32	1.68
				C Loading sum	3.55
160	2	FF	0.24	380.51	1.83
	2	FF	0.24	313.81	1.51
	2	FF	0.24	175.17	1.26
				C Loading sum	4.59
150	2	FF	0.33	388.05	2.56
	2	FF	0.33	320.77	2.12
	2	FF	0.33	189.10	1.25
				C Loading sum	5.93
100	2	FF	0.24	187.94	0.90
	2	FF	0.24	153.13	0.74
	2	FF	0.24	127.61	0.61
				C Loading sum	2.25
Mean C loading in FF = 4.08					

Table 22. Summary of C loadings to a depth of 24 cm in mineral soil profiles of the least invaded pits of the 2009 samples with the mean C loading reported at the bottom.

Pit	Depth (cm)	Horizon	BD (g/cm^3)	C (mg/g)	C Loading (kg/m^2)
190	0-3	A	0.86	64.97	1.68
	3-7	E	0.81	21.11	0.68
	7-11	E	0.81	16.47	0.53
	11-21	E	1.13	9.98	1.13
	21-24	E	1.13	6.79	0.23
				C Loading sum	4.25
160	0-2	A	0.61	48.09	0.59
	2-5	A	0.61	29.18	0.53
	5-10	E	1	19.14	0.96
	10-18	E	1.2	11.14	1.07
	18-24	E	1.31	9.86	0.78
				C Loading sum	3.92
150	0-2	A	0.5	50.23	0.5
	2-5	A	0.5	24.94	0.37
	5-11	E	0.9	13.52	0.73
	11-21	E	1.24	8	0.99
	21-24	E	1.24	10.21	0.38
				C Loading sum	2.98
100	0-3	A	0.24	76.57	0.55
	3-8	A	0.56	19.32	0.54
	8-15	E	1.3	11.95	1.09
	15-24	E	1.3	9.86	1.15
				C Loading sum	3.33
Mean C loading in uninvaded soil (combined pits 190, 160, 150, 100)= 3.62					

Table 23. Summary of C loadings to a depth of 24 cm in mineral soil profiles of the most invaded pits of the 2009 samples with the mean C loading reported at the bottom.

Pit	Depth (cm)	Horizon	BD (g/cm^3)	C (mg/g)	C Loading (kg/m^2)
50	0-2	A	0.55	106.44	1.17
	2-4	A	0.55	85.85	0.94
	4-6	A	0.55	71.93	0.79
	6-8	A	0.55	54.93	0.60
	8-10	A	0.55	24.94	0.27
	10-18	E	1.09	12.65	0.96
	18-24	E	1.32	9.05	0.72
				C Loading sum	5.47
0	0-2	A	0.67	106.44	1.43
	2-4	A	0.67	91.94	1.23
	4-6	A	0.67	80.92	1.08
	6-8	A	0.67	72.80	0.98
	8-10	A	0.67	57.08	0.76
	10-18	E	1.14	13.92	1.27
	18-24	E	1.1	8.64	0.57
				C Loading sum	7.32
Mean C loading in invaded soil (combined pits 50 and 0) = 6.39					

Table 24. Summary of C delta (δ) values in the forest floor of the least invaded pits of the 2009 samples with the mean delta value reported at the bottom.

Pit	Horizon	BD g/cm^3	C (mg/g)	Zr (ppm)	%LOI	δ C (mg/cm^2)
190	FF	0.27	347.45	103.15	59.9	134.83
	FF	0.27	310.32	132.44	53.5	107.03
					δ sum	107.03
160	FF	0.24	380.51	67.81	65.6	152.84
	FF	0.24	313.81	130.99	54.1	103.14
	FF	0.24	175.17	262.30	30.2	31.01
					δ sum	286.99
150	FF	0.33	388.05	61.54	66.9	221.79
	FF	0.33	320.77	132.42	55.3	150.65
	FF	0.33	189.10	271.12	32.6	51.11
					δ sum	423.56
100	FF	0.24	187.94	295.28	32.4	33.69
	FF	0.24	153.13	329.88	26.4	22.06
	FF	0.24	127.61	355.26	22	15.08
					δ sum	70.83
Mean of δ sums: 222.10						

Table 25. Summary of C delta (δ) values for A horizons of all soil profiles of the 2009 samples with the mean delta values reported at the bottom.

Pit	Depth (cm)	Horizon	BD (g/cm^3)	C (mg/g)	Zr (ppm)	δ C (mg/cm^2)
190	0-3	A	0.86	64.97	326.05	18.54
					δ sum	18.54
160	0-2	A	0.61	48.09	382.67	4.64
	2-5	A	0.61	29.18	400.59	1.92
					δ sum	6.56
150	0-2	A	0.5	50.23	417.40	4.57
	2-5	A	0.5	24.94	444.04	1.23
					δ sum	5.80
100	0-3	A	0.24	76.57	406.02	7.64
	3-8	A	0.56	19.32	462.95	0.96
					δ sum	8.60
50	0-2	A	0.55	106.44	334.37	19.52
	2-4	A	0.55	85.85	348.78	12.35
	4-6	A	0.55	71.93	358.52	8.43
	6-8	A	0.55	54.93	370.41	4.65
	8-10	A	0.55	24.94	391.40	0.67
					δ sum	45.62
0	0-2	A	0.67	106.44	200.30	62.94
	2-4	A	0.67	91.94	224.41	46.08
	4-6	A	0.67	80.92	242.73	35.01
	6-8	A	0.67	72.80	256.23	27.83
	8-10	A	0.67	57.08	282.36	16.24
					δ sum	188.10
Mean δ for least invaded soils (pits 190, 160, 150, 100)= 9.87 Mean δ for most invaded soils (pits 50, 0)= 116.86						

Table 26. Summary of C loadings in the forest floor (FF) of the uninvaded soils of the 2014 samples with the overall mean C loading in FF reported at the bottom. Thickness of all forest floor samples is 8 cm.

Sample ID	Thickness (cm)	Horizon	BD (g/cm^3)	C (mg/g)	C Loading (kg/m^2)
1	8	FF	0.20	224.78	3.55
2	8	FF	0.16	254.81	3.19
3	8	FF	0.17	242.42	3.26
4	8	FF	0.21	207.62	3.42
5	8	FF	0.21	192.20	3.30
6	8	FF	0.19	200.76	2.99
7	8	FF	0.32	184.88	4.74
8	8	FF	0.25	246.76	4.92
9	8	FF	0.28	233.91	5.25
10	8	FF	0.20	274.21	4.40
11	8	FF	0.23	378.03	6.99
12	8	FF	0.19	91.38	1.40
13	8	FF	0.22	175.58	3.13
14	8	FF	0.36	112.59	3.27
15	8	FF	0.19	258.62	3.88
				Mean C loading in FF	3.85

Table 27. Summary of C loadings to a depth of 24 cm in the uninvaded mineral soils of the 2014 samples with the mean C loading reported at the bottom.

Sample ID	Depth (cm)	Horizon	BD (g/cm^3)	C (mg/g)	C Loading (kg/m^2)
1	0-4	A	0.90	28.53	1.03
1	4-24	E	1.27	3.51	0.89
2	0-3	A	0.96	30.80	0.88
2	3-24	E	1.29	3.75	1.02
3	0-3	A	0.84	29.10	0.73
3	3-24	E	1.33	3.51	0.98
4	0-4	A	0.51	77.65	1.58
4	4-24	E	1.30	7.24	1.88
5	0-1	A	0.73	33.99	1.13
5	1-24	E	1.30	5.13	1.40
6	0-5	A	1.01	16.79	0.85
6	5-24	E	1.32	3.00	0.75
7	0-4	A	0.86	16.56	0.57
7	4-24	E	1.33	3.12	0.83
8	0-5	A	0.87	37.56	1.64
8	5-24	E	1.23	3.71	0.86
9	0-5	A	0.42	84.74	1.78
9	5-24	E	1.20	7.07	1.61
10	0-5	A	0.70	38.97	1.36
10	5-24	E	1.30	2.85	0.70
11	0-5	A	0.46	54.23	1.24
11	5-24	E	1.11	5.99	1.26
12	0-24	E	1.34	3.26	1.05
13	0-24	E	1.39	2.64	0.88
14	0-24	E	1.28	3.98	1.23
15	0-3.5	A	0.54	92.38	1.73
15	3.5-24	E	1.35	5.32	1.47
C loading in uninvaded soil = 2.09					

Table 28. Summary of C loadings to a depth of 24 cm in the invaded mineral soils of the 2014 samples with the mean C loading reported at the bottom.

Sample ID	Depth (cm)	Horizon	BD (g/cm^3)	C (mg/g)	C Loading (kg/m^2)
1	0-8	A	0.78	46.74	2.91
1	8-24	E	1.30	4.37	0.91
2	0-13	A	0.64	56.30	4.68
2	13-24	E	1.05	11.11	1.29
3	0-11	A	0.71	54.36	4.22
3	11-24	E	1.03	5.64	0.75
4	0-9	A	0.77	48.47	3.35
4	9-24	E	1.16	5.47	0.96
5	0-10	A	1.04	38.86	4.05
5	10-24	E	1.39	3.84	0.75
6	0-13	A	0.75	59.18	5.78
6	13-24	E	1.29	8.35	1.19
7	0-11	A	0.73	55.93	4.51
7	11-24	E	1.53	4.63	0.92
8	0-15	A	0.57	91.04	7.77
8	15-24	E	1.40	11.09	1.40
9	0-9	A	0.89	39.30	3.15
9	9-24	E	1.16	5.14	0.89
10	0-8	A	0.95	41.90	3.18
10	8-24	E	1.13	4.96	0.90
11	0-10	A	0.82	42.73	3.52
11	10-24	E	1.18	6.32	1.04
12	0-11	A	0.73	41.08	3.29
12	11-24	E	1.00	14.65	1.91
13	0-10	A	0.86	40.06	3.46
13	10-24	E	1.15	3.96	0.64
14	0-10	A	0.72	45.08	3.24
14	10-24	E	1.10	7.30	1.12
15	0-11	A	0.92	36.63	3.71
15	11-24	E	1.18	7.59	1.16
C Loading in invaded soil = 5.11					

Table 29. Summary of C delta (δ) values in the forest floor of the uninvaded pits of the 2014 samples with the mean delta value reported at the bottom.

Sample	Horizon	BD (g/cm^3)	C (mg/g)	Zr (ppm)	%LOI	δ C (mg/cm^2)
1	FF	0.20	224.78	199.94	38.75%	164.42
2	FF	0.16	254.81	176.24	43.93%	168.03
3	FF	0.17	242.42	186.02	41.79%	163.73
4	FF	0.21	207.62	213.48	35.79%	145.86
5	FF	0.21	192.20	204.50	37.76%	148.79
6	FF	0.19	200.76	218.89	34.61%	124.08
7	FF	0.32	184.88	231.43	31.87%	177.97
8	FF	0.25	246.76	182.60	42.54%	251.19
9	FF	0.28	233.91	192.74	40.33%	251.64
10	FF	0.20	274.21	160.93	47.27%	250.85
11	FF	0.23	378.03	79.01	65.17%	550.62
12	FF	0.19	258.62	173.24	44.59%	207.29
					Mean δ value	217.04

Table 30. Summary of C delta (δ) values in the uninvaded mineral soil of the 2014 samples with the mean delta value reported at the bottom.

Sample	Horizon	Depth (cm)	BD (g/cm^3)	C (mg/g)	Zr (ppm)	δ C (mg/cm^2)
1	A	0-4	0.90	28.53	354.31	4.93
2	A	0-3	0.96	30.80	355.67	3.85
3	A	0-3	0.84	29.10	357.98	3.07
4	A	0-4	0.51	77.65	335.68	15.62
5	A	0-1	0.73	33.99	356.77	1.04
6	A	0-5	1.01	16.79	362.12	2.70
7	A	0-4	0.86	16.56	365.06	0.81
8	A	0-5	0.87	37.56	355.61	7.83
9	A	0-5	0.42	84.74	334.89	17.07
10	A	0-5	0.70	38.97	351.40	8.26
11	A	0-5	0.46	54.23	347.68	8.37
12	A	0-3.5	0.54	92.38	303.05	31.99
					Mean δ value	8.80

Table 31. Summary of C delta (δ) values in the invaded mineral soil of the 2014 samples with the mean delta value reported at the bottom.

Sample	Horizon	Depth (cm)	BD (g/cm^3)	C (mg/g)	Zr (ppm)	δ C (mg/cm^2)
1	A	0-8	0.78	46.74	299.54	55.42
2	A	0-13	0.64	56.30	283.65	97.94
3	A	0-11	0.71	54.36	286.87	92.96
4	A	0-9	0.77	48.47	296.67	65.08
5	A	0-10	1.04	38.86	312.65	63.62
6	A	0-13	0.75	59.18	282.95	127.91
7	A	0-11	0.73	55.93	284.26	104.00
8	A	0-15	0.57	91.04	225.90	287.92
9	A	0-9	0.89	39.30	311.92	48.44
10	A	0-8	0.95	41.90	307.59	52.99
11	A	0-10	0.82	42.73	305.88	58.50
12	A	0-11	0.73	41.08	308.95	41.00
13	A	0-10	0.86	40.06	310.65	56.06
14	A	0-10	0.72	45.08	302.31	55.68
15	A	0-11	0.92	36.63	316.35	49.11
					Mean δ value	83.77

Appendix III

WARBA SERIES

The Warba series consists of very deep, moderately well and well drained soils formed in loamy calcareous glacial till on moraines. Permeability is moderate to moderately rapid in the upper part and moderately slow in the lower part. Slopes range from 1 to 25 percent. Mean annual precipitation is about 25 inches. Mean annual air temperature is about 39 degrees F.

TAXONOMIC CLASS: Fine-loamy, mixed, superactive, frigid Haplic Glossudalfs

TYPICAL PEDON: Warba very fine sandy loam, on a northeast-facing, convex slope of 4 percent, about 50 feet below the crest of a knoll, on a till plain, under northern hardwoods forest. This pedon represents the moderately well drained phase. (Colors are for moist soils unless otherwise noted.)

O--0 to 2 inches; dark reddish brown (5YR 2/2) forest litter derived from leaves, twigs and roots. (0 to 3 inches thick)

A--2 to 3 inches; very dark gray (10YR 3/1) very fine sandy loam, gray (10YR 5/1) dry; weak very fine granular structure; very friable; many fine and very fine roots; about 4 percent gravel; moderately acid; abrupt smooth boundary. (0 to 2 inches thick)

E1--3 to 8 inches; grayish brown (10YR 5/2) very fine sandy loam; light gray (10YR 7/2) dry; weak thin platy structure; very friable; many very fine and fine roots; few vesicular pores; about 5 percent gravel; strongly acid; clear wavy boundary.

E2--8 to 13 inches; light brownish gray (10YR 6/2) very fine sandy loam; light gray (10YR 7/1) dry; moderate thin platy structure; friable; many fine and very fine roots; common vesicular pores; about 3 percent gravel; moderately acid; abrupt wavy boundary. (Combined thickness of the E horizon is 5 to 13 inches.)

E/B--13 to 17 inches; 70 percent light brownish gray (10YR 6/2) very fine sandy loam (E); massive; friable; tongued into and surrounding 30 percent brown (10YR 4/3) clay loam (Bt); weak coarse subangular blocky structure; firm; many fine and very fine roots; few pores; about 3 percent gravel; moderately acid; clear wavy boundary.

B/E--17 to 20 inches; 75 percent brown (10YR 4/3) clay loam (Bt); moderate medium and coarse subangular blocky structure; firm; with 25 percent tongues of light brownish gray (10YR 6/2) loamy very fine sand (E); massive; friable; few fine and very fine roots; few pores; about 3 percent gravel; moderately acid; clear wavy boundary. (Combined thickness of the glossic horizon is 3 to 14 inches.)

Bt1--20 to 26 inches; light olive brown (2.5Y 5/4) clay loam; strong medium prismatic structure that parts to moderate medium angular blocky structure; firm; few very fine and fine roots; few pores; many distinct brown (10YR 4/3) clay films on faces of peds and in

pores; few faint ped coats of E material; about 3 percent gravel; moderately acid; clear wavy boundary.

Bt2--26 to 31 inches; light olive brown (2.5Y 5/4) clay loam; moderate coarse prismatic structure parting to moderate medium angular blocky structure; firm; few very fine roots; few pores; many distinct thin brown (10YR 4/3) clay films on faces of peds and in pores; few clean sand grains on some of the vertical faces of peds; about 4 percent gravel; moderately acid; clear wavy boundary.

Bt3--31 to 39 inches; light olive brown (2.5Y 5/4) clay loam; weak very coarse prismatic structure; friable; few very fine roots; few pores; common distinct brown (10YR 4/3) clay films on faces of peds; very few fine soft manganese nodules; about 4 percent gravel; moderately acid; clear wavy boundary. (Combined thickness of the Bt horizon is 12 to 36 inches.)

C1--39 to 44 inches; light olive brown (2.5Y 5/4) loam; massive; friable; few very fine roots; few pores; few fine prominent yellowish red (5YR 5/6) Fe concentrations; about 5 percent gravel; neutral; clear wavy boundary.

C2--44 to 60 inches; light olive brown (2.5Y 5/4) loam; massive; friable; few very fine roots; few pores; few fine prominent yellowish red (5YR 5/6) Fe concentrations; about 6 percent gravel; slightly effervescent; slightly alkaline.

TYPE LOCATION: Cass County, Minnesota; in the Pike Bay Experimental Forest, about 3.5 miles east and 3.7 miles south of the community of Cass Lake; located about 990 feet north and 1,270 feet west of the southeast corner of sec. 31, T. 145 N., R. 30 W.; USGS Pike Bay topographic quadrangle; lat. 47 degrees 19 minutes 34 seconds N. and long. 94 degrees 31 minutes 42 seconds W., NAD 83.

RANGE IN CHARACTERISTICS: Depth to carbonates ranges from 35 and 70 inches. The till has 2 to 12 percent by volume of rock fragments of mixed lithology, but typically high in gray, extremely hard, flat shale. Most pedons have a few cobblestones throughout the soil. The soil moisture control section is not dry in any part for as long as 90 cumulative days in most years. Many pedons have a mantle with a high content of coarse silt and very fine sand. It is as much as 20 inches thick. It has 0 to 5 percent by volume of rock fragments.

The O horizons have hue of 10YR to 5YR, value of 2 to 4, and chroma of 1 to 3. It is Oa, Oe or Oi. It is comprised of accumulated forest litter of deciduous tree leaves, coniferous tree needles and remains of forest floor flora.

The A horizon has value of 2 or 3 and chroma of 1 or 2. The E horizon has value of 4 to 6 and chroma of 2 or value of 6 and chroma of 3. The A and E horizons are very fine sandy loam, silt loam, fine sandy loam or loam. They are strongly acid to slightly acid. Some pedons have an Ap horizon with dry value of 5 or higher.

The glossic horizon consists of an E/B or B/E or both. The E and Bt material each occupy 15 percent or more of the horizon. Colors and textures are similar to E and Bt horizons respectively.

The Bt horizon has matrix hue of 10YR or 2.5Y, value of 4 to 6, and a typical chroma of 3 or 4. Some pedons have a minor amount of chroma of 2 beginning 10 inches or more below the upper boundary of the Bt horizon. It is clay loam, loam or sandy clay loam having 20 to 35 percent of clay. It typically has 30 to 40 percent of fine sand and coarser sand. It averages less than 45 percent sand. It commonly is moderately acid to neutral but may be strongly acid in the upper part. It has manganese oxide nodules in the lower part in some pedons. Some pedons have a Bk horizon.

The C horizon has hue of 2.5Y or 10YR, value of 4 to 6, and chroma of 3 or 4. Most pedons have high chroma Fe concentrations. It is loam, sandy clay loam, or clay loam. It is neutral to moderately alkaline. Below the upper few inches it has calcium carbonate equivalent in the range of about 5 to 15 percent.

COMPETING SERIES: These are the Bamfield, Cushing, Duluth, Lozeau, and Sol series. The Cushing soils average less than 25 percent clay and greater than 45 percent total sand in the Bt and C horizon. The Bamfield and Duluth soils have hue of 7.5YR or redder in the middle and lower third of the series control section. Lozeau soils have a paralithic contact above a depth of 40 inches. The Sol soils have less than 18 percent clay in the lower one-third of the series control section and have more than 45 percent sand in the argillic horizon and below.

GEOGRAPHIC SETTING: The Warba soils have convex and plane slopes on moraines. Slope ranges from 1 to 25 percent, mainly 1 to 6 percent. They formed in calcareous loamy till in the late Wisconsinan glaciation. Mean annual air temperature ranges from 36 to 42 degrees F. Mean annual precipitation ranges from 22 to 28 inches. Frost-free period ranges from 88 to 135 days. Elevation ranges from 1,000 to 1,600 feet above sea level.

GEOGRAPHICALLY ASSOCIATED SOILS: These are Stuntz and Talmoon soils, members of a hydrosequence with Warba soils. The somewhat poorly drained Stuntz soils are less sloping with slightly concave slopes and the very poorly drained Talmoon soils are in shallow depressions. Cathro, Greenwood, Lupton, Mooselake, and Seelyeville are organic soils in adjacent depressions.

DRAINAGE AND PERMEABILITY: Moderately well and well drained. Permeability is moderate to moderately rapid in the upper part and moderately slow in the lower part. Runoff is moderately low to high depending upon slope. The moderately well drained phase has an apparent water table at 3.5 to 6.0 feet at some time during April to May in normal years.

USE AND VEGETATION: Most of this soil is forested. Main trees are basswood, quaking aspen, red oak, sugar maple, and white spruce. A minor amount is cleared for the production of hay, pasture, and small grains.

DISTRIBUTION AND EXTENT: North-central Minnesota. Extensive.

MLRA SOIL SURVEY REGIONAL OFFICE (MO) RESPONSIBLE: St. Paul, Minnesota

SERIES ESTABLISHED: Itasca County, Minnesota, 1982.

REMARKS: Diagnostic horizons and features recognized in this pedon are: ochric epipedon - the zone from the mineral soil surface to 15 inches (A, E1, E2, E/B horizons); albic horizons - the zones from 1 to 15 inches (E1, E2, and E/B horizons); glossic horizon - the zone from 6 to 15 inches (E/B and B/E horizons); argillic horizon - the zone from 15 to 37 inches (B/E, Bt1, Bt2 and Bt3 horizons); Base saturation above 60 percent in all parts of argillic horizon.

The moderately wet phase needs field study to determine if it does or does not qualify as an Oxyaquic subgroup of Glossudalfs.

ADDITIONAL DATA: Refer to MAES Central File Code No. 879 for results of some laboratory analyses of the typifying pedon and to Nos. 733 and 796 for data on two other pedons. Soil Interpretation Record numbers are MN0140 and MN0708, moderate wet phase.

National Cooperative Soil Survey
U.S.A.